DWARF GALAXIES OF THE LOCAL GROUP

Mario Mateo

Department of Astronomy, University of Michigan, Ann Arbor, Michigan
48109-1090; e-mail: mateo@astro.lsa.umich.edu

ABSTRACT

The Local Group dwarf galaxies offer a unique window to the detailed properties
of the most common type of galaxy in the Universe. In this review, I update the
census of Local Group dwarfs based on the most recent distance and radial veloc-
ity determinations. I then discuss the detailed properties of this sample, including
(*a*) the integrated photometric parameters and optical structures of these galax-
ies, (*b*) the content, nature, and distribution of their interstellar medium (ISM),
(*c*) their heavy-element abundances derived from both stars and nebulae, (*d*) the
complex and varied star-formation histories of these dwarfs, (*e*) their internal
kinematics, stressing the relevance of these galaxies to the "dark matter prob-
lem" and to alternative interpretations, and (*f*) evidence for past, ongoing, and
future interactions of these dwarfs with other galaxies in the Local Group and
beyond. To complement the discussion and to serve as a foundation for future
work, I present an extensive set of basic observational data in tables that sum-
marize much of what we know and do not know about these nearby dwarfs. Our
understanding of these galaxies has grown impressively in the past decade, but
fundamental puzzles remain that will keep the Local Group at the forefront of
galaxy evolution studies for some time.

*While observing the Andromeda Nebula with a fine 18-ft telescope . . . I saw another small
nebula about one minute in diameter which appeared to throw out two small rays; one to
the right and the other to the left.*

G-J-H-J-B Le Gentil de la Galazière, October 29, 1749

Remarks on the Nebulous Stars (1759)

435

1.   INTRODUCTION

To the rest of the Universe, the Local Group is an ordinary collection of dwarf galaxies dominated by two giant spirals. But to Earthbound astronomers interested in galaxy evolution, the Local Group is particularly special. The dwarfs of the Local Group provide a uniquely well-studied and statistically useful sample of low-luminosity galaxies. Indeed, virtually all currently known dwarfs less luminous than $M_V \sim -11.0$ are found in the Local Group (Whiting et al 1997). Dwarf galaxies represent the dominant population, by number, of the present-day Universe (Marzke & Da Costa 1997), and they were almost certainly much more numerous at past epochs (Ellis 1997). Studies of nearby clusters (Phillips et al 1998 and references therein) suggest that the summed optical luminosity of all dwarfs may rival that of the giant high–surface brightness galaxies in these environments. If low-luminosity galaxies are universally dominated by dark matter (DM) to the extent Local Group dwarfs may be (Section 6), they could account for a large fraction of the mass of galaxy clusters and perhaps the entire Universe. The dwarf galaxies of the Local Group offer the best opportunity to study a representative sample of these important but, by nature, inconspicuous galaxies in detail.

Dwarf galaxies are known to exist in large numbers in other environments, particularly nearby groups (Karachentseva et al 1985, Miller 1996, Côté et al 1997), and clusters (Sandage & Binggeli 1984, Sandage et al 1985b, Ferguson & Sandage 1991, Phillips et al 1998). But there are fundamental reasons why the dwarfs of the Local Group remain especially important:

- What is the relationship, if any, between dwarf irregular (dIrr) and dwarf spheroidal/dwarf elliptical (dSph/dE) galaxies? The Local Group contains a unique mixture of low-luminosity galaxies of both types that provide some ways to address this question (e.g. Bothun et al 1986, Binggeli 1994, Skillman & Bender 1995).

- Low-luminosity dwarfs tend to be metal poor (Section 5); thus, the low-luminosity dwarfs in the Local Group represent a sample of galaxies that is still largely composed of nearly primordial material. Dwarf galaxy abundances are typically determined from their HII regions, but only in the Local Group can we also obtain reliable abundances from resolved stellar populations. The large luminosity range of Local Group dwarfs makes them excellent labs to study how other fundamental parameters vary with luminosity, such as DM content, the interstellar medium (ISM) properties, and star-formation history.

- Dwarfs are the simplest galactic systems known. However, Local Group dwarfs are plainly telling us that "simple" is a relative term. The star-

formation and chemical-enrichment histories of these galaxies are complex, varied, and in most cases triggered and sustained by as-yet unknown mechanisms (Section 6). The Hubble Space Telescope (HST) is capable of reaching the main-sequence turnoff of the oldest stars in galaxies throughout the Local Group (Gregg & Minniti 1997), so these galaxies will likely remain for some time the only well-defined sample for which we can derive complete star-formation histories.

- Dwarf galaxies may be among the darkest single galaxies known (Section 7). They play an important role in addressing the DM problem, having already placed interesting constraints on the nature and distribution of DM, and even whether the DM paradigm is valid for these systems (Ashman 1992, Mateo 1997). The Local Group currently provides our only opportunity to measure the internal kinematics of ultra-low–surface brightness dwarfs.

- There is considerable evidence of ongoing, past, and future interactions between Local Group dwarfs and larger galaxies (Section 8), which may have helped assemble the larger Local Group galaxies over time. Recent measurements of the star-formation histories, space motions, three-dimensional shapes, and detailed internal kinematics of some of these interacting dwarfs in the Local Group offer new constraints on the dwarf/giant relationship and interaction models (Mateo 1996, Unavane et al 1996).

I have two principle goals for this review. First, I present here a set of tables that aim to provide a summary of basic observational data for all of the currently known Local Group dwarf galaxies. These tables also highlight areas where fundamental observations are lacking or remain of poor quality. My second goal is to illustrate ways in which studies of Local Group dwarfs offer unique opportunities to understand galaxy evolution, DM, galaxy interactions, and the relation between stellar populations and the ISM. At the start of most sections, I cite specialized reviews pertinent to the topics that follow. Some recent general reviews relevant to Local Group dwarf galaxies include those by Hodge (1989), Gallagher & Wyse (1994), Ferguson & Binggeli (1994), Binggeli (1994), Skillman & Bender (1995), Da Costa (1994a,b, 1998), and Grebel (1997). I have also found the proceedings of three recent meetings to be particularly helpful: the CTIO/ESO workshop on the Local Group held in La Serena, Chile, in 1994 (Layden et al 1994); the ESO/OHP workshop on dwarf galaxies in France in 1993 (Meylan & Prugniel 1994); and the Tucson workshop on the Galactic halo and in honor of George Preston (Morrison & Sarajedini 1996).

1.1 *Some Words About the Tables and Nomenclature*

The tables are meant to be self-contained with complete notes and references. Although the data are presented in a uniform format, the tables are all based on

Table 1   Local Group galaxies

Galaxy name[a]	Other name[b]	α_{2000}[c]	δ_{2000}[d]	l[e]	b[f]	Type[g]	Subgroup[h]	Images[i]
WLM	DDO 221	00 01 58	−15 27.8	75.9	−73.6	IrrIV-V	LGC	1
NGC 55		00 15 08	−39 13.2	332.7	−75.7	IrrIV	LGC	3, 4, 51
IC 10	UGC 192	00 20 25	+59 17.5	119.0	−3.3	dIrr	M31	5, 6
NGC 147	DDO 3	00 33 12	+48 30.5	119.8	−14.3	dSph/dE5	M31	7, 51
And III		00 35 17	+36 30.5	119.3	−26.2	dSph	M31	8
NGC 185	UGC 396	00 38 58	+48 20.2	120.8	−14.5	dSph/ dE3p	M31	7, 51
NGC 205[j]	M110	00 40 22	+41 41.4	120.7	−21.1	E5p/ dSph-N	M31	7, 51
M32	NGC 221	00 42 42	+40 51.9	121.2	−22.0	E2	M31	9, 10, 51
M31	NGC 224	00 42 44	+41 16.1	121.2	−21.6	SbI-II	M31	10, 50, 51
And I		00 45 43	+38 00.4	121.7	−24.9	dSph	M31	8
SMC	NGC 292	00 52 44	−72 49.7	302.8	−44.3	IrrIV-V	MW	11, 12, 51
Sculptor		01 00 09	−33 42.5	287.5	−83.2	dSph	MW	13, 49
LGS 3	Pisces	01 03 53	+21 53.1	126.8	−40.9	dIrr/dSph	M31	14
IC 1613	DDO 8	01 04 54	+02 08.0	129.8	−60.6	IrrV	M31/LGC	15−17
And II[k]		01 16 27	+33 25.7	128.9	−29.2	dSph	M31	8
M33	NGC 598	01 33 51	+30 39.6	133.6	−31.3	ScII-III	M31	17, 18, 51
Phoenix		01 51 06	−44 26.7	272.2	−68.9	dIrr/dSph	MW/LGC	19, 20
Fornax		02 39 59	−34 27.0	237.1	−65.7	dSph	MW	21
EGB0427+63	UGCA 92	04 32 01	+63 36.4	144.7	+10.5	dIrr	M31	23
LMC		05 23 34	−69 45.4	280.5	−32.9	IrrIII-IV	MW	11, 12, 51
Carina		06 41 37	−50 58.0	260.1	−22.2	dSph	MW	24
Leo A	DDO 69	09 59 24	+30 44.7	196.9	+52.4	dIrr	MW/N3109	29, 51
Sextans B	DDO 70	10 00 00	+05 19.7	233.2	+43.8	dIrr	N3109	27, 28, 51
NGC 3109	DDO 236	10 03 07	−26 09.5	262.1	+23.1	IrrIV-V	N3109	29, 30, 51
Antlia[l]		10 04 04	−27 19.8	263.1	+22.3	dIrr/dSph	N3109	31
Leo I	DDO 74	10 08 27	+12 18.5	226.0	+49.1	dSph	MW	32
Sextans A	DDO 75	10 11 06	−04 42.5	246.2	+39.9	dIrr	N3109	33, 51
Sextans		10 13 03	−01 36.9	243.5	+42.3	dSph	MW	34
Leo II	DDO 93	11 13 29	+22 09.2	220.2	+67.2	dSph	MW	52
GR 8	DDO 155	12 58 40	+14 13.0	310.7	+77.0	dIrr	GR8	36, 37, 54
Ursa Minor	DDO 199	15 09 11	+67 12.9	105.0	+44.8	dSph	MW	38
Draco	DDO 208	17 20 19	+57 54.8	86.4	+34.7	dSph	MW	39
Milky Way		17 45 40	−20 00.5	0.0	0.0	Sbc	MW	
Sagittarius[j]		18 55 03	−30 28.7	5.6	−14.1	dSph-N	MW	40
SagDIG	UKS1927-177	19 29 59	−17 40.7	21.1	−16.3	dIrr	LGC	41, 53
NGC 6822	DDO 209	19 44 56	−14 48.1	25.3	−18.4	IrrIV-V	LGC	42, 43, 51
DDO 210[m]	Aquarius	20 46 46	−12 51.0	34.0	−31.3	dIrr/dSph	LGC	36, 44, 54
IC 5152		22 02 42	−51 17.7	343.9	−50.2	dIrr	LGC	51
Tucana[n]		22 41 50	−64 25.2	322.9	−47.4	dSph	LGC	47, 48
UKS2323-326	UGCA 438	23 26 27	−32 23.3	11.9	−70.9	dIrr	LGC	41
Pegasus	DDO 216	23 28 34	+14 44.8	94.8	−43.5	dIrr/dSph	LGC	25, 44, 51

a large, inhomogeneous set of independent studies. Many entries are subjectively weighted mean values of the results from independent sources. Galaxies are listed in order of increasing right ascension in all the tables. I try to provide realistic estimates of the 1σ errors. Where possible, the errors are taken from the original source, or they reflect the scatter of independent results. In several tables and one figure, errors were omitted for photometric results if ≤ 0.04 mag. ASCII files containing most of the information in the tables are available via anonymous ftp at ⟨ftp://ra.astro.lsa.umich.edu/pub/mateo/get/LGDtables.dat⟩.

"Transition" galaxies are the five objects listed in Table 1 as dIrr/dSph systems. Sandage & Hoffman (1991) referred to such galaxies as "mixed-morphology" systems. The non-dIrr galaxies of the Local Group may or may not belong to a single family; hence, when I wish the discussion to include M32 (a dE system) and the five transition galaxies, I use "early-type" galaxies.

2.   THE CENSUS OF LOCAL GROUP DWARFS

In 1971, Paul Hodge wrote an influential review in these volumes devoted to dwarf galaxies. The total dwarf population of the Local Group at that time was 14 galaxies, including the Magellanic Clouds, with six additional uncertain cases. As we see below, the current census of likely dwarf members of the Local Group now stands at 38^{+6}_{-2}. More dwarfs have been confirmed or identified as Local Group members in the past 27 years than during the previous 222 years beginning with Le Gentil's discovery of M32! And it is almost certain that the full census of Local Group dwarfs is not yet complete (Section 2.2).

Merely making a list of Local Group dwarf galaxies demands reliable distances and radial velocities, as well as agreement on the definition of a dwarf galaxy. Table 1 lists all the galaxies that I consider potential Local Group

---

[a]Entries in italics refer to the five giant Local Group galaxies that are not discussed in this review in any detail.

[b]A common alternative name.

[c,d]Right ascension and declination for epoch J2000.0, respectively.

[e,f]Galactic longitude and latitude, respectively.

[g]Galaxy type following van den Bergh (1994a).

[h]Subgroup membership within the Local Group.

[i]References to optical and 21-cm images (if available): 1, Sandage & Carlson 1985b; 2, Lautsen et al 1977; 3, Hummel et al 1986; 4, Puche et al 1991; 5, de Vaucouleurs & Ables 1965; 6, Shostak & Skillman 1989; 7, Young & Lo 1997a; 8, Caldwell et al 1992; 9, Kent 1987; 10, Hodge 1981; 11, de Vaucouleurs & Freeman 1972; 12, Mathewson & Ford 1984; 13, Carignan et al 1998; 14, Young & Lo 1997b; 15, Ables 1971; 16, Lake & Skillman 1989; 17, Sandage 1961; 18, Corbelli et al 1989; 19, van de Rydt et al 1991; 20, Carignan et al 1991; 21, Hodge 1971; 22, Saha & Hoessel 1991; 23, Hoessel et al 1988; 24, Smecker-Hane et al 1994; 25, Sandage 1986b; 26, Young & Lo 1996a; 27, Sandage & Carlson 1985a; 28, Skillman et al 1988; 29, Sandage & Carlson 1988; 30, Jobin & Carignan 1990; 31, Whiting et al 1997; 32, Hodge 1963a; 33, Sandage & Carlson 1982; 34, Mateo et al 1995a; 35, deleted in proof; 36, Fisher & Tully 1979; 37, Carignan et al 1990; 38, van Agt 1967; 39, Baade & Swope 1961; 40, Ibata et al 1997; 41, Longmore et al 1978; 42, Hodge 1978; 43, Gottesman & Weliachew 1977; 44, Lo et al 1993; 45, deleted in proof; 46, deleted in proof; 47, Lavery & Mighell 1992; 48, Oosterloo et al 1996; 49, van Agt 1978; 50, Hodge 1992a; 51, Sandage & Bedke 1994; 52, Vogt et al 1995; 53, Cesarsky et al 1977; 54, Hopp & Schulte-Ladbeck 1995.

[j]The N suffix has been added to indicate that these systems may be nucleated.

[k]The position listed here is based on an independent measurement by Paul Hodge (private communication).

[l]Also known as PGC 29194 (Fouqué et al 1990) before it was rediscovered as a probable Local Group member by Whiting et al (1997). A thorough discussion of "pre-discovery" observations of Antlia is provided by Aparicio et al (1997a).

[m]Marconi et al (1990) claimed that the original position of DDO 210 (Fisher & Tully 1975) was significantly in error. However, Lo et al (1993) noted that the original position seemed to be correct, and Marconi et al (1995) subsequently agreed. The position listed here corresponds to the original one from Fisher & Tully (1975).

[n]Tucana was known prior to its rediscovery by Lavery & Mighell (1992), who thoroughly document all listings of the galaxy in earlier catalogs. Lavery & Mighell (1992) did first claim Tucana to be a possible Local Group member.

members, without regard to whether they may be dwarf or "giant" galaxies. Also listed are their Hubble types (van den Bergh 1994a), with some modifications and additions for galaxies discovered since that paper. M31, the Milky Way, and M33 are normal "giant" spirals, and I do not consider them in any detail in this review. The Magellanic Clouds—particularly the Small Magellanic Cloud—have a more valid claim to dwarfhood, but I do not discuss them here either. Both have been the subject of recent comprehensive reviews (Olszewski et al 1996b, Westerlund 1990, 1998). All remaining galaxies listed in Table 1 are considered "dwarfs" for the purposes of this review.

2.1   *Membership in the Local Group*

RESOLVABILITY AND THE BRIGHTEST STARS   A common method of flagging possible Local Group members is to identify "resolved" galaxies with low heliocentric velocities. This has been useful to confirm the proximity of candidate Local Group members; some recent examples include galaxies studied by Hoessel et al (1988; EGB 0427+63), Lavery & Mighell (1992; Tucana), and Whiting et al (1997; Antlia). A quantitative variation of this technique is to identify and measure the brightest red and blue stars in a resolved system (Sandage 1986b; Sandage & Carlson 1982, 1985a,b, 1988). Piotto & Capaccioli (1992) and Rozanski & Rowan-Robinson (1994) reassessed this technique, and both concluded that it is a crude distance indicator ($\sigma > 0.5$ mag in the distance modulus) in the optical and the infrared (IR). In contrast, Karachentsev & Tikhonov (1993) and Lyo & Lee (1997) concluded that the systematic uncertainties are considerably smaller: $\sim$0.4 mag in the optical and even smaller in the K band for the brightest red stars (Lyo & Lee 1997). In view of the wide range of star-formation histories exhibited by Local Group dwarfs (Section 6) and these contradictory conclusions, the brightest blue and red stars should be used with care as distance indicators. However, this approach clearly remains suitable for identifying possible Local Group members worthy of further study.

DISTANCES   Table 2 lists the latest information on distances for all the dwarf members and candidates of the Local Group. It is satisfying that nearly all of the galaxies listed now have reasonable distance determinations based on one or more high-precision distance indicator, including (*a*) Cepheid variables (e.g. Madore & Freedman 1991, Capaccioli et al 1992, Piotto et al 1994, Saha et al 1996, Wilson et al 1996), (*b*) the I-band tip of the red giant branch (TRGB) (e.g. Da Costa & Armandroff 1990, Lee et al 1993c, Aparicio 1994, Aparicio et al 1997b), (*c*) RR Lyr stars (Saha & Hoessel 1990, Saha et al 1990, 1992a,b), (*d*) SX Phe stars (McNamara 1995, Mateo et al 1998b), and (*e*) the luminosity of the horizontal branch (HB) (Ibata et al 1994, Smecker-Hane et al 1994, Caputo

Table 2 Distances and heliocentric velocities of Local Group galaxies

Galaxy name[a]	l[b]	b[c]	E(B−V) mag[d]	(m−M)$_0$ mag[e]	Distance (kpc)	Ref[f]	V$_{\odot,opt}$ (km s^{-1})[g]	V$_{\odot,radio}$ (km s^{-1})[h]	Ref[i]
WLM[j]	75.9	−73.6	0.02±0.01	24.83±0.08	925±40	1–3,135	—	−123±3	4,5
NGC 55[j]	332.7	−75.7	0.03±0.02	25.85±0.20	1480±150	8,9	—	124±6	4,8,136,137
IC 10	119.0	−3.3	0.87±0.12	24.58±0.12	825±50	10,11	−344±5	−342±6	4,5,12–14
NGC 147	119.8	−14.3	0.18±0.03	24.30±0.12	725±45	1,15	−193±3	—	16,22
And III[k]	119.3	−26.2	0.05±0.02	24.40±0.10	760±40	18	—	—	4,19
NGC 185	120.8	−14.5	0.19±0.02	23.96±0.08	620±25	1,20	−210±7	−204±4	16,21–25
NGC 205[l]	120.7	−21.7	0.04±0.02	24.56±0.08	815±35	1,26,27	−242±3	−229±5	4,16,22,29–31,138
M32	121.2	−22.0	0.08±0.03	24.53±0.08	805±35	32	−197±3	—	4,34,157
M31	121.2	−21.6	0.08	24.43	770	159	−297	—	159
And I[k]	121.7	−24.9	0.04±0.02	24.53±0.10	805±40	36,37	—	—	4,19
SMC	302.8	−44.3	0.08	18.82	58	125,159	175	—	159
Sculptor[k,m]	287.5	−83.2	0.02±0.02	19.54±0.08	79±4	39,40,145	108±3	102±5	4,41,42,44,142
LGS 3	126.8	−40.9	0.08±0.03	24.54±0.15	810±60	45,151–153	−282±4	−272±6	4,46,155
IC 1613	129.8	−60.6	0.03±0.02	24.22±0.10	700±35	1,27,47,48	−237±5	−234±3	4,49–51,156
And II	128.9	−29.2	0.08±0.02	23.6±0.4	525±110	52	—	—	159
M33	133.6	−31.3	0.08	24.62	840	159	−181	—	159
Phoenix[m]	272.2	−68.9	0.02±0.01	23.24±0.12	445±30	53,55	—	56±3/−23±2	54,144
Fornax[k]	237.1	−65.7	0.03±0.01	20.70±0.12	138±8	56	53±3	—	4,57,142
EGB 0427+63	144.7	−10.5	0.30±0.15	25.6±0.7	1300±700	61,146,147	—	−87±6	4
LMC	280.5	−32.9	0.06	18.45	49	125,159	324	—	159
Carina[k]	260.1	−22.2	0.04±0.02	20.03±0.09	101±5	63–66,148	224±3	—	67–69

(Continued)

Table 2 (*Continued*)

Galaxy name[a]	l[b]	b[c]	E(B−V) mag[d]	(m−M)₀ mag[e]	Distance (kpc)	Ref[f]	V_⊙,opt (km s⁻¹)[g]	V_⊙,radio (km s⁻¹)[h]	Ref[i]
Leo A[n]	196.9	+52.4	0.01±0.01	24.2±0.3	690±100	70, 141, 161	—	26±2	4, 5, 46, 139
Sextans B	233.2	+43.8	0.01±0.02	25.64±0.15	1345±100	71	—	303±2	4, 46, 50, 152
NGC 3109[j]	262.1	+23.1	0.04±0.02	25.48±0.25	1250±165	1, 72–75, 143	—	404±2	4, 76, 77
Antlia	263.1	+22.3	0.05±0.03	25.46±0.10	1235±65	78, 79, 158	—	361±2	80
Leo I[k]	226.0	+49.1	0.01±0.01	21.99±0.20	250±30	81, 82	286±2	—	4, 83, 84, 142
Sextans A	246.2	+39.9	0.03±0.02	25.75±0.15	1440±110	71, 86	328±5	325±3	4, 49, 87
Sextans[k]	243.5	+42.3	0.03±0.01	19.67±0.08	86±4	88–90	227±3	—	44, 91–93
Leo II[k]	220.2	+67.2	0.02±0.01	21.63±0.09	205±12	95–97	76±2	—	4, 98, 142
GR 8	310.7	+77.0	0.02±0.02	26.0±0.7	1590±600	100–102, 162	—	215±3	4, 46, 50, 154
Ursa Minor[k]	105.0	+44.8	0.03±0.02	19.11±0.10	66±3	103, 104	−248±2	—	105, 106, 142
Draco[k]	86.4	+34.7	0.03±0.01	19.58±0.15	82±6	108, 160	−293±2	—	105, 109, 142
Milky Way	0.0	0.0	—	14.52	8	125	—	—	—
Sagittarius[k,o]	5.6	−14.1	0.15±0.03	16.90±0.15	24±2	111–114, 149	140±5	—	111, 115, 116,
SagDIG	21.1	−16.3	0.22±0.06	25.2±0.3	1060±160	117–119	−75±5	−79±2	4, 119, 144
NGC 6822[j]	25.3	−18.4	0.26±0.04	23.45±0.15	490±40	1, 2	−53±4	−54±6	4, 49, 121–123, 136
DDO 210[n]	34.0	−31.3	0.06±0.02	24.6±0.5	800±250	120, 124, 125	—	−137±3	4, 5, 46
IC 5152	343.9	−50.2	0.01±0.02	26.01±0.25	1590±200	126, 134	—	124±3	4, 5
Tucana[p]	322.9	−47.4	0.00±0.02	24.73±0.08	880±40	127–129	—	—	132
UKS2323−326	11.9	−70.9	0.07±0.03	25.6±0.5	1320±350	118	—	62±6	119
Pegasus[o]	94.8	−43.5	0.02±0.01	24.90±0.10	955±50	130, 131, 150	—	−182±2	4, 5, 46, 144

[a]Names in italic are "giant" galaxies, included here for convenience but not discussed in any detail in this review.

[b,c]Galactic longitude and latitude, respectively.

[d]Foreground reddening.

[e]True distance modulus.

[f]Distance/reddening references: 1, Lee et al 1993c; 2, Gallart et al 1996c; 3, Minniti & Zijlstra 1996; 4, Huchtmeier & Richter 1986; 5, Richter et al 1987; 6, Heisler et al 1997; 7, Côté 1995; 8, Puche et al 1991; 9, Pritchet et al 1987; 10, Wilson et al 1996; 11, Saha et al 1996; 12, Saitô et al 1992; 13, Wilson & Reid 1991; 14, Shostak & Skillman 1989; 15, Han et al 1997; 16, Bender et al 1991; 18, Armandroff et al 1993; 19, Thuan & Martin 1979; 20, Lee et al 1993b; 21, Held et al 1992; 22, Young & Lo 1997a;

Table 2 Footnote (*Continued*)

23, Wiklind & Rydbeck 1986; 24, Welch et al 1996; 25, Ford et al 1977; 26, Lee 1996; 27, van den Bergh 1995; 29, Carter & Sadler 1990; 30, Held et al 1990; 31, Peterson & Caldwell 1993; 32, Grillmair et al 1996; 33, deleted in proof; 34, Dressler & Richstone 1988; 36, Da Costa et al 1996; 37, Mould & Kristian 1990; 39, Schweitzer et al 1995; 40, Da Costa 1984; 41, Queloz et al 1995; 42, Armandroff & Da Costa 1986; 44, Carignan et al 1998; 45, Lee 1995b; 46, Lo et al 1993; 47, Saha et al 1992a; 48, Huterer et al 1995; 49, Tomita et al 1993; 50, Hoffman et al 1996; 51, Lake & Skillman 1989; 52, König et al 1993; 53, Ortolani & Gratton 1988; 54, Carignan et al 1991; 55, van de Rydt et al 1991; 56, Beauchamp et al 1995; 57, Mateo et al 1991b; 59, Karachentsev & Tikhonov 1993; 60, deleted in proof; 61, Hoessel et al 1988; 62, deleted in proof; 63, Smecker-Hane et al 1994; 64, Hurley-Keller et al 1998; 65, Mighell 1997; 66, McNamara 1995; 67, Mateo et al 1993; 68, Godwin & Lynden-Bell 1987; 69, Mould et al 1990; 70, Hoessel et al 1994; 71, Piotto et al 1994; 72, Lee 1993; 73, Capaccioli et al 1992; 74, Musella et al 1997; 75, Richer & McCall 1992; 76, Jobin & Carignan 1990; 77, Carignan 1985; 78, Whiting et al 1997; 79, Aparicio et al 1997c; 80, Fouqué et al 1990; 81, Lee et al 1993a; 82, Demers et al 1994a; 83, Mateo et al 1998c; 84, Zaritsky et al 1989; 86, Sakai et al 1996; 87, Skillman et al 1988; 88, Mateo et al 1995a; 89, Mateo et al 1991a; 90, Irwin et al 1990; 91, Hargreaves et al 1994a; 92, Suntzeff et al 1993; 93, Da Costa et al 1991; 95, Mighell & Rich 1996; 96, Demers & Irwin 1993; 97, Lee 1995b; 98, Vogt et al 1995; 100, Tolstoy et al 1995; 101, Wyatt & Dufour 1993; 102, Aparicio et al 1988; 103, Nemec et al 1988; 104, Olszewski & Aaronson 1985; 105, Armandroff et al 1995; 106, Hargreaves et al 1994b; 108, Nemec 1985; 109, Hargreaves et al 1996b; 111, Ibata et al 1994; 112, Mateo et al 1995b; 113, Alard 1996; 114, Alcock et al 1997; 115, Ibata et al 1997; 116, Koribalski et al 1994; 117, Longmore et al 1978; 119, Longmore et al 1982; 120, Marconi et al 1990; 121, Gottesman & Wiliachew 1977; 122, Israel 1997; 123, Wilson 1994b; 124, Greggio et al 1993; 125, van den Bergh 1994a; 126, Caldwell et al 1988; 127, Saviane et al 1996; 128, Da Costa 1994a; 129, Castellani et al 1996; 130, Aparicio 1994; 131, Hoessel et al 1990; 132, Oosterloo et al 1996; 133, Richter et al 1991; 134, Burstein & Heiles 1982; 135, Hodge & Miller 1995; 136, Israel et al 1995; 137, Hummel et al 1986; 138, Sage & Wrobel 1989; 139, Young & Lo 1996a; 140, deleted in proof; 141, Demers et al 1984; 142, Knapp et al 1978; 143, Davidge 1993; 144, Young & Lo 1997b; 145, Kaluzny et al 1995; 146, Karachentseva et al 1996; 147, Karachentsev et al 1994; 148, Mateo et al 1998b; 149, Sarajedini & Layden 1995; 150, Aparicio et al 1997b; 151, Aparicio et al 1997a; 152, Mould 1997; 153, Tikhonov & Makarova 1996; 154, Carignan et al 1990; 155, KH Cook, EW Olszewski, C Stubbs, private communication; 156, Lu et al 1993; 157, Nolthenius & Ford 1986; 158, Sarajedini et al 1997; 159, Karachentsev & Makanov 1996; 160, Grillmair et al 1998; 161, Tolstoy et al 1998; 162, Dohm-Palmer et al 1998.

[g]Heliocentric velocity based on optical measurements.

[h]Heliocentric velocity based on radio measurements.

[i]Velocity references; see footnote *f*.

[j]Photographic spectra were obtained by Humason et al (1956), from which they measured velocities of -78, 210, and 441 km s^{-1} for WLM, NGC 55, and NGC 3109, respectively. The typical uncertainty in these results is approximately 50 km s^{-1}.

[k]No HI detected. See Table 5 for limits.

[l]HI, CO, and optical velocities differ by small but possibly significant amounts.

[m]Ambiguous HI detection; the velocity of the most plausible component is listed. For Phoenix, one or both of two HI clouds could be associated with the galaxy (Carignan et al 1991).

[n]Large distance discrepancy or uncertainty; see text.

[o]All values refer to the central regions of the galaxy, taken to coincide with the globular cluster M 54.

[p]A nearby HI cloud ($v_\odot \sim 130$ km s^{-1}) is observed about 15 arcmin from Tucana, which may be associated with the Magellanic Stream (Oosterloo et al 1996).

et al 1995, Da Costa et al 1996). Other indicators that serve for more luminous galaxies such as supernovae, surface brightness fluctuations, Tully-Fisher (TF), or D_n-σ relations are either inapplicable or remain uncalibrated for very low-luminosity dwarfs. Since many individual Local Group galaxies have distances determined with independent techniques, an analysis similar to that of Huterer et al (1995)—which seeks simultaneous consistency of all distance indicators in all galaxies considered—would be of great interest. Generally, when two or more groups have studied the same galaxy, the agreement of CCD-based results is excellent.

There are exceptions. Aparicio (1994) used the TRGB method to argue that the distance of the Pegasus dIrr galaxy is considerably closer than the Cepheid-based distance of Hoessel et al (1990). Aparicio noted that many of the putative Cepheids are located on or near the red giant branch (RGB). Wilson (1994a) identified variables in IC 10 that she tentatively claimed might be Cepheids and proposed a surprisingly small distance for the galaxy. Soon afterwards, Wilson et al (1996) and Saha et al (1996) obtained IR and optical photometry of bona fide Cepheids in IC 10 to settle the issue, finding good consistency for $D \sim 830$ kpc. Hoessel et al (1994) identified five possible Cepheids in Leo A, deriving a distance of 2.2 Mpc. This result is inconsistent with the low velocity of Leo A relative to the Local Group barycenter (Figure 1), implies a pathologically large red-to-blue supergiant ratio (Wilson 1992a), forces the HI mass of Leo A to exceed the kinematic mass of the entire galaxy (Section 7), and results in an abnormally low M/L ratio for the galaxy (Young & Lo 1996). Tolstoy et al (1998) have readdressed this problem using new HST and ground-based photometry, and they concluded that Leo A is $\sim 0.8 \pm 0.2$ Mpc away. This result resolves all of the problems noted above for Leo A.

Evidently, some dwarf galaxies contain red variables (possibly classical long-period variables or semiregular variables) or other sorts of variables (W Vir stars?) that can mimic classical Cepheids. This underscores the crucial need for color information during searches for variable stars in nearby galaxies, the importance of careful windowing to minimize aliases, and the utility of IR photometry of suspected variables in nearby systems. Given the recent improvements in large optical and IR detectors, this may be a good time to reconsider the Cepheid populations in Local Group dwarfs.

DYNAMICAL CONSIDERATIONS   Yahil et al (1977) introduced a dynamical approach that uses only the observed radial velocities to determine the motions of candidate group members relative to the Local Group barycenter. Sandage (1986a) extended this approach by defining the zero-velocity surface separating the Local Group from the local Hubble expansion field. This method acknowledges that the size and internal dispersion of the Local Group (1.5–2 Mpc in
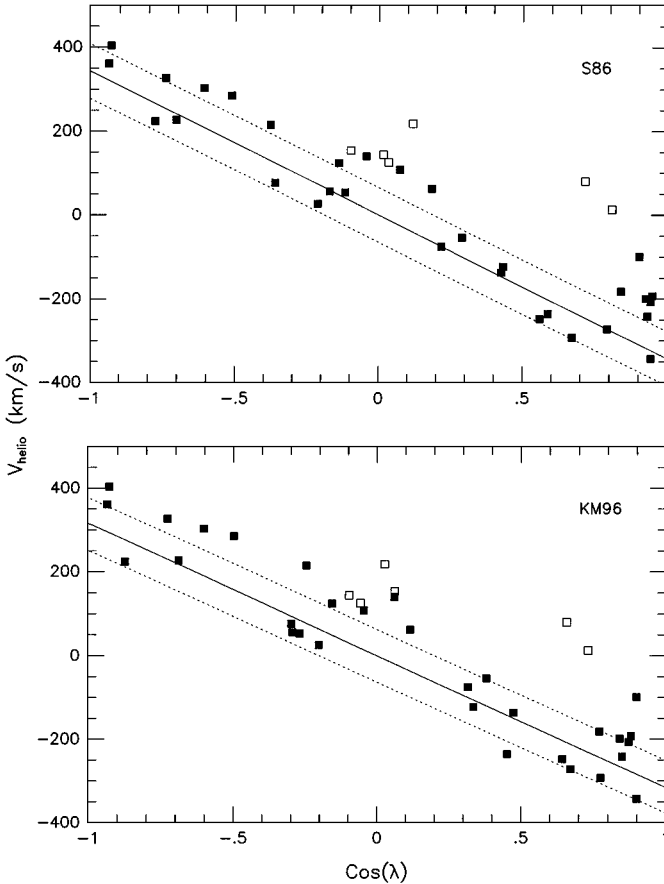
Figure 1   The heliocentric velocities of nearby galaxies plotted as a function of cos(λ), where λ is the angle between the galaxy and the location of the apex of the Sun's motion relative to the center of mass of the Local Group. The *upper plot* adopts the solution for the solar motion from Sandage (1986), for which the apex is located at $(l, b) = (101°, −11°)$ and the Sun's velocity component in this direction is 343 km s^{-1}. The *lower plot* is for the solution from Karachentsev & Makarov (1996), for which $(l, b) = (93°, −4°)$ and the solar velocity is 316 km s^{-1}. The *filled squares* denote the galaxies adopted as Local Group members in this paper; the *open squares* represent a sample of other nearby galaxies—SclDIG (Heisler et al 1997), NGC 300 (Puche et al 1990), Maffei 1 (Luppino & Tonry 1993), DDO 187, and UGCA 86 (van den Bergh 1994a)—that are shown here as a representative sample of galaxies that have at some time or other been considered to be Local Group members (see van den Bergh 1994a for other examples).

radius and ~ 60 km s^{-1}, respectively) imply a crossing time comparable to or longer than a Hubble time. Thus, some bound Local Group members may not yet have reached the outer limit of their first orbit and consequently are still receding from the Local Group center of mass. Sandage's approach requires an estimate of the Local Group mass. The current consensus for the mass of the Galaxy has risen since 1986 to about $1.4 \pm 0.7 \times 10^{12}$ M$_{\odot}$ within 200 kpc from the Galactic Center (Zaritsky et al 1989, Fich & Tremaine 1991, Lin et al 1995, Peebles 1995, Kochanek 1996). If we assume that M31 is 30% more massive than the Milky Way (Peebles 1989), the total mass of the Local Group is $M_{LG} = 3.3 \pm 1.6 \times 10^{12}$ M$_{\odot}$; the zero-velocity surface is about 1.8 Mpc from the Local Group barycenter (Sandage 1986a).

A simple variant of this approach that I use here recognizes that for a bound system traveling at velocity v along a radial orbit, the enclosed mass is $M_{enc} \leq v^2 R/G$ for a distance R from the barycenter. For radial orbits, heliocentric velocities can be used to estimate the mass of the Local Group for each dwarf galaxy with or without corrections for the Sun's offset from the Local Group barycenter. Galaxies that imply large values of M_{enc} are probably not bound to the Local Group and are well into the Hubble flow. Using the radial velocities compiled in Table 2, I have calculated M_{enc} for all Local Group dwarf-galaxy candidates in Table 1. Karachentsev (1996) developed a related method that employs estimates of both the energy and orbital time scales of individual dwarfs to establish membership.

The results of this analysis are shown in Figure 1. Following Yahil et al (1977), I plot the heliocentric velocity, $V_{\odot}$, vs cos λ for individual Local Group candidates, where λ is the angle between the galaxy and the apex of the solar motion relative to the Local Group barycenter. The two panels correspond to the solar-motion solutions of Sandage (1986a) and Karachentsev & Makharov (1996; their equation 4). For the most distant galaxies, the correction from heliocentric to barycentric velocity is small. Galaxies for which M_{enc} exceeds the observed Local Group mass are denoted as *open squares*. For both solar-motion solutions, NGC 55—usually considered a member of the Sculptor Group—is consistent with Local Group membership, as are NGC 3109 and the other galaxies near it (see Section 2.3). EGB 0427+63 and GR 8 are marginal Local Group members; both galaxies imply M_{enc} is slightly larger than the adopted Local Group mass.

Of course, galaxies with large tangential velocities might still be unbound even if their radial velocities relative to the Local Group barycenter are low (Dunn & Laflamme 1993). Proper motions have now been measured (impressively) for some Milky Way satellites: Sculptor (Schweitzer et al 1995), Ursa Minor (AE Schweitzer, KM Cudworth, SR Majewski, in preparation), the Large Magellanic Cloud (LMC) (Jones et al 1994), and Sagittarius (Ibata et al 1997).

We can expect to measure the tangential motions of other Local Group galaxies out to ~1 Mpc over four- to five-year baselines using HST. For now it is probably not possible to unambiguously determine membership for galaxies near the outer fringe of the Local Group armed with only radial velocities and distances. This is further complicated by the effects that nearby groups must have had on the orbits of galaxies in the outer Local Group (Sandage 1986a, Peebles 1989, 1995).

2.2   *What's Missing?*

van den Bergh (1995) suggests that about 98% of the luminous mass of the Local Group has already been identified. But have we identified all of the individual galaxies? Since 50% of the members listed in Table 2 have been found since 1971, the era of discovery within the Local Group probably is not yet over. If we assume that the Local Group galaxy distribution is uniform on the sky (though see Section 2.3), the cumulative number of galaxies should increase from the Galactic poles as $1 - \sin |b|$, where b is Galactic latitude. Figure 2 shows the cumulative number of all Local Group members (*top panel*) and MW satellites (*bottom panel*) as a function of $1 - \sin |b|$. For comparison, the *dotted lines* show how a uniformly distributed sample would appear in these diagrams. Note that in both samples, the observed number of galaxies exceeds the predicted distribution at high galactic latitude (small values of $1 - \sin |b|$). This suggests that many Local Group galaxies remain to be found at low latitudes. If I extrapolate from the observed number of galaxies at the fiftieth and sixty-seventh percentile values of $1 - \sin |b|$ (the *vertical lines* in Figure 2), as many as 15–20 more Local Group galaxies may be hidden at low latitudes, up to half of which may be satellites of the Milky Way. Using the technique of Yahil et al (1977), Grebel (1997) has identified three to four additional Local Group candidates from the catalog of Schmidt & Boller (1992); none of these have even preliminary distance estimates yet. Karachentseva & Karachentsev (1998) have compiled a list of nearby dwarfs that contain additional candidate Local Group members (also see Karachentsev & Makarov 1998).

The recent discoveries of Sextans (Irwin et al 1990) and Sagittarius (Ibata et al 1994) illustrate that nearby galaxies can also hide if they are too diffuse. Caldwell et al (1998) recently found a low–surface brightness, but relatively luminous, dwarf in the M81 group with $\Sigma_{0,V} = 25.4$ mag arcsec^{-2} and $M_V = -14.3$. If this galaxy—which has a core radius of 1.6 kpc—were located 1 Mpc from us, it would contribute 22 stars arcmin^{-2} brighter than I $= 22$ (corresponding to the more luminous giants), or only 0.8 stars arcmin^{-2} brighter than I $= 18.5$ if located 200 kpc away. The apparent core radius would be 5.4 and 27 arcmin, respectively. An object like this would be difficult to identify even at intermediate Galactic latitude (Irwin 1994), though methods
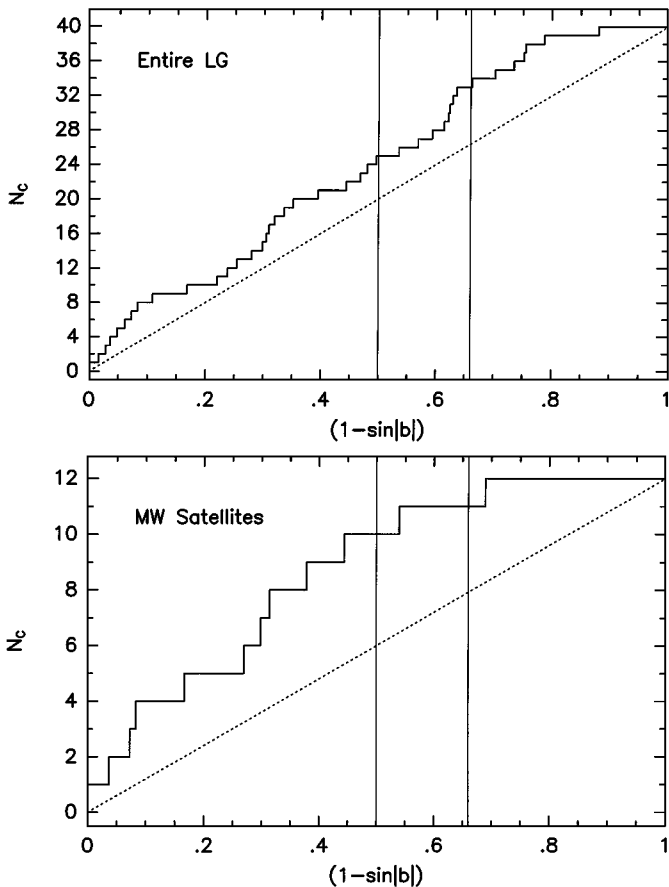
Figure 2   Plots of the cumulative distribution of all Local Group galaxies (*upper plot*) and of the galaxies in the MW subgroup (*lower plot*) as a function of $(1 - \sin|b|)$, where b is Galactic latitude. The *dotted lines* show the expected distribution of a uniform sample of 40 and 12 objects. The *vertical lines* show where 50% (*left*) and 67% (*right*) of a uniform cumulative distribution would be found. For example, based on the fiftieth percentile value of $N_c = 10$ in the *lower panel*, a total of 20 MW satellites would be expected if they were uniformly distributed and if there was no gradient in Galactic extinction as a function of latitude.

designed to find stars far from the centers of known dwarfs might succeed (e.g. Gould et al 1992, Mateo et al 1996, Kuhn et al 1996, Siegel et al 1998).

Henning (1997) summarizes prospects for finding "hidden" galaxies from HI observations at low latitudes. Although the Galaxy is transparent at 21 cm, confusion with Galactic emission at low velocities would present a major obstacle to finding Local Group galaxies in this manner. Of course, only gas-rich objects would be found, effectively ruling out detection of gas-poor early-type dwarfs at low latitudes. Ongoing IR surveys such as DENIS (Epchtein et al 1997) and 2MASS (Kirkpatrick et al 1997) may successfully penetrate much of the foreground dust in some regions of the Galactic Plane. Although the stellar density of Galactic field stars would be quite high, the signature of a nearby dwarf galaxy might be possible to detect as a concentrated excess of faint stars at low latitudes.

2.3   *The Structure of the Local Group*

Because they are so numerous, the Local Group dwarfs can be used effectively as tracers of substructure. Gurzadyan et al (1993) and Karachentsev (1996) have previously carried out substructure analyses of the Local Group; both found the well-known concentration of galaxies towards M31 and the Milky Way (see also van den Bergh 1995 and Grebel 1997). A powerful—but more subjective—way to visualize local substructure is via stereoscopic images of the distribution of Local Group galaxies. Three stereo views are shown in Figure 3*a*, corresponding to observers located well outside the Local Group along the orthogonal axes $(l, b) = (0°, 0°)$, $(90°, 0°)$, and $b = +90°$, centered on the Galactic Center. Figure 3*b* identifies some of the more distant individual galaxies for each of three viewing positions of Figure 3*a*.

Four subgroups are evident in Figure 3. The prominent group located near the center is the Milky Way and its satellites (the origin of the coordinate system is the center of our Galaxy). The second surrounds M31. The third forms an extended "cloud" populated only by dwarfs, mostly dIrr systems. This "Local Group Cloud" is best seen in the *middle panel* of Figure 3*a*. The fourth subgroup is relatively isolated and contains NGC 3109 as its most luminous member. The individual members of these four subgroups are identified in Table 1. Remarkably few galaxies have ambiguous subgroup assignments: IC 1613 and Phoenix could both be plausibly placed in the MW or M31 subgroups; Leo A's new distance (Tolstoy 1998) places it in an isolated location between the MW and N3109 subgroups. Only GR 8—a marginal Local Group member—cannot be clearly assigned to any of these four subgroups.

It is interesting that the N3109 subgroup "points" toward the nearby Maffei/ IC 342 group (Karachentsev et al 1996), while the Local Group Cloud very

roughly points toward the Sculptor group (Côté et al 1997). NGC 55 is located on the far side of the Local Group Cloud, closest to the Sculptor group. Perhaps the substructure of the Local Group reflects a dynamical history in which the Maffei and Sculptor groups have had an important role and have "stretched out" the Local Group in these directions (Byrd et al 1994). Alternatively, this may reflect a false excess of candidates in these directions where the surface densities of galaxies just beyond the Local Group are relatively high. NGC55 in particular may be an example of this effect.

3.   OPTICAL PHOTOMETRIC AND STRUCTURAL PROPERTIES OF LOCAL GROUP DWARFS

Measurement of the integrated photometric and structural properties of Local Group dwarfs is challenging. Because they are so close, many Local Group dwarfs are quite extended, ranging from under 10 arcmin in diameter to over $40°$. Few telescope/detector combinations can survey the entire extent of the larger systems in one or even several exposures (though see Kent 1987, Bothun & Thompson 1988). Nearly all Local Group dwarfs have very low surface brightnesses, which not only makes it difficult to discover these galaxies but greatly complicates obtaining reliable follow-up photometry. Nonetheless, there have been many attempts over the past 35 years to study the integrated properties and structural parameters of Local Group dwarfs. Hodge, de Vaucouleurs, and Ables pioneered these studies, and in many cases their results remain the only ones available (e.g. Hodge 1963a,b, 1973; deVaucouleurs & Ables 1965, 1968, 1970; Ables 1971; Ables & Ables 1977).

⟶

Figure 3   Stereoscopic views of the Local Group based on the data in Tables 1 and 2. From *top* to *bottom*, these views are from $(l, b) = (0°, 0°)$, $(90°, 0°)$ and the NGP, respectively. The directions of the principle orthogonal axes in the plane of the paper are indicated on the *top* and *right edges* of each stereoscopic pair. The "viewer" is located 2.6 Mpc from the center of the Milky Way, which is represented by the *large cross closest to the center of each panel*; the *other large cross* represents M31; and the *small cross* is M33. *Open squares* represent the dSph and E galaxies (see Table 1 for galaxy types); *closed squares* are Irr galaxies; *small xs* are transition systems (denoted dIrr/dSph in Table 1). To produce the stereo effect, the viewer's "eyes" were set about 250 kpc apart.

The MW, M31, and NGC 3109 subgroups are easily seen in all three stereo pairs; the Local Group Cloud is best appreciated in the middle pair but is also evident as a distinct structure in the other two panels. Only GR 8 (and possibly Leo A) is unattached to any subgroup; this is best seen in the *lower panel* where the galaxy is particularly near the observer. The *set of three single panels on the opposite page* serve to aid identification of individual galaxies in the stereo pairs. The galaxies closest to M31 and the Milky Way have not been labeled to avoid excessive clutter in the diagram. Because of the strong perspective effects required to make a stereo pair, none of the panels represents orthogonal projections of the galaxy positions onto the various planes.
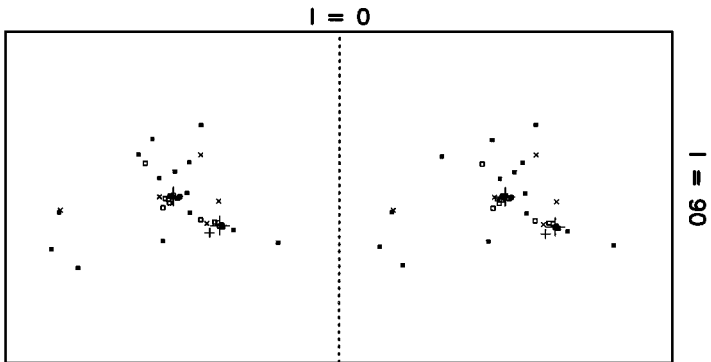
(a)

b = 90

View from (l,b) = (0,0)

l = 90

b = 90

View from (l,b) = (90,0)

l = 0

l = 0
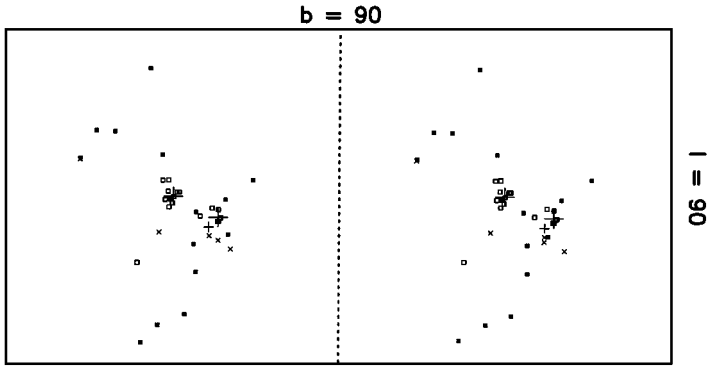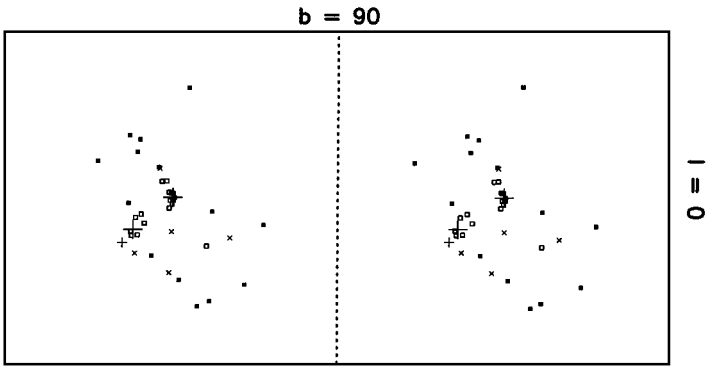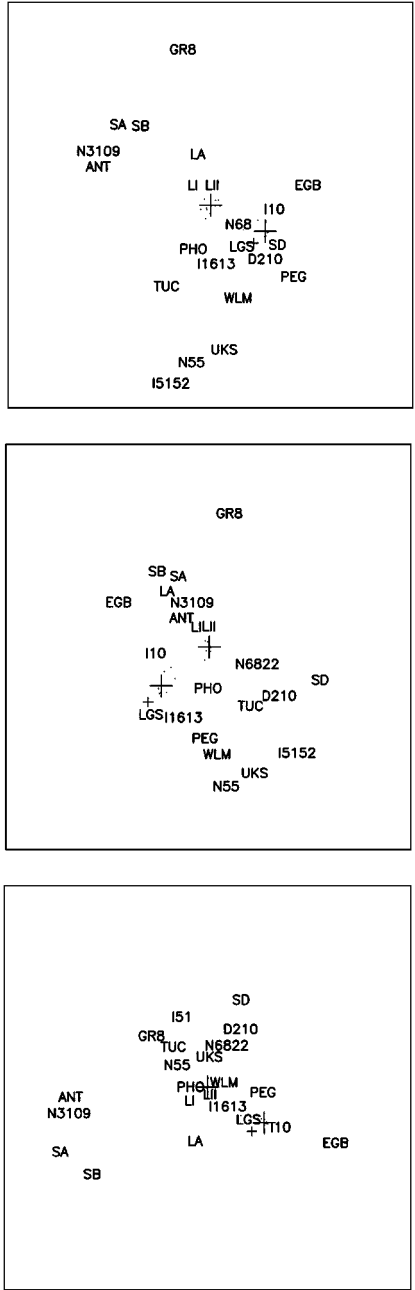
View from NGP (b = 90)

l = 90

(b)

Figure 3 (*Continued*)

3.1   *Integrated Photometry*

Table 3 lists the integrated V-band magnitudes and, when available, the integrated colors of Local Group dwarfs. In some cases, these values are based on observations of only a small fraction of the galaxy. For example, less than 1% of the surface area of Sagittarius has been measured photometrically (Mateo et al 1995c, 1996; Fahlman et al 1996), though a large fraction has been mapped photographically (Ibata et al 1997). Combined with the distance and reddening values in Table 2, the photometry in Table 3 can be used to derive integrated absolute magnitudes and luminosities (Table 4) and the luminosity function (LF) of the Local Group (Figure 4). For $M_B \lesssim -14$, the Local Group LF matches that of the "poor" groups studied by Ferguson & Sandage (1991). The best-fitting Schechter (1976) LF for the poor groups of Ferguson & Sandage (1991) is also shown. Note that the analytic expression, if extrapolated as in Figure 4, implies that the Local Group contains many galaxies less luminous than $M_B \sim -12$ that have yet to be discovered.

Figure 5 is the color-magnitude diagram of the Local Group based on the integrated V-band absolute magnitudes (M_{V_0}) and $(B - V)_0$ colors. The giant/dIrr galaxies are segregated from the early-type galaxies (denoted as a *dotted line* in Figure 5). EGB 0427+63 is the only dIrr that lies redward of this boundary, but its photometric properties and reddening are poorly known (Karachentseva et al 1996). The transition galaxies—so named in Table 1 solely on the basis of their morphological properties—are located close to but on both sides of the dIrr–early-type dividing line. NGC 205 is a luminous dSph system that contains a bright central region of recent star formation and has a luminous blue nucleus (Hodge 1973, Price 1985); it is located on the dIrr side of the dividing line in Figure 5. The smaller region of young stars in NGC 185 (Hodge 1963b) has a negligible effect on that galaxy's integrated colors (Price 1985).

3.2   *Structural Properties*

In the optical, the structure of Local Group dIrr galaxies is dominated by star-forming complexes and OB associations with typical diameters of 200–300 pc (Fisher & Tully 1979, Hodge et al 1991a,b; see the "Images" references in Table 1). These clumps are usually not found near the optical center of symmetry of the galaxies. NGC 3109—one of the most luminous dIrr galaxies in the sample—shows clear evidence for spiral structure underlying a patchy morphology (Demers et al 1985, Sandage & Carlson 1988). In all suitably studied Local Group dIrr systems, the clumpy young stellar populations are superimposed on a more extended, smoother, and symmetric distribution of older stars (Hodge et al 1991a,b; Minniti & Zijlstra 1996). Either dynamical effects smooth out the structures with time, or else the star-formation regions migrate through individual galaxies, eventually forming a more symmetric sheet of old stars (Skillman & Bender 1995, Hunter & Plummer 1996, Dohm-Palmer et al 1997).

Table 3 Integrated photometric properties and structural parameters of Local Group dwarf galaxies

Galaxy name	V_T^a (mag)	$(B-V)_T^b$ (mag)	Other colors[c] [mag (bands)]	Σ_0^d [mag (arcsec^{-2})]	r^e (arcmin)	R^f (arcmin)	Major-axis position angle[g] (deg)	e^h	r_{exp}^i (arcmin)	Ref[j]
WLM	10.42±0.2	0.62±0.12	−0.21 [1]	20.36±0.05	2.2	5.5	175±5	0.59±0.04	3.3±0.2	57, 61
NGC 55	7.95±0.15	0.50±0.04	0.87 [3]; 0.77 [4]; 0.42 [5]; −0.05±0.2 [6]	20.8±0.5	4.6	20.2	105±5	0.77	3.4±0.2	1, 2, 4, 60, 73
IC 10	11.55±0.3	1.37	0.28 [1]	22.1±0.4	—	5.0±2.0	140±20	0.3±0.1	1.9±0.3	1, 67, 70, 71, 75
NGC 147	9.35±0.15	0.92±0.07	0.55 [2]; 1.12 [3]	21.6±0.2	1.1	20	34±4	0.46±0.03	2.1±0.3	1, 5–8, 11, 82
And III	14.21±0.15	—	—	24.49±0.05	1.27±0.17	6.2±1.0	135±5	0.6	0.75±0.01	5, 8
NGC 185	9.09±0.15	0.96±0.06	0.30±0.05 [1]; 0.60 [2]; 1.25 [3]; 2.06 [6]	20.1±0.4	1.0±0.3	16±2	41±5	0.26	1.7±0.3	1, 5, 6, 8–11, 74, 82
NGC 205[k,l]	8.05±0.15	0.70±0.10	0.34 [1]; 0.52 [2]; 1.23 [3]; 3.08 [5]	20.4±0.4	1.5±0.5	6.2±2.0	165±5	0.46±0.03	1.7	1, 5, 6, 8, 63–65, 79, 82
M32[l,m]	8.10±0.15	0.99±0.05	0.64 [1]; 0.42 [2]; 1.07 [3]; 3.06 [5]; 0.64 [6]; 0.85 [7]	<11.6	—	9±2	165±5	0.18±0.03	—	1, 6, 12–14, 65, 76
And I	12.75±0.2	0.75±0.06	0.29 [1]	24.37±0.01	1.58±0.08	13.4±1.4	—	0.0	1.46±0.06	1, 5, 47
Sculptor	8.5±0.3	—	—	23.7±0.4	5.8±1.6	76.5±5.0	99±1	0.32±0.03	6.7±0.2	5, 8, 20, 77
LGS 3	14.26±0.15	0.74±0.06	0.47 [2]; 1.00 [3]	24.7±0.2	0.82±0.05	14.5±4.5	175±5	0.26±0.06	0.78	16–18, 78
IC 1613	9.59±0.15	0.60±0.10	−0.25 [1]	22.8±0.3	3.3±1.0	11±3	83±6	0.24±0.06	5.4±3.0	48, 49, 75
And II	12.7±0.2	—	—	24.47±0.05	1.64±0.08	17.2±1.0	160±10	0.3	1.57±0.03	5, 8
Phoenix	13.2±0.2	0.61±0.05	−0.21 [1]	—	13.8±0.8	>8.6	160±10	0.3±0.1	10.2	1, 19
Fornax	7.6±0.3	0.63±0.05	0.08 [1]; 0.45 [2]; 1.02 [3]	23.4±0.3	13.8±0.8	71±4	48±6	0.31±0.03	10.2	5, 20–22, 24, 50
EGB 0427+63[n]	13.88±0.12	1.34±0.05	—	23.9±0.3	0.5	1.0	73±5	0.55±0.05	—	16, 72
Carina	10.85±0.25	—	—	25.5±0.4	8.8±1.2	28.8±3.6	65±5	0.33±0.05	5.5	5, 20, 26, 83
Leo A	12.8±0.2	0.15±0.2	−0.2±0.1 [1]	—	2.3	3.5	94±5	0.36	—	1, 2, 57, 59
Sextans B	11.43±0.15	0.48	−0.16 [1]	—	3.0	3.9	130±15	0.23	—	2, 42, 57, 58
NGC 3109	9.88±0.15	0.52	−0.12 [1]	23.6±0.2	2.8	13.3	92±1	0.80	3.1	1, 53, 84
Antlia[o]	14.8±0.2	—	0.5±0.1 [2]; 1.2±0.2 [3]	24.3±0.2	0.80±0.05	5.2±0.2	145±5	0.35±0.03	1.1, 0.3	28, 29
Leo I	10.1±0.3	0.8±0.2	0.15 [1]	22.4±0.3	3.3±0.3	12.6±1.5	79±3	0.21±0.03	1.8±0.2	5, 8, 20
Sextans A	11.30±0.15	0.38±0.07	−0.32 [1]	23.5±0.3	3.2	4.0	52±5	0.21	1.5±0.3	1, 2, 75

Sextans	10.3±0.3	—	—	26.2±0.5	16.6±1.2	160±50	56±5	0.35±0.05	12.3±3.0	5, 8, 20, 30
Leo II	12.0±0.2	0.65±0.15	—	24.0±0.3	2.9±0.6	8.7±0.9	12±10	0.13±0.05	1.5	1, 20, 32, 33
GR 8	14.40±0.15	0.37±0.05	−0.51[1]; 0.39[2]	22.3±0.2	*0.7*	*1.0*	47±7	0.31±0.04	0.24±0.02	1, 8, 35, 55–57
Ursa Minor	10.3±0.4	1.3±0.3	−0.1±0.3[1]	25.5±0.5	15.8±1.2	50.6±3.6	53±5	0.56±0.05	8.0±2.5	1, 5, 20, 42, 64
Draco	10.9±0.3	0.95±0.2	0.1±0.3[1]	25.3±0.5	9.0±0.7	28.3±2.4	82±1	0.29±0.01	4.5	20, 42
Sagittarius	4.0±0.5	—	—	25.4±0.3		>10°	120±10	0.80±0.15	—	38–40, 68, 69
SagDIG	13.5±0.4	0.4±0.2	—	24.4±0.3	*0.9*	*1.7*	90±10	0.47±0.10	—	41, 54
NGC 6822[n]	9.1±0.2	0.73±0.05	0.04±0.20[1]	21.4±0.2	2.5±1.0	40±10	10±5	0.47±0.03	2.4±0.4	1, 80–82
DDO 210	14.71±0.15	0.15	−0.18[1]; 1.11[4]	—	*0.9*	*1.6*	100±10	0.44	—	1, 2, 57, 58
IC 5152	11.2±0.2	0.34±0.1	−0.16[1]	—	*2.3*	*2.8*	95±10	0.18	—	1, 42, 62
Tucana	15.15±0.2	0.7±0.1	0.55[2]	25.05±0.06	0.70±0.10	3.7±1.2	97±2	0.48±0.03	0.49±0.08	43, 44
UKS2323−326	13.8±0.4	0.4±0.2	—	24.6±0.5	*1.1*	*1.2*	135±25	0.05±0.03	—	41, 54
Pegasus	12.04±0.15	0.61	0.06±0.06[1]	—	*2.3*	*3.9*	125±15	0.40	—	1, 2, 57, 58

a Integrated apparent V-band magnitude.

b Integrated B−V color.

c Other integrated colors. [1] = U−B; [2] = V−R; [3] = V−I; [4] = B−R; [5] = V−K; [6] = J−H; [7] = H−K.

d V-band central surface brightness; values in italics are B-band results.

e Roman type: core radius in arcmin; italic type: semi-minor axis dimension to the Holmberg limit of $\Sigma_{0,B}$ = 26.5 mag arcsec^{-2}.

f Roman type: tidal radius in arcmin; italic type: semi-major axis dimension to the Holmberg limit as for core radius.

g Major-axis position angle, with N = 0° and E = 90°.

h The ellipticity of the galaxy defined as e = (1 − b/a), where b = minor axis and a = major axis.

i The exponential scale length of the surface-brightness distribution, typically along the major axis.

j References: 1, Longo & de Vaucouleurs 1983; 2, de Vaucouleurs et al 1991; 3, deleted in proof; 4, Pierce & Tully 1992; 5, Caldwell et al 1992; 6, Kent 1987; 7, Hodge 1976; 8, de Vaucouleurs et al 1981; 9, Price 1985; 10, Hodge 1963b; 11, Buta & Williams 1995; 12, Lugger et al 1992; 13, Michard & Nieto 1991; 14, Silva & Elston 1994; 15, deleted in proof; 16, Karachentseva et al 1996; 17, Lee 1995a; 18, Schild 1980; 19, van de Rydt et al 1991; 20, Irwin & Hatzidimitriou 1995; 21, Hodge & Smith 1974; 22, de Vaucouleurs & Ables 1968; 23, deleted in proof; 24, Poulain & Nieto 1994; 26, Mateo et al 1993; 27, deleted in proof; 28, Aparicio et al 1997a; 29, Whiting et al 1997; 30, Mateo et al 1991a; 31, deleted in proof; 32, Hodge 1982; 33, Vogt et al 1995; 34, deleted in proof; 35, Hopp & Schulte-Ladbeck 1995; 36, deleted in proof; 37, deleted in proof; 38, Ibata et al 1994; 39, Mateo et al 1995c; 40, Ibata et al 1997; 41, Longmore et al 1982; 42, Longo & de Vaucouleurs 1985; 43, Saviane et al 1996; 44, Lavery & Mighell 1992; 45, deleted in proof; 46, deleted in proof; 47, Mould & Kristian 1990; 48, Hodge et al 1991a; 49, Hodge 1978; 50, Demers et al 1994b; 51, deleted in proof; 52, deleted in proof; 53, Carignan 1985; 54, Longmore et al 1978; 55, Carignan et al 1990; 56, de Vaucouleurs & Moss 1983; 57, Fisher & Tully 1975; 58, Fisher & Tully 1979; 59, Allsopp 1978; 60, Puche et al 1991; 61, Ables & Ables 1977; 62, Sérsic & Cerruti 1979; 63, Hodge 1973; 64, Lee 1996; 65, Peletier 1993; 67, de Vaucouleurs & Freeman 1972; 68, Mateo et al 1996; 69, Fahlman et al 1996; 70, Shostak 1974; 71, de Vaucouleurs & Ables 1965; 72, Hoessel et al 1988; 73, Fitzgibbons 1990; 74, Lee 1993; 75, Ables 1971; 76, Burstein et al 1987; 77, Hodge 1966; 78, Tikhonov & Makarova 1996; 79, Price & Grasdalen 1983; 80, Hodge 1977; 81, Hodge et al 1991b; 82, Kodaira et al 1990; 83, Demers et al 1983; 84, Jobin & Carignan 1990; 85, Hodge 1964.

k The major axis position angle varies significantly outward from the galaxy center.

l Σ_0 is determined from the extrapolation of the outer–surface-brightness profile to r = 0. For NGC 205, r_c is estimated from surface-brightness profile as the location where the central surface brightness drops a factor of two below the level listed in this table. Both M32 and NGC 205 exhibit composite–surface-brightness profiles; no single King model, exponential profile, or power-law profile can fit the observed profiles at all radii.

m The outer isophotes of M32 are not truncated according to Kent (1987).

n The position angle and e values refer to the inner bar structure.

o Aparicio et al (1997a) found that the radial–surface-brightness profile is best fit with two exponential components. The values of r_{exp} refer to the inner and outer components, respectively. The two exponential components meet at a radial distance of 40 arcsec from the center of the galaxy.

Table 4 Derived photometric and kinematic properties of Local Group dwarf galaxies

Galaxy name	M_V[a] (mag)	M_B[b] (mag)	L_V[c] ($10^6\,L_\odot$)	R_c[d] (pc)	ρ_0[e] ($M_\odot\,pc^{-3}$)	I_0[f] ($L_\odot\,pc^{-3}$)	Total mass[g] ($10^6\,M_\odot$)	$(M/L)_{0,V}$[h] (solar)	$(M/L)_{tot,V}$[i] (solar)	M_{HI}/M_{tot}[j]	M_{HI}/L_B[k] ($M_\odot\,L_\odot$)	(v_r/σ)[*l]
WLM[m,n]	−14.5	−13.9	50.2	710	(0.46)	0.19	150	—	3.0	0.40	1.2	(2.8)
NGC 55[m-o]	−18.0	−17.5	1290	875	(0.26)	0.10	15600	—	12	0.09	0.94	(10.8)
IC 10	−15.7	−15.2	160	475	0.047	0.63	1580	0.1	9.9	0.10	0.86	5.8
NGC 147	−15.5	−14.8	131	170	2.8	0.39	110	7.1	0.8	<0.001	<0.001	0.32
And III[m]	−10.3	−9.7	1.13	180	(0.044)	0.018	—	—	—	—	<0.07	—
NGC 185	−15.5	−14.7	125	155	4.3	1.76	130	2.5	1.0	0.001	0.001	0.08
NGC 205	−16.6	−16.0	366	260	5.1	0.43	740	12	2.0	0.001	0.001	0.04
M32[p]	−16.7	−15.8	383	635	1.0	786	2120	0.0	5.6	<0.001	<0.009	0.51
And I[n]	−11.9	−11.2	4.71	375	(0.023)	0.009	—	—	—	—	<0.02	—
Sculptor	−11.1	−10.4	2.15	110	0.60	0.055	6.4	11	3.0	0.004	0.01	—
LGS 3	−10.5	−9.9	1.33	160	0.37	0.018	13	21	9.7	0.03	0.33	—
IC 1613	−14.7	−14.2	63.6	585	0.035	0.025	795	1.4	12	0.07	0.81	4.3
And II[m]	−11.1	−10.5	2.35	205	(0.043)	0.017	—	—	—	—	—	—
Phoenix	−10.1	−9.5	0.90	310	0.14	—	33	—	37	0.006	0.21	—
Fornax	−13.2	−12.6	15.5	460	0.086	0.018	68	4.8	4.4	<0.001	<0.001	—
EGB 0427+63[m,n]	−12.6	−11.6	9.12	85	(0.33)	0.13	—	—	—	—	2.6	(3.7)
Carina	−9.3	−8.6	0.43	210	0.17	0.006	13	30	31	<0.001	<0.002	—
Leo A	−11.4	−11.3	3.03	185	0.20	—	11	—	3.5	0.72	1.6	1.1
Sextans B	−14.2	−13.8	40.7	445	0.27	0.018	885	—	22	0.05	0.96	2.1
NGC 3109	−15.7	−15.2	160	630	0.042	0.016	6550	2.4	41	0.11	3.8	6.8
Antlia	−10.8	−10.2	1.73	230	0.12	0.092	12	7.4	7.1	0.08	0.58	—
Leo I	−11.9	−11.1	4.79	215	0.28	0.011	22	3.1	4.6	<0.001	<0.007	—
Sextans A	−14.6	−14.2	55.7	700	0.022	0.002	395	2.0	7.1	0.20	1.1	4.1
Sextans	−9.5	−8.8	0.50	335	0.065	0.029	19	34	39	<0.001	<0.001	—
Leo II	−9.6	−9.0	0.58	160	0.29	0.20	9.7	10	17	<0.001	<0.02	—
GR 8	−11.6	−11.2	3.43	110	1.7	0.006	7.6	8.3	2.2	0.59	1.0	1.1
Ursa Minor	−8.9	−7.6	0.29	200	0.35	0.008	23	60	79	<0.002	<0.25	0.48
Draco	−8.8	−7.8	0.26	180	0.46	—	22	58	84	<0.001	<0.02	—
Sagittarius[r]	−13.4	−12.8	18.1	550	0.030	—	—	22	52	<0.001	<0.001	<0.18
SagDIG[q]	−12.3	−12.1	6.85	125	0.58	0.044	9.6	13	1.4	9.2	8.6	—
NGC 6822[m,n]	−15.2	−14.7	94.4	260	(0.97)	0.39	1640	—	17	0.08	1.2	(6.4)
DDO 210	−10.0	−9.9	0.81	95	0.84	—	5.4	—	6.7	0.35	1.4	—

	a	b	c	d		e		f	g	h	i
IC 5152[m]	-14.8	-14.5	70.3	390	0.000	—	400	—	5.7	0.15	0.64	(4.7)
Tucana[n]	-9.6	-8.9	0.55	130	(0.032)	0.013	—	—	—	—	<0.18	—
UKS2323-326[n]	-12.0	-11.7	5.25	150	(0.051)	0.020	—	—	—	—	0.90	—
Pegasus	-12.9	-12.3	12.0	280	0.16	—	58	—	4.8	0.09	0.44	1.7

[a] Integrated V-band absolute magnitude.

[b] Integrated B-band absolute magnitude.

[c] Visual luminosity in units of 10^6 $L_\odot$.

[d] "Core" radius in parsecs, corresponding to the observed core radius, r_c, when available, or $1.25 \times r_{exp}$ if r_c is not measured but the exponential scale length is measured (compare with Bender et al 1991; the average of r_c/r_{exp} for the 18 galaxies in Table 3 with both radii is 1.27 ± 0.12), or $a/3$ if neither r_c nor r_{exp} is available, where a is the observed Holmberg semi-major axis as defined in Table 3.

[e] The central mass density in $M_\odot$ pc^{-3}, here approximated as $\rho_0 = 166\sigma_0^2/R_c$, where σ_0 is the central velocity dispersion in km s^{-1} and R_c is in parsecs; this is computed only for systems that are pressure supported (see Mateo et al 1991b for details). For rotating LG dwarfs, the central mass density is dominated by the visible material and has been approximated as $2.5I_0$, where I_0 is defined in footnote f (also see footnote n).

[f] The central luminosity density in $L_\odot$ pc^{-3}, taken as $I_0 = S_0/2 r_c$, where S_0 is the central surface brightness expressed in units of $L_\odot$ pc^{-2}, and r_c is in pc (see Mateo et al 1991b for details).

[g] The total mass; if a central velocity dispersion is known and exceeds the rotational velocity, then total mass $M_{tot} = 167\beta R_c\sigma_0^2$, where β is a scaling factor for King profiles taken here to be 8.0, appropriate for low-concentration King models. If $v_{rot} > \sigma_0$, then $M_{tot} = R_{rot}v_{rot}^2/G$, where v_{rot} is the rotational velocity—corrected for the galaxy inclination—at the projected distance R_{rot} from the Galaxy center.

[h] The central V-band mass-to-light ratio, defined as ρ_0/I_0, in solar units.

[i] The integrated V-band mass-to-light ratio defined as M_{tot}/L_V, in solar units.

[j] The ratio of integrated HI mass to the total mass, M_{tot} (see footnote g).

[k] The ratio of the integrated HI mass to the blue luminosity, in solar B-band units.

[l] The parameter $(v_{rot}/\sigma)^*$ is simply (v_{rot}/σ_0) for dIrr systems or $(v_{rot}/\sigma_0)(e/(1 - e))^{-1/2}$, where e is the ellipticity, for ellipsoidal systems (Bender et al 1991). See footnote m for details about values in parentheses.

[m] The interstellar medium (ISM) velocity dispersion of these galaxies is assumed to be 8 km s^{-1} (see Table 7).

[n] The central mass density has not been determined kinematically for these galaxies. Instead, we assume $\rho_0 = 2.5I_0$.

[o] The results given here for NGC 55 are especially uncertain because of internal reddening that affects the inferred total luminosity and central luminosity density. See Puche et al (1991) for a complete discussion and for more precise estimates of the luminosity and mass of this galaxy. Note that these authors assumed a distance of 1.6 Mpc for NGC 55, in contrast to the distance of 1.48 ± 0.15 Mpc used here (Table 2).

[p] Owing to the possible presence of a massive central black hole, the nuclear kinematics are too complex for the simple analysis used here. See Kormendy & Richstone (1995) for details.

[q] $M_{HI}/M_{tot} \gtrsim 1.0$. This indicates an error in the distance ($M_{HI}/M_{tot} \propto D$, where D is the distance), a misinterpretation of or error in the kinematic data, an error in the HI flux measurement, or some combination of these.

[r] Sagittarius probably violates the assumption of equilibrium that is implicitly adopted in the analysis used here and its structural parameters remain highly uncertain. The mass and M/L ratios given here are taken directly from Ibata et al (1997). R_c and ρ_0 are also taken from this source.
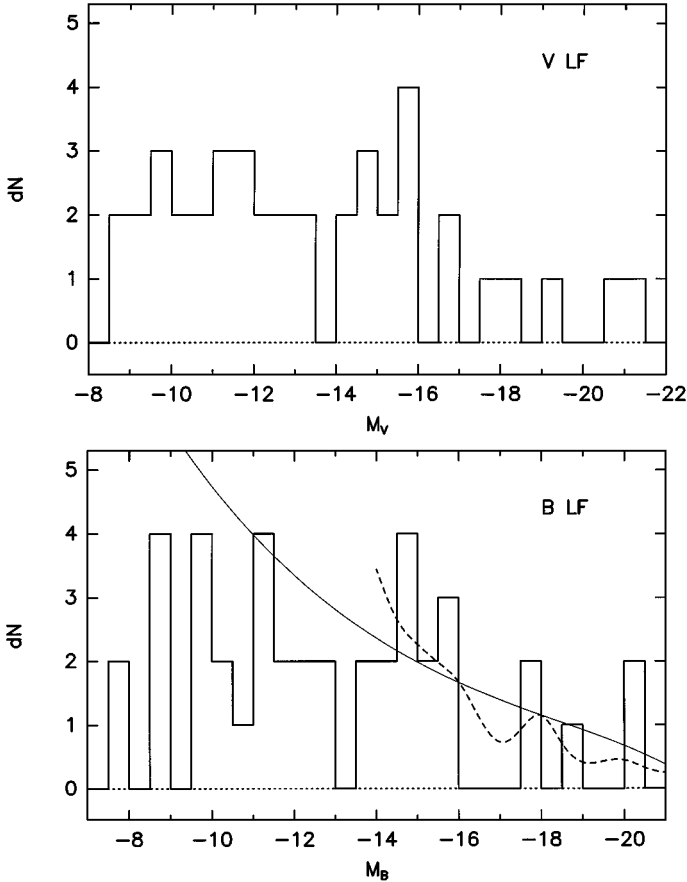
Figure 4 The differential luminosity function of galaxies in the Local Group based on the data in Table 4. The *upper* and *lower panels* show the V- and B-band luminosity functions (LFs), respectively. The *lower panel* also shows a best-fitting Schechter (1976) function ($\alpha = -1.16$, $M_{*,B} = -21.42$) and the empirical LF that Ferguson & Sandage (1991) derived for their sample of "poor" groups. Both LFs are scaled to match approximately the cumulative galaxy counts for $M_B \lesssim -14$.

The early-type dwarfs of the Local Group are dominated by a symmetric spheroidal component (Hodge 1971, Irwin & Hatzidimitriou 1995), with occasional instances of superimposed concentrations of relatively young stars (NGC 185 and NGC 205: Hodge 1963b, 1973; Price & Grasdalen 1983; Price 1985; Lee et al 1993b). Of interest, the star-forming regions in NGC 185 and NGC 205 are similar in size to those seen in dIrr galaxies, but these young stars are found near, though slightly offset from, the centers of the galaxies.
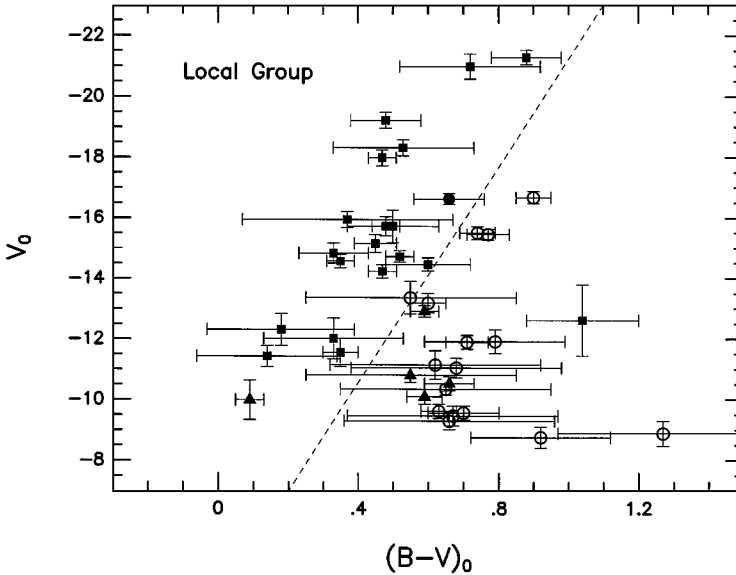
Figure 5   The M_{V_0}-$(B-V)_0$ color-magnitude diagram of Local Group galaxies based on the data from Tables 2 and 3. The *diagonal dashed line* separates galaxies classified as Spirals, or Irregular systems (*filled squares*; Table 1), and dSph or Elliptical systems (*open circles*). Five "transition" objects, Antlia, LGS 3, Phoenix, Pegasus, and DDO 210, are plotted as *filled triangles*; NGC 205 is plotted as a *filled circle*.

Demers et al (1994b, 1995) carefully searched for substructure in a number of dSph systems but found weak evidence for such structure only in Ursa Minor (Olszewski & Aaronson 1985).

Only three Local Group dwarfs contain nuclei: NGC 205, Sagittarius, and M32. The latter is now widely believed to contain a massive central black hole (Kormendy & Richstone 1995). The nucleus of NGC 205 is extremely blue (Price & Grasdalen 1983, Lee 1996), dynamically colder than the surrounding galaxy envelope (Carter & Sadler 1990), and has a spectrum dominated by young stars (Bica et al 1990, Jones et al 1996). The existence of a nucleus of Sagittarius—the globular cluster M54—is somewhat controversial. Da Costa & Armandroff (1995) argued that the velocity dispersion and metallicity of M54 are incompatible with its identification as a normal dSph nucleus. However, M54 is the second most luminous globular cluster in the entire Milky Way, nearly as luminous as the nucleus of NGC 205 (Peterson 1993); exhibits an internal abundance dispersion (Sarajedini & Layden 1995); and is located close to the center of symmetry of Sagittarius (Ibata et al 1994, 1997). Such an unusual object seems unlikely to have been merely an isolated globular cluster in a dSph galaxy such as Sagittarius.

The observed structural parameters of Local Group dwarfs are listed in Table 3, including ellipticity, major-axis position angle, King core and tidal radii, Holmberg radii, and exponential scale lengths. The corresponding derived structural parameters are listed in Table 4. Historically, the surface-brightness profiles for the dIrr galaxies are fit with exponential profiles, whereas for early-type systems, King profiles are preferred. Many authors have noted that both profiles produce acceptable fits to the red populations of dIrr and dSph systems (Eskridge 1988a,c; Hodge et al 1991a,b; Irwin & Hatzidim-itriou 1995). Aparicio et al (1997a) found that the best fit to the surface-brightness profile of Antlia requires two exponential profiles (Table 3). Sérsic (1968) profiles may be better suited to describing these varied types of surface-brightness profiles with only a single additional parameter (Prugniel & Simien 1997). Sagittarius and NGC 205 show highly elongated or otherwise disturbed outer structures, indicative of strong interactions with the Milky Way and M31, respectively. All galaxies with exponential scale lengths >500 pc are dIrr systems, while 90% with smaller scale lengths are early-type systems (James 1991).

4.   THE INTERSTELLAR MEDIUM OF LOCAL GROUP DWARFS

Some aspects of the relationship of the stellar populations and the interstellar medium (ISM) in Local Group dwarfs are acutely puzzling. This partly reflects the great detail with which we can now study the ISM in these nearby systems, but it also reflects some fundamental deficiencies in our understanding of dwarf galaxy evolution. In this section, I discuss the basic properties of the ISM in Local Group dwarfs and comment on some of these puzzles. The chemical and kinematic properties of the ISM are discussed in Sections 7 and 8, respectively. Good reviews on the ISM in Local Group dwarfs have been written by Wilson (1994a), Kennicutt (1994), and Skillman (1998); a more general review of the ISM in dwarf galaxies can be found by Brinks & Taylor (1994).

4.1   *HI Content and Distribution*

DIRR GALAXIES   Single-dish and aperture-synthesis radio observations provide total fluxes (see Table 5) and detailed HI maps of many of the dwarfs in the Local Group. Many HI properties show a clear progression from dIrr to dSph galaxies. For example, Table 4 shows that the ratios of HI to total masses of dIrr galaxies range from about 7% to over 50% (SagDIG is anomalous), which is consistent with expectations from standard closed chemical-enrichment models of galaxies with low mean abundances (see Section 7). Four of the five transition galaxies (denoted dIrr/dSph in Table 1) have HI-to–total mass ratios

between 1 and 10%. The exception, DDO 210, has a particularly uncertain distance (Table 2). The Local Group dSph galaxies are all comparatively devoid of neutral hydrogen; the few with detectable emission contain $\lesssim$0.1% of their mass in the form of interstellar neutral hydrogen.

The spatial distribution of HI emission in most Local Group dIrr galaxies is clumpy on scales of 100–300 pc scales (Shostak & Skillman 1989, Carignan et al 1990, Hodge et al 1991a,b, Lo et al 1993, Young & Lo 1996a, 1997b). Diffuse HI emission is inferred for many galaxies from the large differences in integrated flux from single-dish and synthesis observations. Only the most luminous systems—NGC 3109 and NGC 55—have comparatively smooth HI distributions (Jobin & Carignan 1990, Puche et al 1991).

The peak emission of individual HI clouds is generally found near regions of optically active star formation, but the clouds are often offset by 50–200 pc from the locations of the nearest star-forming complexes (Gottesman & Weliachew 1977; Hodge et al 1990, 1991a,b, 1994; Hodge & Lee 1990). Skillman et al (1988) and Saitō et al (1992), among others, have suggested that star formation requires a minimum HI column density of about $N(\mathrm{HI}) \sim 10^{21}$ cm^{-2} to proceed. However, for some galaxies, the peak HI surface density exceeds this limit and yet there is no current or recent star formation (Shostak & Skillman 1989, Young & Lo 1997b). It seems that a trigger is needed to initiate star formation in these cases. There are also counter-examples—mostly in dSph or transition galaxies—where recent or ongoing star formation is apparent, yet $N(\mathrm{HI}) < 10^{20}$ cm^{-2} (Hodge et al 1991a,b, Lo et al 1993, Young & Lo 1997a,b).

On the largest scales, the HI emission is generally centered on the optical centroids of Local Group dIrr galaxies even systems with complex HI morphology (e.g. Lo et al 1993, Young & Lo 1996a, 1997b; see also Puche & Westpfahl 1994 for examples beyond the Local Group). Transition galaxies are more complicated: The neutral hydrogen in LGS 3 is centered on the optical galaxy, while in Phoenix the HI—if it is in fact associated with the galaxy—is distinctly offset from the optical light (Young & Lo 1997b). In most Local Group dIrr galaxies, the neutral gas is more extended than the optical emission (Hewitt et al 1983, Lake & Skillman 1989, Young & Lo 1996a, 1997b). However, for the two most luminous dIrr systems in the sample (NGC 55 and NGC 3109; Table 4), the surface-brightness profile scale lengths and shapes are similar for the HI emission and optical light (Jobin & Carignan 1990, Puche et al 1991).

Young & Lo (1996, 1997b) have found evidence that the atomic component of the ISM in Leo A has two distinct phases. The warm component has a velocity dispersion of 9 km s^{-1} and pervades much of the galaxy, while the cooler component ($\sigma \sim 3$ km s^{-1}) is found principally near optical HII regions and contributes 10–20% of the total HI flux. Remarkably, though, Leo A is 400 times fainter than the LMC, both exhibit this two-phase HI structure. The HI gas

Table 5 Integrated and derived properties of the interstellar medium of Local Group dwarf galaxies

Galaxy name	$S(\text{HI})$[a] (Jy km s^{-1})	$M(\text{HI})$[b] ($10^6\,M_\odot$)	Ref[c]	$S(\text{CO})$[d] (Jy km s^{-1})	M_{mol}[e] ($10^6\,M_\odot$)	Ref[f]	$\log(F_\alpha)$[g]	Star-formation rate[h] ($M_\odot$ year^{-1})	Ref[i]	f_{60}[j] (mJy)	f_{100}[k] (mJy)	$M_d(\text{FIR})$[l] ($10^2\,M_\odot$)	Dust[m]	Ref[n]
WLM	300±25	61±6	1	<70	<1900	80	6.38	0.003	2, 3	320	1,040	4.7±0.3	Yes?	13, 64
NGC 55	2,680±200	1,390±224	1, 4	43±8	99±23	5, 6	7.85	0.18	7, 8	77,000	174,090	1,050±150	Yes	13, 76
IC 10	950±140	153±35	1	80±25	57±20	9, 80	8.11	(0.71)	2, 10	31,230	71,250	136±12	Yes	13–51, 81
NGC 147	<0.04	<0.005	1, 11, 82	—	—	—	—	—	—	<56	<160	0.34±0.03	No	11, 12
And III	<0.6	<0.08	1, 14	—	—	—	—	—	—	—	—	—	—	—
NGC 185[p]	1.4±0.2	0.13±0.02	1, 11, 82	69±15	28±6	11, 15–17, 84	4.47	0.0	11	440	1,720	5.0±0.3	Yes	12, 56
NGC 205	2.4±0.2	0.38±0.04	1, 11	62±17	43±12	11, 17, 18, 83	<1.88	0.0	11	570	3,130	33±2	Yes	12, 68–70
M 32	<17.8	<2.7	1	—	—	—	—	—	—	<40	<144	0.60±0.04	No	12, 19, 79
And I	<0.65	<0.1	1, 14	—	—	—	—	—	—	—	—	—	—	—
Sculptor[q]	17.3±1.5	0.026±0.003	20, 46	<2.8	<0.05	46	—	—	—	—	—	—	—	—
LGS 3[r]	2.7±0.1	0.42±0.05	14, 21, 22	28±5	19±4	23, 31	<2.10	0.0	2, 3	<75	<109	<0.1	—	13
IC 1613	480±40	54±11	58, 60	<3.0	<4.6	24, 80	6.73	0.003	2, 25, 26	1,420	3,690	6.3±0.4	Yes	12, 13, 63
And II	—	—	—	—	—	—	—	—	—	—	—	—	—	—
Phoenix (+55)[s]	2.0±0.4	0.08±0.02	21, 27	—	—	—	—	—	—	—	—	—	—	—
Phoenix (−23)[s]	2.6±0.1	0.11±0.01	21, 27	—	—	—	—	—	—	—	—	—	—	—
Fornax	<1.05	<0.005	1, 20	—	—	—	5.40	0.0004	3	<17	<86	0.0	—	12
EGB 0427+63	105±2	16±6	1	—	—	—	—	—	—	—	—	—	—	—
Carina	<0.29	<0.0007	29	<1.6	<2.4	31, 80, 85, 86	—	—	—	—	—	—	—	—
Leo A	68±3	80±8	1, 22	<1.6	<2.4	33, 80	4.77	0.0003	32	<90	<270	<6	—	13
Sextans B	106±10	45±6	1, 60	<70	<400	80	5.58	0.0008	2, 32	246	689	5.0±0.5	—	13
NGC3109	1,880±110	690±140	61, 62	<1.0	<4.9	33, 80	7.08	0.02	2, 33, 57	3,410	7,970	38±5	Yes	13, 52
Antlia[t]	2.7±0.5	0.97±0.19	34	—	—	—	—	—	—	—	—	—	Yes?	—
Leo I	<2.1	<0.03	1, 20	—	—	—	—	—	—	<33	<72	0.0	No?	12, 66
Sextans A	160±20	78±13	1, 35	<4.1	<27	24, 80, 85	5.98	0.002	2, 36, 78	503	849	3.0±0.3	—	13
Sextans	<0.08	<0.0001	46	—	—	—	—	—	—	—	—	—	—	—
Leo II	<1.05	<0.01	1, 20	—	—	—	—	—	—	—	—	—	—	—
GR 8	8.4±0.6	4.5±1.4	22, 59, 60	<1.6	<12	24, 31, 67	5.47	0.0007	37	20	143	9.2±2.7	—	13
Ursa Minor	<42	<0.04	20	—	—	—	—	—	—	<27	<73	<0.1	—	12
Draco	<18	<0.003	20	—	—	—	—	—	—	—	—	—	—	—
Sagittarius[u]	<0.56	<0.0001	38	—	—	—	—	—	—	—	—	—	—	—
SagDIG	33±2	8.8±1.9	21, 22, 39	—	—	—	4.72	0.0001	32	<94	<204	<0.6	—	13
NGC6822[o]	2,370±150	134±18	1	91±17	23±5	24, 41, 42, 47	8.11	(0.06)	2, 43	47,630	95,420	52±4	Yes	13, 72–75

Galaxy	F(HI)	M_{HI}	HI ref	S(CO)	M_{CO}	log Hα	SFR	Hα ref	f_{60}	f_{100}	M_d	dust	IR ref
DDO210	12.8±1.4	1.9±0.8	1, 22	<2.0	<70	<4.0	<560	23, 31, 85	139	<449	<4.8	—	13
IC5152	98±8	59±11	1	<70	<560	—	—	80	2,461	6,861	69±12	—	13
Tucana[v]	<0.48	<0.09	45	—	—	—	—	—	—	—	—	—	—
UKS2323-326	15±3	6.2±2.6	1, 39	—	—	—	—	23, 31, 80, 85	<55	<531	—	—	13
Pegasus	25±2	5.4±0.6	22, 60	<2.1	<6.0	3.80	0.0	23, 31, 80, 85	2.77	—	<34	—	13

[a] Integrated 21-cm flux.

[b] Total HI Mass in solar units $M_{HI} = 2.36 \times 10^{11} F(HI) d^2$, where d is the galaxy distance in Mpc and F(HI) in Jy km s^{-1}.

[c] HI references: 1, Huchtmeier & Richter 1986; 2, Hunter et al 1993; 3, Hodge & Miller 1995; 4, Hummel et al 1986; 5, Israel et al 1995; 6, Dettmar & Heithausen 1989; 7, Hoopes et al 1996; 8, Ferguson et al 1996; 9, Wilson 1995; 10, Hodge & Lee 1990; 11, Young & Lo 1997a; 12, Knapp et al 1985; 13, Melisse & Israel 1994a,b; 14, Thuan & Martin 1979; 15, Sofue & Wakamatsu 1993; 16, Welch et al 1996; 17, Roberts et al 1991; 18, Sage & Wrobel 1989; 19, van Dokkum & Franx 1995; 20, Knapp & Franx 1991; 21, Young & Lo 1997b; 22, Lo et al 1993; 23, Young et al 1995; 24, Ohta et al 1993; 25, Hodge et al 1990; 26, Price et al 1990; 27, Carignan et al 1991; 28, deleted in proof; 29, Mould et al 1990; 30, deleted in proof; 31, Tacconi & Young 1987; 32, Strobel et al 1991; 33, Bresolin et al 1993; 34, Fouqué et al 1990; 35, Skillman et al 1988; 36, Hodge et al 1994; 37, Hodge et al 1989; 38, Koribalski et al 1994; 39, Longmore et al 1982; 40, deleted in proof; 41, Israel 1997; 42, Wilson 1994b; 43, Collier & Hodge 1994; 44, deleted in proof; 45, Oosterloo et al 1996; 46, Carignan et al 1998; 47, Wilson 1992b; 48, deleted in proof; 49, Ohta et al 1988; 50, de Vaucouleurs & Ables 1965; 51, Klein & Gräve 1986; 52, Davidge 1993; 53–55, deleted in proof; 56, Hodge 1963b; 57, Hodge 1969a; 58, Lake & Skillman 1989; 59, Carignan et al 1990; 60, Hoffman et al 1996; 61, Jobin & Carignan 1990; 62, Carignan 1985; 63, Hodge 1978; 64, Ables & Ables 1977; 65, Gottesman & Weliachew 1977; 66, Bowen et al 1997; 67, Verter & Hodge 1995; 68, Hodge 1973; 69, Price & Grasdalen 1983; 70, Lee 1996; 71, Hodge 1976; 72, Hodge et al 1991b; 73, Hodge 1977; 74, Wilson 1992a; 75, Gallart et al 1996b; 76, Fitzgibbons 1990; 77, Aparicio & Gallart 1995; 78, Aparicio & Rodríguez-Ulloa 1992; 79, Bendinelli et al 1992; 80, Rowan-Robinson et al 1980; 81, Yang & Skillman 1993; 82, Johnson & Gottesman 1983; 83, Young & Lo 1996b; 84, Wiklind & Rydbeck 1986; 85, Taylor, private communication 1988; 86, Young & Lo 1996a.

[d] The integrated CO flux, S(CO), in Jy km s^{-1}. If the CO intensity, I(CO), is given, I derived S(CO) from the relation $S(CO) = gI(CO)$, where I(CO) is in K km s^{-1}, and g is a factor (in Jy K^{-1}) that accounts for the beam response of a point source. I adopt g from Roberts et al (1991) or use $g = 14.2$ or 1.7 for SEST and the Nobemaya 50m, respectively. When necessary, I assume $S_{2-1}/S_{1-0} = 0.75$. Upper limits are 3σ values and assume a velocity dispersion of 12 km s^{-1} if necessary.

[e] Total molecular mass computed as $M_{CO} = 1.61 \times 10^4 d^2 I(CO)$ in solar units for d in Mpc (Roberts et al 1991, Wilson 1995).

[f] CO references; see footnote c.

[g] The base-10 logarithm of the integrated Hα flux in units of 10^{-18} ergs sec^{-1} cm^{-2}.

[h] The current star formation rate in $M_\odot$ year^{-1} as prescribed by Kennicutt (1983) using the extinction-corrected Hα fluxes.

[i] Hα references; see footnote c.

[j,k] The IRAS 60- and 100-μm integrated fluxes, respectively.

[l] The total mass of cool dust in solar units: $M_d = 0.00478 f_{100} d^2 [\exp(2.94 R^{0.4}) - 1]$, where $R = f_{100}/f_{60}$ and the distance d is in Mpc. If only the 100-μm fluxes are available, $M_d = 2.6 f_{100} d^2$. Fluxes are in mJy and d is in Mpc (Roberts et al 1991).

[m] A flag indicating whether there are optical indicators of dust in the galaxy either through detection of internal reddening or direct observation of opaque dust clouds.

[n] Far-infrared (IR) and dust references; see footnote c.

[o] Internal reddening is probably significant. The star-formation rate estimated from the Hα flux (along with most other photometric parameters) may be greatly underestimated.

[p] Young & Lo (1997a) argued that the Hα emission is unlikely to be related to star-formation processes but may instead arise from shock-excited gas in an old supernova remnant. Ho et al (1997) classified NGC 185 as a Seyfert 2!

[q] HI emission extended on a scale comparable to the beam size; the HI flux and mass may be significantly underestimated (Carignan et al 1998).

[r] The extended HI distribution is much larger than the beam sizes of the earliest observations; the largest reported HI flux is listed here.

[s] Young & Lo (1997b) reported two distinct HI clouds in the vicinity of Phoenix, one at $v_\odot = +55$, the other at $v_\odot = -23$. Results for each cloud are listed separately. The stellar velocity is not known.

[t] Aparicio et al (1997a) note a possible small HII region near the center of Antlia. This HII region is visible in the color photograph of Whiting et al (1997).

[u] HII observations obtained only in fields near the center of the galaxy.

[v] A nearby neutral-hydrogen cloud has F(HI) = 7.7 Jy km s^{-1} and $v_\odot = 130 \pm 2$ km s^{-1}. Oosterloo et al (1996) favor an association with the Magellanic Stream rather than Tuscana. Ho

in NGC 185 and NGC 205 also seems to exhibit the same two-phase structure, even though in these cases the HI is clearly in a nonequilibrium configuration and has a much lower column density (Young & Lo 1997a).

EARLY-TYPE DWARFS   Deep single-dish HI observations have failed to detect most of the early-type Local Group dwarfs (Knapp et al 1978, Mould et al 1990, Koribalski et al 1994, Oosterloo et al 1996). Knapp et al (1978) detected HI emission near Sculptor, but lacking a precise optical velocity for the galaxy, they tentatively concluded that it was not associated with the galaxy. HI emission has long been known to exist in NGC 185 and NGC 205, but no HI is detected in NGC 147 and M32 to similar limits (Johnson & Gottesman 1983, Huchtmeier & Richter 1986, Young & Lo 1997a; Table 5).

The unique case of Sculptor recently has been revisited by Carignan et al (1998), who found that the emission reported earlier (Knapp et al 1978) is probably associated with Sculptor (the optical velocity is now accurately known; Table 2). Figure 6 is a plot of the HI map and the optical image of Sculptor. The systemic optical and HI velocities agree to within their combined errors (Armandroff & Da Costa 1986, Queloz et al 1995), though there is a hint that the HI velocity may be larger. For NGC 185 and NGC 205, the HI emission is clearly offset spatially and kinematically from the optical counterparts (Young & Lo 1997a, Carignan et al 1998). As in dIrr systems, the HI emission in these two galaxies is also spatially offset from the young stars (Johnson & Gottesman 1983, Young & Lo 1997a).

Because the extent of Sculptor's HI emission is comparable to the beam size, the map in Figure 6 may be highly incomplete. The actual distribution could be a ring or some other more complex bimodal geometry (Puche & Westpfahl 1994, Young & Lo 1997b). What is certain, however, is that the flux received from the small central HI emission is much less than the flux from the extended component. Because past HI observations of dSph galaxies were centered on the optical image, they could conceivably have missed all of the emission from even a relatively strong extended component. It would be extremely interesting to reexamine the nearby dSph at 21 cm, taking particular care to search for extended HI structures.

4.2   *Dust and Molecular Gas*

Evidence of interstellar dust clouds is seen optically as compact absorption regions in some Local Group dIrr galaxies and near the cores of some dSph systems (Hodge 1963b, 1973, 1978; Price 1985). The dust is generally clumped into small clouds ($D \sim$ 20–40 pc) with inferred masses of a few hundred solar masses. In NGC 185, Price (1985) argued that the extinction law of the dust regions differs significantly from the standard Galactic extinction law.
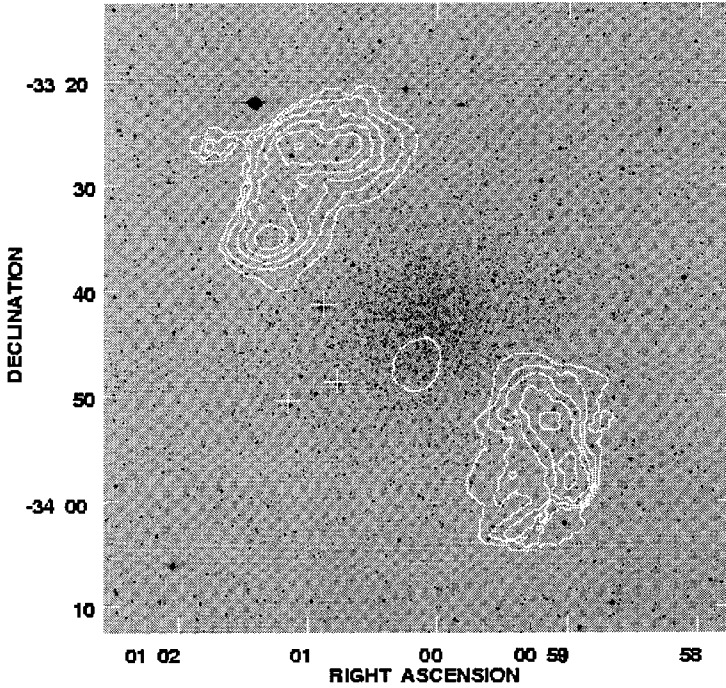
Figure 6   A plot of the Sculptor dSph galaxy showing the optical and 21-cm radio components (Carignan et al 1998). The stellar and HI velocities agree to within 5 km s^{-1}; the gas is almost certainly associated with Sculptor. Considerable HI flux in the outer regions of Sculptor may have been missed by these VLA observations; the actual morphology (total flux) of the HI emitting gas may be quite different (larger) than the bimodal distribution shown (or the flux reported in Table 5). The key point is that what little neutral H gas there is in Sculptor is distributed away from the galaxy's center. For reference, the tidal radius of Sculptor is approximately 76 arcmin (Table 3), slightly larger than the dimensions of the sides of the figure. The HI *contours* correspond to 0.2, 0.6, 1.0, 1.4, 1.8, and 2.2 $\times$ 10^{19} cm^{-2}.

Both the total optical extinction and total mass of individual dust clouds in low-luminosity dIrr seem to be smaller for the clouds—when seen—in dSph galaxies (Ables & Ables 1977, Hodge 1978, Hodge & Lee 1990). Some Local Group dIrr galaxies suffer variable internal extinction, presumably from a pervasive, nonuniform dust sheet (Gallart et al 1996a). van Dokkum & Franx (1995) found no optical evidence of dust clouds in the core of M32 using archival HST observations. Bendinelli et al (1992) claimed to see a central reddening in M32, possibly due to a central dust component; however, Peletier (1993) found no optical color gradients to within 1 arcsec of the center of the galaxy.

Nearly 25% of the Local Group dwarfs have now been detected in CO emission (Table 5). These detections include the lowest luminosity galaxies in which molecular gas has been observed (Roberts et al 1991). The CO emission is typically confined to distinct clouds with diameters of $\lesssim$50 pc (Ohta et al 1988, Saitō et al 1992, Wilson 1995, Welch et al 1996, Young & Lo 1997a). By combining spectra from fields without direct detections, Israel (1997) has found evidence of a diffuse CO component in NGC 6822. Many Local Group dwarfs have been detected with IRAS at 60 and 100 μm (Melisse & Isreal 1994a,b, Knapp et al 1985). All of the Local Group IRAS sources either contain dust and/or a significant population of stars younger than about 10 Myr. Submillimeter observations have also proven useful to tracking dust in Local Group dwarfs, both from their continuum emission (e.g. Thronson et al 1990, Fich & Hodge 1991) and from carbon line emission (Massen et al 1997).

In general, the spatial and kinematic distribution of dust, CO emission, HI, and optical star-formation regions are well correlated, but there are some interesting exceptions. Hodge & Lee (1990), Richer & McCall (1992), and Welch et al (1996) found small spatial offsets between HI and CO emission regions in IC 10, NGC 3109, and NGC 185, respectively. The locations of optical HII regions often correlate very well with CO emission regions (Hodge & Lee 1990, Saitō et al 1992). However, the CO and Hα emission lines are often redshifted relative to HI (Tomita et al 1993), which is perhaps indicative of infall or collapse in the denser regions where CO is observed. In NGC 185, some regions with strong CO emission appear devoid of optical dust (Welch et al 1996), but when optical dust is present, the regions are usually detected in CO (Gallagher & Hunter 1981; IC 1613 may be an exception; Hodge 1978, Ohta et al 1993).

Numerous studies have used Local Group dwarfs to measure the conversion factor, X, between CO emission and H$_2$ molecular mass as a function of metallicity. $X \equiv N_{H_2}/S(CO)$, where N_{H_2} is the molecular hydrogen column density, and $S(CO)$ is the integrated CO flux density or intensity. Low-luminosity— hence low-metallicity (Section 5.2)—dwarfs should have larger H$_2$-CO conversion factors because CO formation will be hindered at low abundances for a given molecular mass. Two methods are used to estimate the molecular masses needed to calculate X. First, the observed CO line width is taken as a measure of the cloud velocity dispersion from which the virial mass is determined (e.g. Wilson 1994b, 1995). The second approach combines IRAS and HI fluxes throughout a galaxy to determine the total hydrogen column density (neutral plus molecular) where CO is observed (Israel 1997). Recent studies all agree that X is higher for low-luminosity dwarfs, but the precise form, slope, and zero point of the L-X relation is still controversial (Ohta et al 1993, Verter & Hodge 1995, Wilson 1995). In NGC 6822 ([Fe/H] ~ -0.7; Section 5) X is about two to five times higher than in the Galaxy (Ohta et al 1993, Wilson 1995, Israel

1997), while for GR 8 ([O/H] $\sim$ -1.3), $X \geq 10$ times the Galactic value (Ohta et al 1993, Verter & Hodge 1995). Ohta et al (1993) and Israel (1997) both noted that X shows considerable scatter at a given metallicity, implying that some other parameter affects the H_2-CO ratio.

4.3 HII Regions, Supernova Remnants, and X Rays

The integrated Hα fluxes of the Local Group dwarfs are listed in Table 5. All of the dIrr galaxies in the Local Group contain HII regions. Hodge & Lee (1990) introduced a morphological classification scheme for these HII regions; Hunter et al (1993) have published deep Hα images of many Local Group dwarfs that provide an excellent way to appreciate this rich morphological variety. The distribution of morphological types of HII regions differs between galaxies (Hodge & Lee 1990, Hunter et al 1993), though the size distribution of HII regions is generally well fit as a power law truncated at a maximum HII region diameter of about 200–400 pc (Strobel et al 1991, Hodge et al 1994, Hodge & Miller 1995).

Only one dSph galaxy (NGC 185) and one transition system (Antlia) have detected HII emission. The Hα emission from NGC 185 appears to be related to an old supernova remnant (Gallagher et al 1984, Young & Lo 1997a); the high excitation led Ho et al (1995, 1997) to classify the galaxy as a Seyfert 2. In Antlia, the HII region is extremely faint (Aparicio et al 1997a; the region is visible in the color image of Whiting et al 1997). As in Pegasus (Aparicio & Gallart 1995, Skillman et al 1997), its presence may merely reflect the stochastic nature of high-mass star formation in systems with relatively low average star-formation rates (Aparicio et al 1997b).

Using radio continuum observations, Yang & Skillman (1993) identified an unusually large nonthermal source in IC 10 that they argued is the remnant of multiple recent supernovae shells. This conclusion received support from the subsequent observations of optical filaments from the radio-continuum shell (Hunter et al 1993). Nonthermal sources have also been observed in IC 1613 and NGC 6822 (Klein & Gräve 1986), which are also probably from old supernova remnants. Virtually all other sources identified in these galaxies are thermal sources associated with optical HII regions or nonthermal background sources.

No diffuse X-ray emission has been detected in any Local Group dwarf (Markert & Donahue 1985, Fabbiano 1989, Gizis et al 1993). This is not surprising: If hot gas was produced during periods of active star formation in any Local Group dwarf, it would have been rapidly expelled from the galaxy and faded to invisibility. The nearby dwarf NGC 1569 appears to be the closest example of a dwarf galaxy experiencing this short-lived X-ray emitting phase (Heckman et al 1995). In general, Local Group dwarfs contain few X-ray sources of any kind, though some possible X-ray binaries have been detected in

a few systems (Brandt et al 1997, Eskridge & White 1997, and the references above, but see Eskridge 1995).

4.4   *The Interstellar Medium "Crisis" in dSph Galaxies*

NGC 147 and NGC 185 are virtually twins; their luminosities, masses, mean abundances, abundance dispersions, average star-formation rates, sizes, and core and exponential radii are extremely similar (Tables 3–7). NGC 147 does have a significantly fainter central surface brightness than NGC 185 (Table 3), but the latter contains young stars in its core (see Section 6), which probably boosts its central luminosity density. However, their kinematic properties indicate that both galaxies have very similar central mass densities (Tables 4 and 7). Yet when considering their gaseous component (Table 5), it is immediately apparent that while NGC 185 contains a significant ISM, NGC 147 has none. This is extremely puzzling. Many authors agree that the gas replenishment time scale in galaxies such as these would be approximately 0.1–1 Gyr from internal sources such as planetary nebulae or red giant winds (Ford et al 1977, Mould et al 1990, Gizis et al 1993, Welch et al 1996, Young & Lo 1997a). Paradoxically, NGC 185 contains young stars and even an old supernova remnant (Price 1985, Lee et al 1993b, Young & Lo 1997a), yet this activity has not blown out its gas. Since NGC 147 has no stars younger than 1 Gyr (Han et al 1997), we cannot simply claim that we have caught it just after an energetic star-formation episode that consumed or expelled all of its gas.

Few early-type Local Group galaxies have been mapped at HI, but most of the ones that have contain distinct HI clouds with masses $\sim 10^5$ M$_\odot$ (if at the distance of the galaxy) and diameters of ~ 200 pc or larger (Carignan et al 1991, 1998, Young & Lo 1997a). This gas is always significantly offset from the optical centers of the galaxies. Young & Lo (1997a) further emphasize that the configuration and kinematics of the gas are highly unstable: These HI clouds must be short-lived structures. As we see in Section 6, most Local Group dwarfs—including the early-type systems—have surprisingly complex and varied star-formation histories. In many cases, there is evidence of star formation in the past 10^9 years, yet few seem to contain any gas that could have fueled this activity (though see Section 4.1).

If the gas is of internal origin and we have not come onto the scene just as all dSph systems used up all their gas, then these galaxies somehow would have had to avoid accumulating any gas between star-formation episodes (as the lack of central HI and the NGC 147/185 paradox seem to be telling us). Could structures such as those seen in Sculptor serve as "holding tanks" for such quasi-expelled gas? Another option is that the gas is of external origin (Knapp et al 1985). This possibility superficially explains the generally asymmetric distribution of gas in early-type systems (except LGS 3; Young & Lo 1997b), the kinematic offsets

of the gas and stars in these galaxies, and the possibly complex chemical-enrichment history of at least one dSph system (Smecker-Hane et al 1994; accreted clouds could have any metallicity); it even provides a repository—the halo—for gas expelled from these galaxies during earlier episodes. The dIrr galaxies may have less chance to accrete clouds because they are further from M31 and the Milky Way (Figure 3). IC 10 shows evidence of a disturbed outer HI velocity field and has a very high current star-formation rate (Table 5; Shostak & Skillman 1989). However, these authors warn that many other isolated dIrr systems show similarly complex kinematics, so such characteristics do not necessarily imply a recent encounter or merger with another galaxy or HI cloud. Past surveys for high-latitude HI clouds would have missed low-velocity clouds under 10 arcmin in diameter and with $M(\text{HI}) \sim 10^5$–$10^6\,M_\odot$ if located $>50\,\text{kpc}$ away (Wakker & van Woerden 1997). The crucial dilemma for any accretion model faces is to understand how systems with escape velocities as low as 10–15 km s^{-1} can snare gas in any quantity within a halo with a velocity dispersion that is at least 10 times larger.

5. CHEMICAL ABUNDANCES IN LOCAL GROUP DWARFS

Photometric and spectroscopic techniques can be used to estimate heavy-element abundances in Local Group dwarfs. For early-type galaxies, the properties of the RGB constrain [Fe/H] and, in some cases, the abundance dispersion, $\sigma_{[\text{Fe/H}]}$. Apart from helium and some molecular species, photometry is poorly suited to determining abundances of individual elements. Photometric abundances have now been measured in some Local Group dIrr systems where the old/intermediate-age RGB population can be observed directly in deep color-magnitude diagrams (e.g. Sextans A: Dohm-Palmer et al 1997; Leo A: Tolstoy et al 1998; various: Lee et al 1993c; see Table 6 for other examples). Spectroscopy can be used to determine abundances of both individual stars and emission nebulae, such as HII regions and planetary nebulae. Generally, spectroscopy provides abundances for specific elemental, ionic, or molecular species, which somewhat complicates comparisons with photometric [Fe/H] abundance estimates. Some good recent reviews of dwarf abundances can be found by Skillman & Bender (1995) and Skillman (1998).

5.1 *The Observational Basis for Local Group Dwarf Abundances*

RED GIANT BRANCH ABUNDANCES   Da Costa & Armandroff (1990) observed RGB sequences using the V and Cousins I bands in a number of globular clusters ranging from −0.7 to −2.3 in [Fe/H]. These sequences have helped establish

the (V−I) TRGB method of determining distances (Section 2.2). They also found that the colors of the giant branches define a monotonic sequence with respect to abundance: $[Fe/H] = -15.16 + 17.0(V - I)_{-3} - 4.9(V - I)^2_{-3}$, where $(V - I)_{-3}$ is the reddening-corrected $(V - I)$ color of the giant branch at $M_I = -3.0$. This relation is valid for $-0.7 > [Fe/H] > -2.2$. Lee et al (1993c) reevaluated this expression at $M_I = -3.5$ for easier application in distant galaxies: $[Fe/H] = -12.64 + 12.6(V - I)_{-3.5} - 3.3(V - I)^2_{-3.5}$. This relation has the same range of validity as the earlier one because both were derived from the same data (Da Costa & Armandroff 1990).

Photometric abundance indicators such as the RGB color run into complications in dwarf galaxies. Unlike clusters, most dwarfs exhibit significant abundance dispersions. Because dwarf galaxies are considerably more distant on

Table 6 Heavy-element abundances of Local Group dwarf galaxies

Galaxy name	[Fe/H][a] (dex)	$\sigma_{[Fe/H]}$[b] (dex)	Ref[c]	$12 + \log(O/H)$[d] (dex)	[N/O][e] (dex)	Ref[f]
WLM	-1.5 ± 0.2	—	1, 2	7.75 ± 0.2	-1.46 ± 0.15	3, 4
NGC 55	—	—	—	8.32 ± 0.15	-1.44 ± 0.15	67, 75, 76
IC 10[g]	—	—	—	8.19 ± 0.15	-1.37 ± 0.12	5, 74
NGC 147[h,i,j]	-1.1 ± 0.2	0.4 ± 0.1	7–9	—	—	—
And III	-2.0 ± 0.2	$\leq 0.2 \pm 0.04$	10	—	—	—
NGC 185[j,k]	-1.22 ± 0.15	0.4 ± 0.1	11	8.2 ± 0.2	—	6
NGC 205[j,k,l]	-0.8 ± 0.1	0.5 ± 0.1	12–14	8.6 ± 0.2	—	6
M32[l]	-1.1 ± 0.2	0.7 ± 0.2	15, 16	—	—	—
And I	-1.5 ± 0.2	0.3 ± 0.1	17, 71	—	—	—
Sculptor	-1.8 ± 0.1	0.3 ± 0.05	18, 19	—	—	—
LGS 3	-1.8 ± 0.3	0.3 ± 0.2	20, 65	—	—	
IC 1613	-1.3 ± 0.2	—	2	7.8 ± 0.2	—	67
And II	-1.6 ± 0.3	0.5 ± 0.1	21	—	—	—
Phoenix	-1.9 ± 0.1	0.5 ± 0.1	22, 23	—	—	—
Fornax[j,k]	-1.3 ± 0.2	0.6 ± 0.1	24, 50	7.98 ± 0.4	—	6, 72
EGB 0427+63	—	—	—	7.62 ± 0.1	≤ -1.5	4
Carina	-2.0 ± 0.2	<0.1	51, 52	—	—	—
Leo A[k]	—	—	—	7.3 ± 0.1	—	25
Sextans B[m]	~ -1.2	—	60	7.84 ± 0.3	—	25, 26
NGC 3109	-1.5 ± 0.3	<0.3	2, 28–30	8.06 ± 0.2	—	6
Antlia	-1.8 ± 0.25	0.3 ± 0.1	48, 49, 77	—	—	—
Leo I	-1.5 ± 0.4	0.3 ± 0.1	31, 32, 69, 70	—	—	—
Sextans A	-1.9 ± 0.3	—	61	7.49 ± 0.2	—	25
Sextans	-1.7 ± 0.2	0.2 ± 0.05	33–36	—	—	—
Leo II	-1.9 ± 0.1	0.3 ± 0.1	31, 37, 38	—	—	—
GR 8[m]	—	—	—	7.62 ± 0.1	—	26
Ursa Minor	-2.2 ± 0.1	$\lesssim 0.2$	39	—	—	—
Draco	-2.0 ± 0.15	0.5 ± 0.1	40, 41	—	—	—
Sagittarius[j,k,n]	-1.0 ± 0.2	0.5 ± 0.1	54–57, 63, 64	8.30 ± 0.08	-1.0 ± 0.3	62
SagDIG	—	—	—	7.42 ± 0.3	—	3
NGC 6822[k,m]	-1.2 ± 0.3	0.5 ± 0.1	2, 43, 44	8.2 ± 0.2	-1.7 ± 0.1	3, 59, 68
DDO 210[o]	< -1.0	—	30	—	—	—
IC 5152	—	—	—	8.36 ± 0.2	—	67
Tucana	-1.7 ± 0.15	0.3 ± 0.2	45, 46	—	—	—
UKS2323-326	—	—	—	—	—	—
Pegasus	-1.0 ± 0.3	—	47, 49, 66	7.93 ± 0.14	-1.24 ± 0.15	73

average than Galactic globular clusters, few galaxies have reliable HB photometry (though see Da Costa et al 1996); those that do often reveal unusual HB morphologies, such as bimodal (in luminosity) HB sequences (Carina: Smecker-Hane et al 1994; Sagittarius: Sarajedini & Layden 1995) or compact, super-red HBs (Leo I: Lee et al 1993a, Caputo et al 1995). It is not always feasible to use abundance indices such as $(B-V)_{0,g}$ (the $B-V$ color of the RGB at the level of the HB; Sandage & Wallerstein 1960, Sandage & Smith 1966, Zinn & West 1984) to estimate the metallicities of these galaxies. Another complication is that most Local Group dwarfs exhibit complex star-formation histories (Section 6). It remains to be seen how reliably these abundance indices—derived for globular clusters—can measure the composite populations of nearby dwarfs (see also Grillmair et al 1996). It would clearly be useful to extend the range of photometric abundance indicators with

---

[a]The mean iron abundance for the old and intermediate-age stellar populations where [Fe/H] $\equiv \log(Z/Z_{\odot})$.

[b]The intrinsic dispersion in [Fe/H]. If the reference gave a full metallicity range instead of a dispersion, I assumed $\sigma = 0.5 \, \Delta$[Fe/H]. This reasonably approximates the scaling between these quantities for the few galaxies that have independent estimates of both $\sigma_{\text{[Fe/H]}}$ and Δ[Fe/H].

[c]References for the stellar abundances: 1, Minniti & Zijlstra 1996; 2, Lee et al 1993c; 3, Skillman et al 1989b; 4, Hodge & Miller 1995; 5, Garnett 1990; 6, Richer & McCall 1995; 7, Davidge 1994; 8, Mould et al 1983; 9, Han et al 1997; 10, Armandroff et al 1993; 11, Lee et al 1993b; 12, Mould et al 1984; 13, Lee 1996; 14, Richer et al 1984; 15, Davidge & Jones 1992; 16, Grillmair et al 1996; 17, Da Costa et al 1996; 18, Kaluzny et al 1995; 19, Da Costa 1984; 20, Lee 1995a; 21, König et al 1993; 22, van de Rydt et al 1991; 23, Ortolani & Gratton 1988; 24, Beauchamp et al 1995; 25, Skillman et al 1989a; 26, Moles et al 1990; 27, deleted in proof; 28, Lee 1993; 29, Davidge 1993; 30, Greggio et al 1993; 31, Suntzeff et al 1986; 32, Reid & Mould 1991; 33, Suntzeff et al 1993; 34, Mateo et al 1995a; 35, Mateo et al 1991a; 36, Da Costa et al 1991; 37, Demers & Irwin 1993; 38, Lee 1995b; 39, Olszewski & Aaronson 1985; 40, Lehnert et al 1992; 41, Carney & Seitzer 1986; 42, deleted in proof; 43, Gallart et al 1996a; 44, Gallart et al 1996b; 45, Saviane et al 1996; 46, Castellani et al 1996; 47, Aparicio & Gallart 1995; 48, Whiting et al 1997; 49, Aparicio et al 1997b; 50, Buonanno et al 1985; 51, Smecker-Hane et al 1994; 52, Mould & Aaronson 1983; 53, Hurley-Keller et al 1998; 54, Mateo et al 1995c; 55, Ibata et al 1997; 56, Sarajedini & Layden 1995; 57, Da Costa & Armandroff 1995; 58, deleted in proof; 59, Pagel et al 1980; 60, Tosi et al 1991; 61, Dohm-Palmer et al 1997; 62, Walsh et al 1997; 63, Whitelock et al 1996; 64, Marconi et al 1998; 65, Aparicio et al 1997c; 66, deleted in proof; 67, Talent 1980; 68, Dufour & Talent 1980; 69, Lee et al 1993a; 70, Demers et al 1994a; 71, Mould & Kristian 1990; 72, Maran et al 1984; 73, Skillman et al 1997; 74, Lequeux et al 1979; 75, Stasinska et al 1986; 76, Webster & Smith 1983; 77, Sarajedini et al 1997.

[d]The oxygen abundance defined as $12 + \log(O/H)$, where (O/H) is the number ratio of oxygen to hydrogen atoms.

[e]The nitrogen to oxygen ratio defined as [N/O] $=$ $\log(N/O)$, where (N/O) is the number ratio of nitrogen to oxygen atoms.

[f]References for the oxygen and nitrogen abundances; see footnote c.

[g]The sulfur abundance was also determined: $12 + \log(S/H) = 6.77$ (Richer & McCall 1995).

[h]A weak abundance gradient is seen with [Fe/H] increases with radius from the galaxy center (Han et al 1997).

[i]The stellar metallicity dispersion is higher in the center of the galaxy than in the outer region (Han et al 1997).

[j]The globular clusters of this galaxy are more metal poor on average than the field stars.

[k]The oxygen abundance was derived, at least in part, from one or more planetary nebula.

[l]The metallicity distribution seems to be skewed towards positive values of [Fe/H] (NGC 205: Mould et al 1984; M32: Grillmair et al 1996).

[m]The helium abundance, N(He)/N(H), was determined: 0.098 (GR 8; Moles et al 1990); 0.097 (Sextans B; Moles et al 1990); 0.074 (NGC 6822; Pagel et al 1980).

[n]The associated globular clusters of this galaxy exhibit a considerably larger spread in [Fe/H] than the field stars.

[o]At the closer distance adopted in Table 2, the stellar iron abundance is likely to be considerably lower than that found by Greggio et al (1993) for their assumed distance of over 2.5 Mpc.

observations of the RGBs in populous clusters in the Galaxy and the Magellanic Clouds.

With few exceptions, every Local Group dwarf for which abundances have been determined from the RGB shows evidence of a significant abundance dispersion (Table 6). In M32 (Grillmair et al 1996) and NGC 205 (Mould et al 1984), the color distribution of the RGB implies an abundance distribution that is skewed toward higher abundances. Although these color dispersions principally reflect variations in abundances, an age dispersion can also (slightly) broaden the RGB (e.g. Bertelli et al 1994, Meynet et al 1993). Carina has a large age spread and populations with distinct abundances (Da Costa 1994a, Smecker-Hane et al 1994), yet it has a narrow RGB. Leo I also exhibits a large

Table 7 Internal kinematic properties of Local Group dwarf galaxies

Galaxy name	σ_* [a] (km s^{-1})	$v_{rot,*}$ [b] (km s^{-1})	Ref [c]	σ_{ISM} [d] (km s^{-1})	$v_{rot,ISM}$ [e] (km s^{-1})	R_{rot} [f] (arcmin)	i [g] (deg)	Ref [h]
WLM[i,j]	—	—		(8)	21 ± 2	4.8	69 ± 5	1
NGC 55[i–k]	—	—		(8)	86 ± 3	21	88 ± 2	1, 2, 49
IC 10[k]	—	—		8 ± 2	30 ± 3	13	40 ± 5	1, 3
NGC 147	22 ± 4	6.5 ± 1.1	4	—	—	—	—	
And III	—	—		—	—	—	—	
NGC 185[l]	25 ± 4	1.2 ± 1.1	4–8	—	—	—	—	7
NGC 205 (Outer)[l]	46 ± 8	1.5 ± 0.8	4, 9–12	16 ± 4	—	—	—	
NGC 205 (Inner)	21 ± 6	—	4, 9–12	—	—	—	—	
M32[m]	50 ± 10	12 ± 3	13, 14, 47, 48, 50	—	—	—	—	
And I	—	—		—	—	—	—	
Sculptor	6.6 ± 0.7	<2.0	15–18	—	—	—	—	
LGS 3	6.5 ± 3.0	—	43	9 ± 3	$<2 \pm 2$	—	50 ± 5	1, 19, 20
IC 1613[k]	—	—		8.5 ± 1.0	21 ± 2	12.5	35 ± 3	1, 21, 22
And II	—	—		—	—	—	—	
Phoenix	—	—		8.9 ± 1.5	<2.0	—	55 ± 4	23
Fornax	10.5 ± 1.5	<2.0	24, 25	—	—	—	—	
EGB 0427+63[j]	—	—		(8)	33 ± 10	—	—	26
Carina	6.8 ± 1.6	—	27	—	—	—	—	
Leo A	—	—		9.3/3.5	<3.0	—	45 ± 5	1, 19, 28
Sextans B[j,k]	—	—		18	22 ± 3	6.6	35 ± 15	22, 51
NGC 3109[k]	—	—		10 ± 2	67 ± 4	17.0	83 ± 6	1, 31, 45
Antlia	—	—		6.3 ± 1.7	—	—	—	32
Leo I	8.8 ± 0.9	—	44	—	—	—	—	
Sextans A[i]	—	—		8 ± 3	19 ± 2	3.7	35 ± 3	1, 30
Sextans	6.6 ± 0.7	—	33, 42	—	—	—	—	
Leo II	6.7 ± 1.1	—	34	—	—	—	—	
GR 8[n]	—	—		11 ± 3	7 ± 3	0.5	48 ± 3	19, 22, 35
Ursa Minor	9.3 ± 1.8	5.0 ± 2.0	36–38	—	—	—	—	
Draco	9.5 ± 1.6	<2.0	37–39	—	—	—	—	
Sagittarius	11.4 ± 0.7	$\lesssim 4.0$	46	—	—	—	—	
SagDIG[o]	—	—		7.5 ± 2.0	<2.0	—	60 ± 10	1, 19
NGC 6822[k]	—	—		(8)	47 ± 3	19	67 ± 3	1, 41
DDO 210	—	—		6.6 ± 1.8	<5.0	—	—	19
IC 5152	—	—		(8)	31 ± 3	2.6	55 ± 5	1
Tucana	—	—		—	—	—	—	
UKS2323-326[o]	—	—		—	—	—	—	
Pegasus	—	—		8.6 ± 1.4	10 ± 5	4.0	42 ± 10	1, 19, 22

spread in age but has a wide giant branch (Lee et al 1993a). In Carina, the age spread seems to compensate for the metallicity dispersion, while in Leo I, it does not. Does this imply radically different chemical-enrichment patterns for the two galaxies? This underscores an obvious, but important, point: The star-formation and chemical-enrichment histories of dwarfs cannot be interpreted independently. To derive one history requires careful consideration of the other (Hodge 1989, Aparicio et al 1997b,c).

SPECTROSCOPIC ABUNDANCES   Among the early-type dwarfs in the Local Group, spectroscopic abundances (typically [Fe/H] or [Ca/H]) have been measured for individual stars in Draco (Lehnert et al 1992 and references therein), Sextans (Da Costa et al 1991, Suntzeff et al 1993), Carina (Da Costa 1994a),

---

[a]The stellar central velocity dispersion.

[b]The rotation velocity from stellar velocity measurements.

[c]Optical kinematic references: 1, Huchtmeier & Richter 1988; 2, Hummel et al 1986; 3, Shostak & Skillman 1989; 4, Bender et al 1991; 5, Held et al 1992; 6, Welch et al 1996; 7, Young & Lo 1997a; 8, Wiklund & Rydbeck 1986; 9, Carter & Sadler 1990; 10, Held et al 1990; 11, Ford et al 1987; 12, Peterson & Caldwell 1993; 13, Bender & Nieto 1990; 14, Dressler & Richstone 1988; 15, Da Costa 1992; 16, Armandroff & Da Costa 1986; 17, Queloz et al 1995; 18, Da Costa 1994a; 19, Lo et al 1993; 20, Thuan & Martin 1979; 21, Lake & Skillman 1989; 22, Hoffman et al 1996; 23, Carignan et al 1991; 24, Mateo et al 1991b; 25, Paltoglou & Freeman 1987; 26, Huchtmeier & Richter 1986; 27, Mateo et al 1993; 28, Young & Lo 1996a; 29, deleted in proof; 30, Skillman et al 1988; 31, Jobin & Carignan 1990; 32, Fouqué et al 1990; 33, Suntzeff et al 1993; 34, Vogt et al 1995; 35, Carignan et al 1990; 36, Hargreaves et al 1994b; 37, Olszewski et al 1995; 38, Armandroff et al 1995; 39, Hargreaves et al 1996b; 40, deleted in proof; 41, Gottesman & Weliachew 1977; 42, Hargreaves et al 1994a; 43, KH Cook, EW Olszewski, C Stubbs, private communication; 44, Mateo et al 1998c; 45, Carignan 1985; 46, Ibata et al 1997; 47, Nolthenius & Ford 1986; 48, Tonry 1984; 49, Puche et al 1991; 50, Carter & Jenkins 1993; 51, Hewitt et al 1983.

[d]The velocity dispersion measured from the ISM (HI line widths, HI clump-clump dispersions, and CO cloud-cloud dispersions). See footnotes i, j, and o for additional details.

[e]The peak or outermost observed rotation velocity of the ISM.

[f]The angular distance from the kinematic center of the galaxy to where the rotation velocity listed in column 6 is observed (see footnote e).

[g]The inclination of the disk of the galaxy from the plane of the sky.

[h]Radio/ISM kinematic references; see footnote c.

[i]Formulae given by Huchtmeier & Richter (1988) to convert the full width at 20% intensity to FWHM. The rotation velocity was taken to be FWHM/2.0. If the inferred rotation was found to be less than 20 km s^{-1}, then the line width was interpreted instead as a measure of the internal velocity dispersion such that $\sigma_0 = \text{FWHM}/2.35$.

[j]σ_{ISM} is assumed to be 8 km s^{-1}. No correction has been applied to v_{rot} for WLM or IC 5152 to account for this (small) dispersion. For the other galaxies, detailed corrections for asymmetric drift have been applied to the velocity curves as necessary in the cited studies.

[k]The higher velocity and spatial resolution study is used here to obtain the rotation velocity.

[l]Streaming motions that cannot be attributed to rotation are observed in the HI velocity maps.

[m]The nuclear kinematics of M32 are complex, possibly owing to the presence of a massive central black hole (Kormendy & Richstone 1995). The dispersion and rotational velocity quoted here refer to regions far outside the nucleus ($r > 10$ arcsec).

[n]The inner parts appear to follow a solid-body rotation curve, but the outer regions do not exhibit organized rotation and appear to be pressure supported (Carignan et al 1990).

[o]Both SagDIG and UKS2323-326 were observed at 21cm by Longmore et al (1982). For SagDIG, their estimate of the velocity dispersion (derived here using the methods described in footnote i above) is highly discrepant compared to the two other independent measurements of the galaxy's dispersion. One of these references (Lo et al 1993) finds no evidence for rotation, so this discrepancy is probably not merely a misinterpretation of the cause for the line broadening. I have chosen to disregard HI velocity widths (of Longmore et al 1982) in this table for both SagDIG (for which other values are available) and UKS2323-326 (for which no other kinematic data are published).

Sagittarius (Da Costa & Armandroff 1995, Ibata et al 1997), and Ursa Minor (EW Olszewski & NB Suntzeff, private communication). Oxygen abundances have been derived from spectroscopy of planetary nebulae in Fornax (Maran et al 1984, Richer & McCall 1995), Sagittarius (Walsh et al 1997), NGC 185, and NGC 205 (Richer & McCall 1995), as well as the dIrr NGC 6822 (Dufour & Talent 1980).

Spectroscopy of HII regions in Local Group dIrr galaxies typically targets oxygen, but abundances of other elements such as nitrogen, sulphur, and helium have also been measured (e.g. Pagel et al 1980; Garnett 1989, 1990; Garnett et al 1991). The improved blue-sensitivity of CCD detectors in recent years has greatly aided nebular abundance studies by making it simpler to derive reliable physical conditions in HII regions. This alone greatly improves the consistency and precision of the oxygen abundances derived in this manner (see Skillman 1998 for details). Table 6 lists the oxygen abundances for Local Group dIrrs that have adequate data. Unlike [Fe/H] in early-type dwarfs, there is no evidence for significant dispersion of the oxygen abundances in any Local Group dIrr in which multiple HII regions have been studied (Pagel et al 1980, Skillman et al 1989a, Moles et al 1990, Hodge & Miller 1995). Because HII regions are associated with young populations (though the gas itself may derive from relatively old stars), these nebular abundances nicely complement those derived from intermediate-age planetary nebula (Olszewski et al 1996b).

Integrated spectroscopy is impractical for most of the dwarfs largely because of their extremely low surface brightnesses [Sembach & Tonry (1996) suggested one method to overcome this problem]. M32 is a famous exception for which a number of integrated spectroscopic studies in the optical and ultraviolet (UV) have been carried out (for reviews, see O'Connell 1992, Grillmair et al 1996). The excess UV light in its spectrum is generally taken as evidence of a population of relatively young stars associated with the IR-luminous asymptotic giant branch (AGB) stars found by Freedman (1992) and Elston & Silva (1992). However, the spectrum only weakly constrains the stellar abundance of M32 (Grillmair et al 1996). Optical spectra reveal complex radial gradients of the Balmer lines (these weaken outward), while the Mg lines remain constant with radius and CH increases in strength (Davidge 1991, González 1993). Oddly, M32 exhibits *no* strong radial color gradients apart from in the UV (Michard & Nieto 1991, O'Connell 1992, Peletier 1993, Silva & Elston 1994). These conflicting tendencies have greatly complicated spectroscopic determinations of the galaxy's abundance even now that deep HST photometry is available (Grillmair et al 1996). The nuclear region of NGC 205 has also been observed spectroscopically (Bica et al 1990), revealing a prominent young population (age $\lesssim 10^8$ years) with a mean metallicity of [Fe/H] ~ -0.5, along with more older, metal-poor stars (ages $\gtrsim 5$ Gyr; [Fe/H] $\lesssim -1.0$). A lower nuclear

abundance has been derived by Jones et al (1996) for NGC 205 ([Fe/H] ~ -1.4) from UV spectra.

5.2 *The Metallicity-Luminosity Relation and the dIrr/dSph Connection*

The fact that the more luminous dwarf galaxies are also on average the most metal rich has been known for some time for both dIrr (Lequeux et al 1979, Talent 1980, Skillman et al 1989a) and dSph galaxies (Aaronson 1986, Caldwell et al 1992). Aaronson (1986) and Skillman et al (1989a) merged the abundance data for both types into a a single luminosity-abundance (L-Z) relation spanning 12 mag in M_B and about 1.6 dex in oxygen/iron abundance. A recent determination of [Fe/H] of a low–surface brightness but relatively luminous dSph galaxy in the M81 group (Caldwell et al 1998) demonstrates clearly that luminosity, not surface brightness, is the principal parameter correlated with metallicity in dSph and, presumably, dIrr galaxies.

Figure 7 is a plot of the mean abundances for all of the galaxies in Table 6 (except DDO 210 for which [Fe/H] is uncertain; Greggio et al 1993) vs their
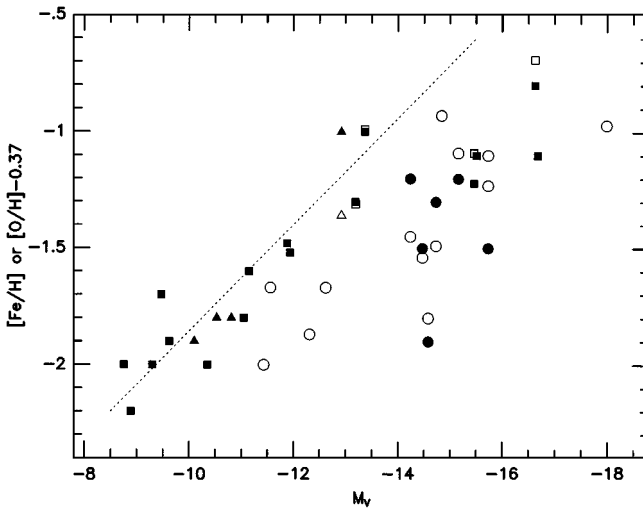
Figure 7 A plot of [Fe/H] (*filled squares*) or [O/H] $- 0.37$ [I assume $12 + \log(O/H)_\odot = 8.93$ after Anders & Grevesse (1989)] vs absolute V-band magnitude. The *dotted line* is a rough fit to the [Fe/H]-M_V relation for the dSph and transition objects. Sagittarius corresponds to the *points* near $(M_V, [Fe/H]) \sim (-13.4, -1.0)$. *Square symbols* refer to dSph or dE galaxies; *triangles* refer to transition galaxies (denoted dIrr/dSph in Table 1); *circles* refer to dIrr systems. *Filled symbols* correspond to [Fe/H] abundances determined from stars, while *open symbols* denote oxygen abundance estimates from analyses of HII regions and planetary nebulae. See Table 6 for details.

mean V-band absolute magnitudes (Table 4). The data have been corrected for external reddening; internal extinction is probably insignificant for most of these systems (see Table 5). In Table 6, 10 galaxies have reliable [Fe/H] *and* oxygen abundances, including some dIrrs with stellar abundance estimates and some early-type dwarfs with oxygen abundances from planetary nebulae. The mean difference between [Fe/H] and [O/H] [defined as $\log(O/H) - \log(O/H)_\odot$] is 0.37 ± 0.06 dex. I have therefore added -0.37 to the oxygen abundances before plotting them in Figure 7.

Even if the offset to the nebular abundances is disregarded, the stellar [Fe/H] abundances show a bimodal, or possibly discontinuous, behavior. The oxygen abundances only reinforce this conclusion. The "upper branch" in Figure 7 (denoted by the *dotted line*) contains only dSph galaxies, and all four transition galaxies (LGS 3, Phoenix, Antlia, and Pegasus; see Table 1) with precise abundance estimates. All of the galaxies fainter than $M_V \sim -13.5$ with nebular abundances are dIrr systems and clearly fall below the dSph relation by about 0.6–0.7 mag. At the other extreme, nearly all of the galaxies brighter than $M_V \sim -13.5$ are dIrr systems—with the important exceptions of NGC 147, NGC 185, NGC 205, and M32. A similar bifurcation of the luminosity-abundance (L-Z) relation was suggested by Binggeli (1994) and Walsh et al (1997). Caldwell et al (1992, 1998) adopted a single relation to fit all the data for early-type dSph and dE galaxies in the Local Group and other groups and clusters. However, a single linear relation in Figure 7 ignores the strong segregation of dIrr and dSph for $M_V \gtrsim -13.5$. The proposed bimodal L-Z relation also helps remove the abundance anomaly exhibited by Sagittarius (Ibata et al 1994, Mateo et al 1995c, Sarajedini & Layden 1995, Ibata et al 1997) for which the L-Z relation of Caldwell et al (1992, 1998) implies that $M_{V,Sgr} \lesssim -16$. This is about 2–3 mag brighter than observed (Mateo et al 1995c, Ibata et al 1997). Based on the current data, there is no correlation between the offset (in magnitudes) from the *dashed line* in the *upper panel* of Figure 7 and the intrinsic color of the galaxy (Skillman et al 1997), as might be expected if the bimodal behavior simply reflects the effects of current star-formation on the integrated luminosities of dIrr galaxies.

Figure 7 addresses the relationship between dwarf ellipsoidal (dSph and dE) galaxies and dIrr systems. Star-formation (Dekel & Silk 1986, Babul & Rees 1992, De Young & Heckman 1994) and ram-pressure stripping (Faber & Lin 1983, van den Bergh 1994c) have been proposed as means of removing gas from dwarfs in the inner Galactic halo. The spatial segregation of dSph and dIrr (e.g. see Figure 3) appears consistent with the latter idea. But there are other fundamental problems if dSph galaxies are supposed to be simply "gas-free" dIrr (see reviews by Binggeli 1994, Ferguson & Binggeli 1994, Skillman & Bender 1995). Hunter & Gallagher (1985) and Bothun et al (1986) showed that the present-day central surface brightnesses of dIrrs will be considerably

lower than in dSph galaxies after evolutionary fading, while James (1991) found large systematic structural differences between Virgo dIrr and dSph galaxies that seem inconsistent with a common origin or a single evolutionary endpoint (see also Section 3.2). Binggeli (1994), Richer & McCall (1995), and Walsh et al (1997) all noted that at a given luminosity, dIrr galaxies are generally more metal poor than dSph systems, which is precisely the effect seen in Figure 7.

If dIrr and dSph galaxies do indeed represent fundamentally different objects, why does a protodwarf galaxy choose one type rather than the other? It is interesting that even the lowest-luminosity dIrr shows evidence for rotation (e.g. GR 8: Carignan et al 1990; Leo A: Young & Lo 1996) even though $v_{rot}/\sigma < 1.0$. The only rotating dSph systems are NGC 147 (Bender et al 1991) and UMi (Hargreaves et al 1994b, Armandroff et al 1995). The latter's rotation may reflect streaming motions induced by external tides (Oh et al 1995, Piatek & Pryor 1995), and both galaxies have $v_{rot}/\sigma_0 < 1.0$. Could angular momentum be the factor that distinguishes dIrr (high angular momentum) and spheroids (low angular momentum)? Alternatively, Skillman & Bender (1995) suggested that the strength of the first star-formation episodes dictates this distinction; galaxies experiencing little or no early star formation become dIrr systems (see also Aparicio et al 1997c). Or is environment the deciding factor after all (van den Bergh 1994c; Figure 3)?

There are serious objections to each possibility. Three of the four early-type dwarf satellites of M31 that lie in the proposed dIrr branch in Figure 7 (NGC 147, NGC 185, and NGC 205) do not significantly rotate (Bender & Nieto 1990, Held et al 1990, 1992, Bender et al 1991), although dIrr galaxies of similar luminosity do (see Section 7). The fourth galaxy, M32, does rotate (Tonry 1984, Dressler & Richstone 1988, Carter & Jenkins 1993), but its structural parameters are not like any dIrr. Many dIrr galaxies do have pronounced ancient populations, while some dSph galaxies exhibit evidence for few or no old stars (Section 6). Thus, the amplitude or timing of the first episodes of star formation do not appear to differentiate dIrr and dSph galaxies. Finally, although galaxy types are segregated as a function of distance from M31 or the Milky Way (Figure 3), there are glaring exceptions. The Magellanic Clouds are dIrr galaxies that lie close to the Milky Way, while Tucana is an example of an inactive dSph far from any large galaxy. Environment also offers no easy explanation of the segregation of faint dSph and dIrr galaxies in Figure 7.

6.   STAR-FORMATION HISTORIES OF LOCAL GROUP DWARFS

Mould & Aaronson (1983) published deep CCD photometry of the nearby Carina dSph galaxy and showed conclusively that it is dominated by intermediate-age (4–8 Gyr) stars. Although there was already compelling evidence to

suggest that some of the dSph galaxies might contain relatively young stars (Zinn 1980), it was still widely assumed that dSph galaxies such as Carina were all ancient stellar systems, much like globular clusters. The balance of opinion has nearly completely reversed, and it is widely believed that few, if any, Local Group dwarf galaxies contain only ancient stars. Some recent reviews of the exciting developments of this field have been written by Da Costa (1994a,b, 1998), Hodge (1994), Stetson (1997), and Grebel (1997).

6.1   *Basic Techniques and Ingredients*

The key ingredient to deciphering the fossil record of star formation in nearby galaxies is deep CCD photometry of individual stars. Methods that rely on analysis of the most luminous young stars, HII regions, or the integrated galaxy colors at a variety of wavelengths (Hodge 1980, Kennicutt 1983, Gallagher et al 1984) invariably lose age resolution for populations older than about 1 Gyr. As shown below, many Local Group dwarfs were very active during that entire time interval.

Recent technical developments have greatly expanded our ability to constrain the star-formation histories of individual galaxies. Optical and IR detectors have greatly improved in quality and size. Improved computing capabilities have also been essential to progress in this field. Extensive simulations of observations are required to correct for effects such as crowding, internal reddening, incompleteness, and photometric errors (e.g. Aparicio & Gallart 1995, Gallart 1996a,b, Tolstoy 1996, Martínez-Delgado & Aparicio 1997, Hurley-Keller et al 1998). The expansion of grids of stellar-evolutionary models has also been crucial (Schaller et al 1992, Bertelli et al 1994): Observations of local dwarf galaxies have driven us into regions of parameter space—low age and low metallicity—where we have never before had to venture.

6.2   *Age Indicators in Local Group Dwarfs*

A galaxy's star-formation history can be determined by simultaneously comparing its photometric data with appropriate composite models, suitably corrected for observational effects (Bertelli et al 1994, Aparicio & Gallart 1995, Gallart et al 1996a,b, Tolstoy & Saha 1996, Hurley-Keller et al 1998). This powerful approach can, in principle, constrain the entire star formation and chemical history of a galaxy. Of course, the method depends critically on the precision of the input models and on its implicit assumptions, e.g. that the chemical enrichment is a monotonically rising function of time. A heuristic drawback of this approach is that the process is not terribly intuitive; consequently, I discuss here specific evolutionary phases that have proven especially useful as age tracers and note the age range over which they can be used. The theoretical Hertzsprung-Russell (HR) diagrams of Schaller et al (1992; their figures 1 and 2) and figure 1 of

Gallart et al (1996b) are particularly helpful guides to the evolutionary phases discussed here. A good general discussion is given by Chiosi et al (1992).

WOLF-RAYET STARS   These high-mass stars signal vigorous star formation during the past 10 Myr (Massey 1998). The frequency of Wolf-Rayet stars depends on mass-loss rates, metallicity, the star-formation rate for high-mass stars, and the high-mass end of the initial mass function (IMF) (Meynet et al 1994, Massey & Armandroff 1995, Massey 1998). Among Local Group dwarfs, only IC 1613, NGC 6822 and IC 10 are known to contain Wolf-Rayet stars.

BLUE-LOOP STARS   Stars of intermediate mass evolve through prolonged "blue loops" after they ignite He in their cores. The luminosities at which the loops occur depend principally on the mass of the star, though the color and extent of the loop is critically sensitive to metallicity. For stars ranging in age from 100–500 Myr, the loop luminosities (L_{BL}) fade monotonically with age. Dohm-Palmer et al (1997) used deep HST photometry that clearly separates the upper main-sequence and blue-loop stars in the color-magnitude diagram of Sextans A. They constructed a luminosity function (LF) for the blue loop stars that is uncontaminated by other evolutionary phases. Because of the nearly one-to-one correspondance of luminosity and age for these stars, they were able to then directly convert the LF into the star-formation history of Sextans A with only an age-L_{BL} relation from models. Cepheid variables are closely associated with blue-loop evolution (Chiosi et al 1992, Schaller et al 1992).

RED SUPERGIANTS   Mermilliod (1981) demonstrated that red supergiants also fade monotonically with age for populations ranging from about 10–500 Myr in age. However, these stars exhibit a moderate spread in luminosity at a given age. For a composite system—such as a dwarf galaxy—the red supergiant LF will contain stars exhibiting a range of ages at a given luminosity. Both the blue-loop and red supergiant phases are short-lived (Maeder & Meynet 1988, Chiosi et al 1992, Schaller et al 1992, Wilson 1992a) and, therefore, subject to added uncertainties from the stochastic nature of star formation, particularly in dwarfs (Aparicio & Gallart 1995).

ASYMPTOTIC GIANT BRANCH STARS   Gallart et al (1996a,b) descriptively refer to the AGB as the "red tail" extending redward from the RGB. They also discuss in detail the practical problems of using the AGB to derive quantitatively the intermediate-age star-formation history of a galaxy. Figure 23 of Gallart et al (1996b) shows clearly that the details the mass-loss prescription used to model the AGB is critical to properly describe AGB evolution (see also Charbonnel et al 1996). Consequently, ages for AGB stars probably cannot be determined to better than a factor of 2–3. Nevertheless, AGB stars often provide our only

constraint on stellar populations older than ~1 Gyr in many distant galaxies within and beyond the Local Group. Long-period variables are often found among luminous AGB stars (Olszewski et al 1996b).

RED GIANT BRANCH STARS   The RGB plays an important role in understanding the chemical-enrichment histories of dwarf galaxies (Section 5.1), largely because its properties are relatively insensitive to age. Unfortunately, for a given metallicity, stars spanning a large age range are funneled into a very narrow corridor within optical color-magnitude diagrams (Chiosi et al 1992, Schaller et al 1992). The RGB serves only as a relatively crude age indicator for populations older than 1 Gyr (Schaller et al 1992, Ferraro et al 1995). Long-period variables are found near the upper tip of the RGB (Caldwell et al 1998, Olszewski et al 1996b).

RED-CLUMP AND HORIZONTAL BRANCH STARS   The He core burning phase occurs in a "red clump" located at the base of the RGB for populations with ages in the range 1–10 Gyr. The detailed evolution of this clump has been studied recently by Caputo et al (1995); its empirical behavior as a function of age in Magellanic Cloud star clusters has been determined by Hatzidimitriou (1991). The clump evolution in luminosity ($\lesssim 1$ mag) and color ($\lesssim 0.5$ mag) is small even for large age differences.

Horizontal branch (HB) stars—also undergoing core He burning—signal the presence of ancient populations ($\gtrsim 10$ Gyr; Olszewski et al 1996b). RR Lyr stars are an easily identified example of HB stars; blue HB stars are also distinctive but are known to exist in only two Local Group dwarfs (Carina and Ursa Minor), while RR Lyr stars have been found in 13 systems (Section 9). The red HB is also indicative of an old population, but distinguishing it from the red clump in an intermediate-age population can be difficult (Lee et al 1993a, Caputo et al 1995). A beautiful example of the relationship of red-clump and blue HB stars is shown by Smecker-Hane et al (1994) for Carina.

SUBGIANT BRANCH STARS   Stars with main-sequence lifetimes longer than about 2–4 Gyr evolve slowly towards the RGB after they exhaust hydrogen in their cores, resulting in a well-populated subgiant branch below the luminosity of the HB/red-clump stars (Meynet et al 1993). At a given metallicity, the minimum luminosity of subgiant branch stars fades monotonically with increasing age. Bertelli et al (1992) and Hurley-Keller et al (1998) rely heavily on the subgiant branch to determine the star-formation history of composite populations.

MAIN-SEQUENCE STARS   The main sequence is the only evolutionary phase present in populations of all ages. Unlike the subgiant branch, the maximum

luminosity of the main sequence (the main-sequence turnoff) fades with increasing age. When an age spread is present, older populations can be hidden by the unevolved main-sequence stars of younger populations. However, used in conjunction with the subgiant branch, the main sequence provides the only method of determining ages for populations older than 1–2 Gyr with ∼1 Gyr resolution (Bertelli et al 1992, Holtzman et al 1997, Hurley-Keller et al 1998). The main sequence has one particularly useful feature: The maximum luminosity on the main sequence can always be related to the age of the youngest population at the precision of sampling uncertainties. Short-period dwarf Cepheids are associated with metal-poor main-sequence populations (Nemec et al 1994, McNamara 1995, Mateo et al 1998b).

6.3   A Compilation of Star-Formation Histories of Local Group Dwarfs

Hodge (1989) introduced the concept of "population boxes" as a way of visualizing the star-formation and chemical-enrichment histories of galaxies. These three-dimensional plots show time, abundance, and star-formation rate on orthogonal axes. Unfortunately, we generally lack sufficiently detailed information to plot real galaxies in this manner, though some recent studies have begun to do so (Gallart et al 1996b,c, Aparicio et al 1997a–c, Grebel 1997). In order to present the star-formation history of Local Group dwarfs in a uniform manner, I choose here to plot only the relative star-formation rate vs time in Figure 8 for 29 of these galaxies (see also van den Bergh 1994c). I have tried to convey the uncertainties of these results as described in the caption; however, sampling errors and systematic effects due to the evolutionary models are extremely difficult to estimate with any precision. References for individual galaxies are listed in the caption.

A number of important conclusions regarding the star-formation history of Local Group dwarf galaxies can be drawn from Figure 8.

1. No two Local Group dwarfs have the same star-formation history.

2. Many dIrr galaxies appear to contain significant old populations as indicated by their pronounced RGBs (WLM, NGC 3109, NGC 6822) or by the presence of RR Lyr stars (IC 1613).

3. The most recent star-formation episodes are relatively short—ranging from 10–500 Myr in duration—in both dIrr and early-type systems (WLM, NGC 205, IC 1613, Fornax, Carina, Sextans B, Sextans A, NGC 6822, Pegasus). Since all age indicators quickly lose resolution for ages exceeding ∼1 Gyr, it is probably safe to assume that short-duration bursts are typical of the entire evolution of these galaxies. For example, the seemingly long
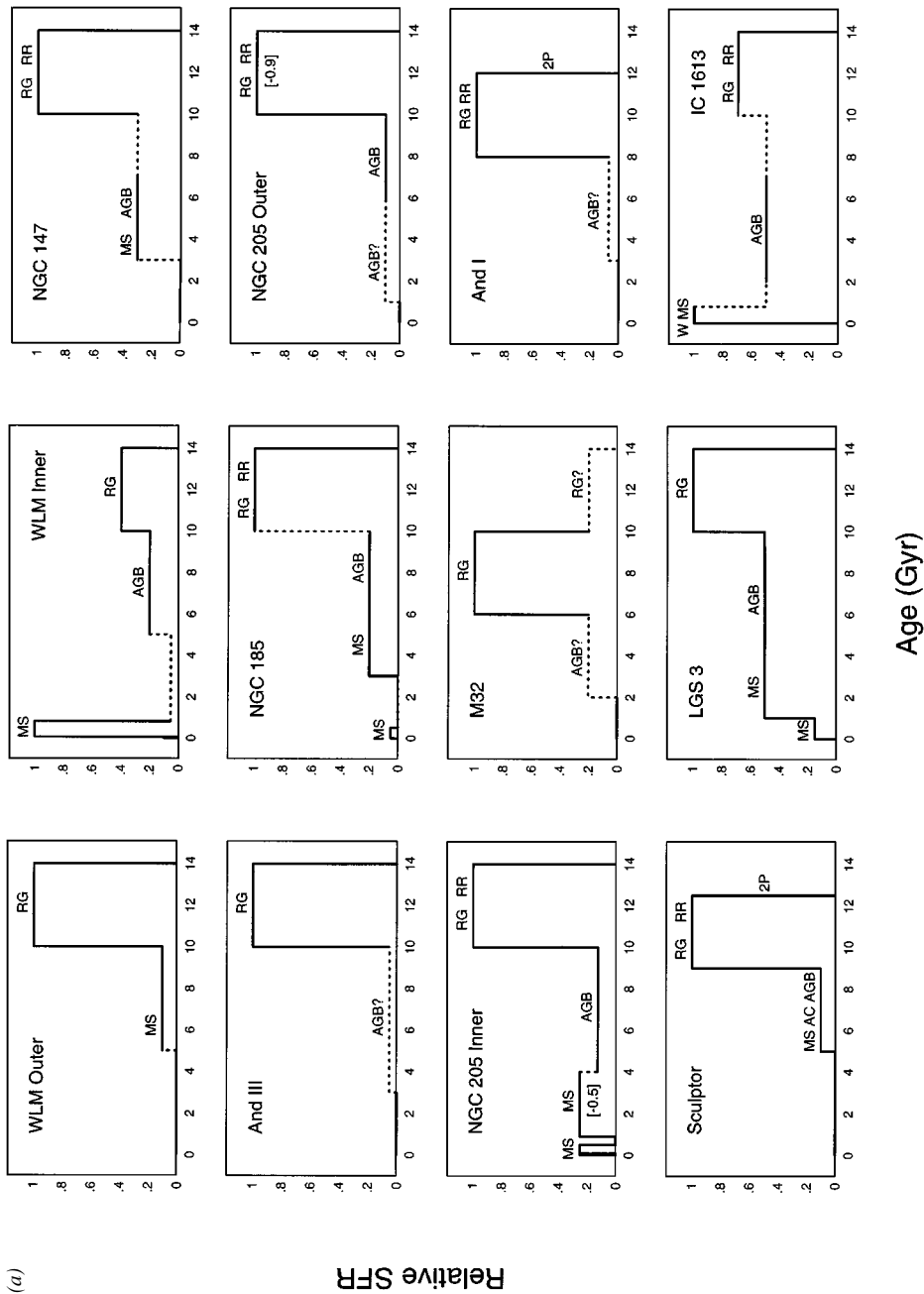
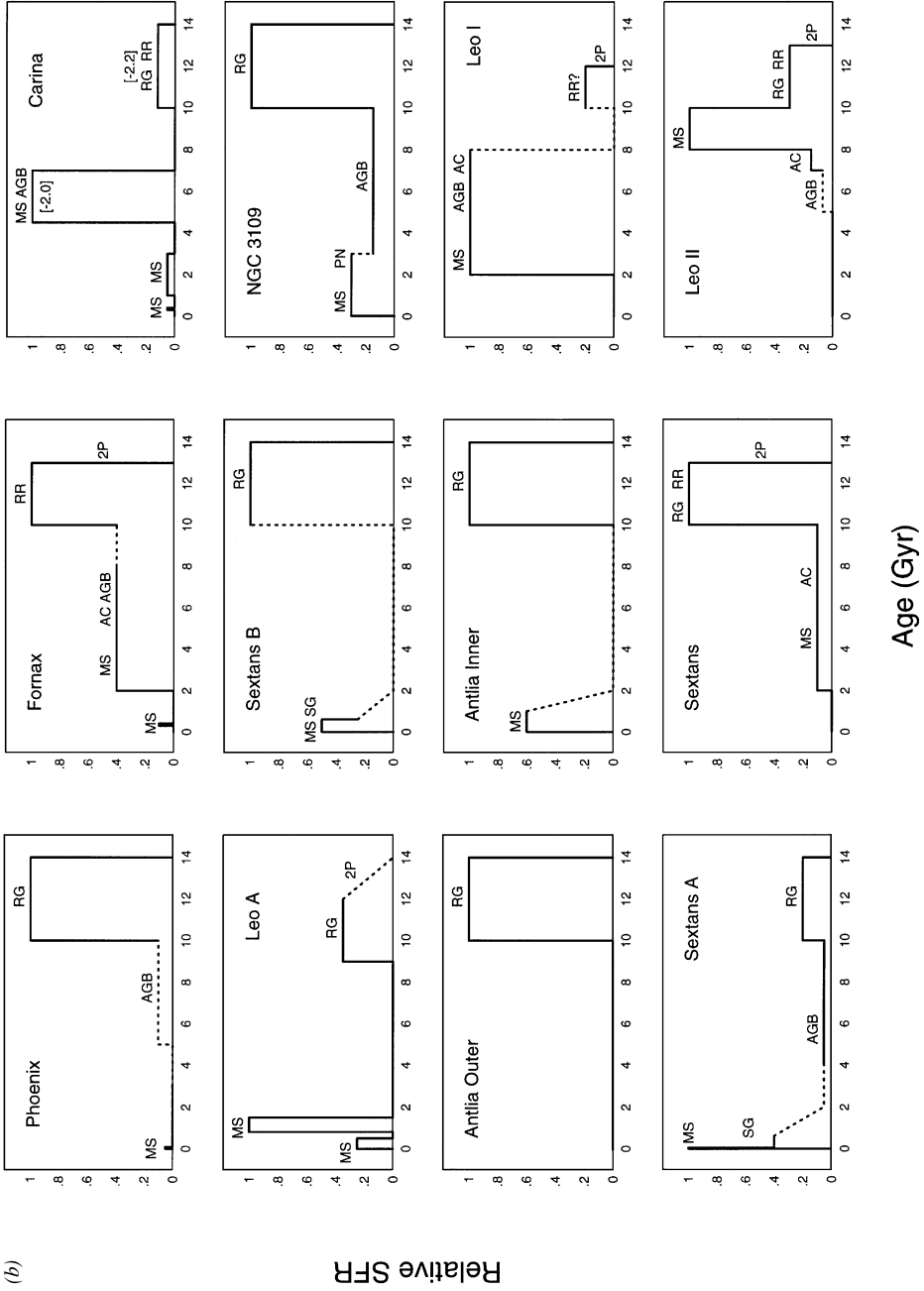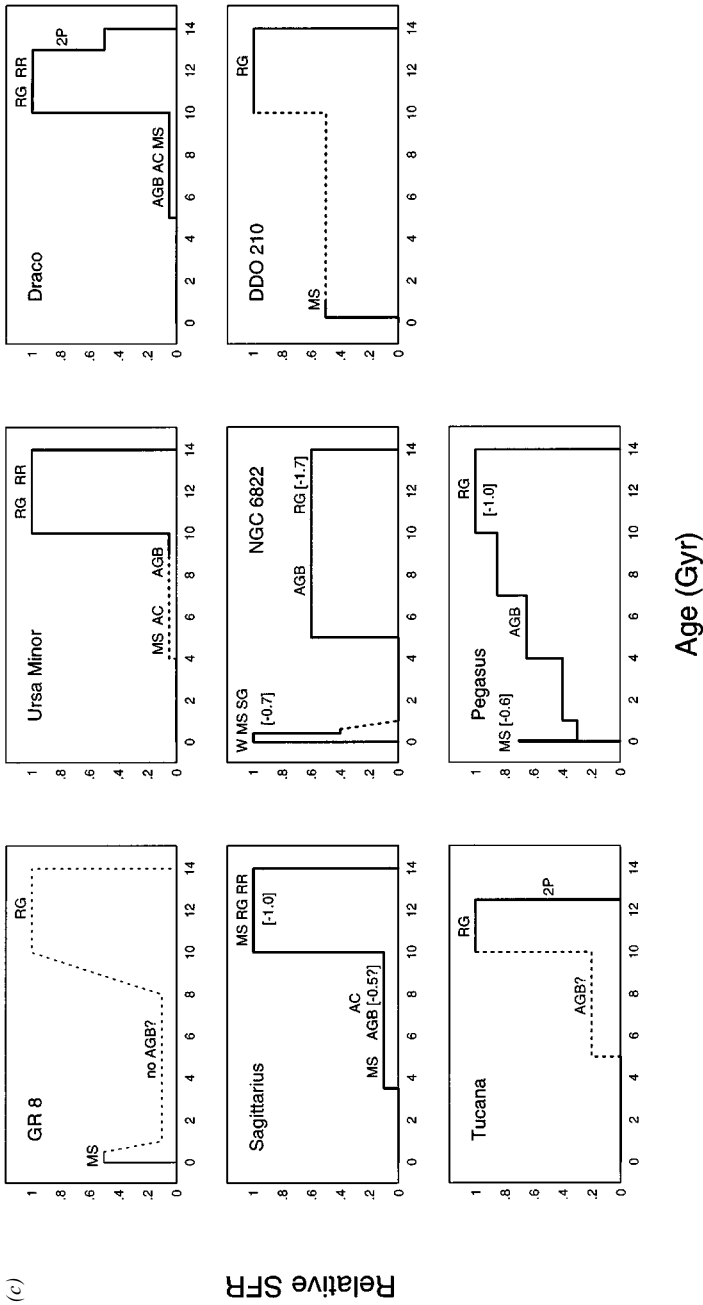*Figure 8*   (*Continued*)

Figure 8   (Continued)

Figure 8 Schematic plots of the star-formation histories of all Local Group dwarfs with sufficient data. The *labels within the individual panels* specify the nature of the stellar indicators used to infer the presence of a given age component: MS = main-sequence stars; AGB = asymptotic giant branch stars; RG = red giants; RR = RR Lyr variables; AC = anomalous Cepheids; SG = blue and red supergiants; W = Wolf-Rayet stars; PN = planetary nebulae. "2P" means that the galaxy has an anomalously red horizontal-branch (HB) population for its (low) metallicity—that is, the galaxy exhibits

the second parameter effect. *Numbers within square brackets* denote the metallicities of specific star-forming epochs; this information is generally quite uncertain and is available for only a few systems.

The reliability of the various star-formation episodes for a given galaxy is denoted by the style of the lines use to plot them: *solid horizontal lines* indicate that the duration of a given age component is fairly well determined; *solid vertical lines* indicate that the relative star-formation rate of a given event with respect to other star-formation episodes is reasonably well constrained; *dashed horizontal and vertical lines* indicate very great uncertainties in the duration or relative strength of individual star-formation periods. The galaxies are plotted in the same order that they are listed in the tables by increasing right ascension. Some of the galaxies listed as Local Group members in Table 2 are not plotted because of insufficient data, usually for the old and intermediate-age populations. Many of these cases are discussed in the text. For a few galaxies, *separate panels* show the star-formation histories of the inner and outer regions.

REFERENCES FOR FIGURE 8: *WLM:* Sandage & Carlson (1985b), Cook et al (1986), Ferraro et al (1989), Minniti & Zijlstra (1996); *NGC 147:* Mould et al (1983), Saha et al (1990), Davidge (1994), Han et al (1997); *And III:* Armandroff et al (1993); *NGC 185:* Saha & Hoessel (1990), Lee et al (1993b); *NGC 205:* Mould et al (1984), Richer et al (1984), Saha et al (1992b), Lee (1996); *M32:* Davidge & Jones (1992), Freedman (1992), Elston & Silva (1992), Grillmair et al (1996); *And I:* Da Costa et al (1996); *Sculptor:* Da Costa (1984), Azzopardi et al (1985, 1986); *LGS 3:* Lee (1995a), Aparicio et al (1997b); *IC 1613:* Freedman (1988), Saha et al (1992a); *Phoenix:* Ortolani & Gratton (1988), van de Rydt et al (1991); *Fornax:* Buonanno et al (1985), Demers et al (1995), Beauchamp et al (1995), Demers et al (1998); *Carina:* Mould & Aaronson (1983), Azzopardi et al (1985, 1986), Mighell (1990, 1997), Smecker-Hane et al (1994), Hurley-Keller et al (1998); *Leo A:* Tolstoy et al (1998); *Sextans B:* Tosi et al (1991), Marconi et al (1995); *NGC 3109:* Richer & McCall (1992), Greggio et al (1993), Davidge (1993), Bresolin et al (1993); *Antlia:* Aparicio et al (1997a), Sarajedini et al (1997), Whiting et al (1997); *Leo I:* Azzopardi et al (1985, 1986), Reid & Mould (1991), Caputo et al (1995), Gallart et al (1998); *Sextans A:* Dohm-Palmer et al (1997); *Sextans:* Mateo et al (1991a), Suntzeff et al (1993), Mateo et al (1995a); *Leo II:* Azzopardi et al (1985), Mighell & Rich (1996); *GR 8:* Dohm-Palmer et al (1998); *Ursa Minor:* Olszewski & Aaronson (1985); *Draco:* Carney & Seitzer (1986), Azzopardi et al (1986), Grillmair et al (1998); *Sagittarius:* Ibata et al (1994), Mateo et al (1995b), Sarajedini & Layden (1995), Mateo et al (1996), Alard (1996), Fahlman et al (1996), Ibata et al (1997), Marconi et al (1998); *NGC 6822:* Hodge (1980), Armandroff & Massey (1991), Gallagher et al (1991), Wilson (1992a), Marconi et al (1995), Gallart et al (1996a–c); *DDO 210:* Marconi et al (1990), Greggio et al (1993); *Tucana:* Lavery & Mighell (1992), Saviane et al (1996), Castellani et al (1996); *Pegasus:* Aparicio & Gallart (1995), Aparicio et al (1997b).

intermediate-age episode of star formation in Carina may actually have been a set of short, but observationally unresolved, bursts.

4. The second-parameter effect is common throughout the Local Group. That is, many galaxies with low metallicities possess relatively red HBs (Zinn 1980, Sarajedini et al 1997). This suggests that the most ancient populations of these galaxies are younger than the oldest Galactic globular clusters. However, Draco (Grillmair et al 1998) seems to present an interesting exception. Main-sequence photometry reveals an old population, yet the galaxy's HB is red. In this case, age does not seem to be the second parameter.

5. No single galaxy is composed exclusively of stars older than 10 Gyr, with the possible exception of Ursa Minor.

6. Some galaxies may contain very few or no stars older than 10 Gyr (M32 and possibly Leo I).

7. van den Bergh (1994b) suggested that dSph galaxies nearest the Milky Way are on average older than more distant systems. But this is not strongly supported by Figure 8. Carina, Fornax, and Leo I are all "young" systems and are found 100–270 kpc from the Milky Way; Ursa Minor, Leo II, and Tucana are predominantly old systems found 70–880 kpc from the Milky Way. NGC 205 contains young stars yet is located near M31 (Section 3.2; Hodge 1973).

Most of the remaining galaxies listed in Table 2 that are not represented in Figure 8 simply have insufficient data for even an educated guess of their entire star-formation histories. One galaxy deserves special mention. Massey & Armandroff (1995) noted that IC 10 has the highest surface density of Wolf-Rayet stars of any region in any Local Group galaxy. Two H_2O masers—also considered to be tracers of high-mass star formation—have been found in IC 10 (Becker et al 1993). Radio continuum and optical $H\alpha$ imaging reveal evidence of an enormous multiple-supernova–driven bubble (Hunter et al 1993, Yang & Skillman 1993). The inferred star-formation rate of IC 10 (Table 5) is the highest by far of any Local Group dwarf. By comparison, if Carina formed its entire dominant intermediate-age population in 10 Myr, its total star-formation rate would only slightly have exceeded what we see today in IC 10 (Hurley-Keller et al 1998).

Some galaxies are plotted in Figure 8 twice because of evidence that they exhibit significantly different star-formation histories in their inner and outer regions. Radial population gradients have been detected in many early-type systems (And I, Leo II, Sculptor, but not Carina: Da Costa et al 1996; NGC 205: Jones et al 1996; Antlia: Aparicio et al 1997a), often as a gradient in the HB

morphology. Aparicio et al (1997a) commented on the core/halo morphology now evident in some Local Group dIrr systems (see also Minniti & Zijlstra 1996). Mighell (1997) argued that the strong intermediate-age burst of star-formation in Carina started in the center of that galaxy and then progressed outward.

7.   INTERNAL KINEMATICS OF LOCAL GROUP DWARFS

For a given mass-to-light ratio, the central velocity dispersion of a self-gravitating system in equilibrium scales as $(R_c S_0)^{1/2}$, where R_c is the characteristic radial scale length of the system and S_0 is the central surface brightness in intensity units (Richstone & Tremaine 1986). Globular clusters have central velocity dispersions of 2–15 km s^{-1}. Pressure-supported dwarf galaxies that have central scale lengths about 10 times larger and surface brightnesses 10^3 times smaller should therefore have central velocity dispersions of ≤ 2 km s^{-1}. They don't. All low-luminosity dwarfs have central velocity dispersions of $\gtrsim 7$ km s^{-1}, independent of galaxy type and regardless of whether the dispersion is measured from the stars or gas. In this section, I review the observational basis for DM in the dwarf galaxies of the Local Group, and discuss some possible alternatives to DM in these systems. The seminal paper of this field was written by Aaronson (1983). Recent reviews include those by Gallagher & Wyse (1994), Mateo (1994), Pryor (1994, 1996), Gerhard (1994), and Olszewski (1998).

7.1   *The Observational Basis for Dark Matter*

To estimate kinematic masses for galaxies, we require a measure of the velocity dispersion for pressure-supported systems, or the rotation velocity for rotationally supported galaxies, and an estimate of the relevant scale length. To determine mass-to-light ratios, we further need the luminosity density or total luminosity. The scale length required depends on the details of the dynamical model used to interpret the kinematics; for nonrotating dwarfs, the King core radius or exponential scale length is commonly used (Table 3), whereas for rotating systems, the relevant length scale is taken from the rotation curve (Table 7).

DSPH GALAXIES   Because they generally lack an ISM component (or when they do, it is not in dynamical equilibrium; see Section 4) and because they have such low surface brightnesses, the internal kinematics of most Local Group dSph galaxies are based on high-precision spectroscopic radial velocities of individual stars (Mateo 1994, Olszewski 1998). There have been at least

four persistent criticisms of the reliability of dSph kinematics derived in this manner.

1. Some early claims of large central velocity dispersions were based on spectra with single-epoch errors exceeding $\sim$5–10 km s^{-1}. Most recent studies rely on spectra and reduction techniques that deliver single-epoch errors of 1–4 km s^{-1} (Mateo et al 1991b; Hargreaves et al 1994b, 1996b; Olszewski et al 1995). These smaller errors have been confirmed from comparisons of results for common stars from independent studies (Hargreaves et al 1994b, 1996b; Armandroff et al 1995; Queloz et al 1995).

2. The most luminous AGB stars are subject to atmospheric motions, or "jitter," with amplitudes of 2–10 km s^{-1}. Virtually all recent studies have pushed far below the upper tip of the RGB to luminosities where jitter is not seen in globular cluster red giants (Mateo et al 1991b, 1993; Hargreaves et al 1994a,b, 1996b; Queloz et al 1995; Vogt et al 1995).

3. Improved simulations of the effects of binaries have convincingly shown that, barring a pathological binary period distribution, dispersions based even on single-epoch observations are negligibly affected by binary motions (Hargreaves et al 1996a, Olszewski et al 1996a). The limited data available suggest that the binary frequency and period distribution are not radically different in dSph galaxies from what is seen in the solar neighborhood (Mateo et al 1991b; Hargreaves et al 1994b, 1996b; Olszewski et al 1995, 1996a; Queloz et al 1995).

4. In recent years, samples of over 90 stars have become available in many dSph galaxies (Armandroff et al 1995, Olszewski et al 1996a, Mateo 1997, Olszewski 1998). It is now possible to meaningfully measure departures from Gaussian distributions for such large samples (Merrifield & Kent 1990, Olszewski 1998) or construct velocity dispersion profiles within single galaxies (Mateo et al 1991b; Da Costa 1994a; Hargreaves 1994a,b, 1996b; Armandroff et al 1995; Mateo 1997).

These observational advances strongly suggest that modern measurements of the velocity dispersions of Local Group dSph galaxies are indeed reliable estimates of the true one-dimensional dispersions of these systems. I conclude that no dSph galaxy has a central velocity dispersion smaller than 6.6 km s^{-1} (Table 7).

DIRR GALAXIES   Standard procedures exist to derive rotation curves for dIrr galaxies within and beyond the Local Group (Jobin & Carignan 1990, Puche et al 1990, 1991). However, only within the Local Group do we encounter dIrr

galaxies whose kinematics are not dominated by rotation at all radii (Carignan et al 1990, 1991; Lo et al 1993; Young & Lo 1996a, 1997b). GR 8 exhibits rotation in its inner regions but then becomes pressure supported at large radii (Carignan et al 1990). The typical measure of the velocity dispersion in gas-rich but nonrotating dwarfs is from the 21-cm line width. Lo et al (1993) addressed this problem in detail; they recommended that where possible, the dispersion be based on the line-of-sight dispersion of the mean velocities of individual clouds. In practice, the two approaches seem to agree to within their combined errors.

7.2   *Constraints on Dark Matter in Local Group Dwarfs*

To determine masses and central mass densities of dSph galaxies, the King formalism is generally adopted (Richstone & Tremaine 1986), along with the simplifying assumptions that mass follows light and that the velocity dispersion is isotropic. Pryor & Kormendy (1990) have investigated the sensitivity of the derived masses for dSph galaxies on these and other assumptions. In general, the resulting M/L ratios for most dSph galaxies with good surface photometry are robust to within a factor of two (Pryor 1994, Mateo 1994, 1997). This same approach is also used to derive masses for pressure-supported dIrr systems (Lo et al 1993, Young & Lo 1997b). The rotation curves of the more luminous Local Group dIrr galaxies are typically fit with two-component models. One component of fixed M/L follows the visible-light or HI distribution; the second dark component is usually fit as an isothermal sphere to represent an extended dark halo. All of the Local Group dwarfs require both components for an adequate fit to the observed rotation curves. These techniques implicitly assume the galaxies are in dynamical equilibrium.

Figure 9 is a plot of the derived M/L ratios for all Local Group dwarfs with adequate data in Table 7. The King method (Richstone & Tremaine 1986) allows calculation of both the central density and total mass under the assumptions listed above. For the pressure-supported galaxies, plotting the central M/L ratio is therefore possible, while for all systems with kinematic data, the global M/L can be derived.

The dIrr and early-type galaxies are clearly separated in the *lower panel* of Figure 9. This is not surprising: The dIrr systems all have masses constrained by rotation curves at large radii that can only be understood if the galaxies possess extended DM halos. For the early-type galaxies, the King formalism assumes that mass follows light. Hence, it is likely that the M/L ratios of all the early-type dwarfs are underestimated. Figure 9 also shows that the distribution of M/L ratios for the early-type dwarfs can be fit with the relation $\log M/L = 2.5 + 10^7/(L/L_\odot)$; these galaxies are consistent with the idea that each is embedded in a dark halo of fixed mass of about $10^7 \, M_\odot$ and contains a luminous
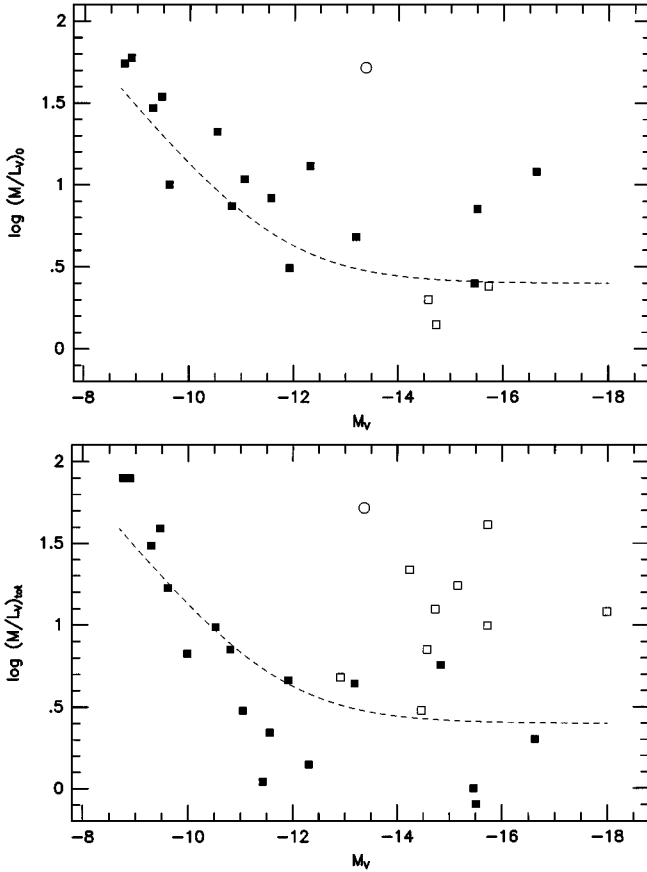
Figure 9 Kinematically determined mass-to-light ratios of local group dwarfs as a function of luminosity. *Top panel*: $\log(M/L)_0$ from Table 4 vs M_V. *Filled squares* are for dSph or dSph/Irr systems for which masses were determined from the central velocity dispersions, while the *open squares* represent Irr systems that have masses derived here from HI rotation curves. See Table 4 for details or the original sources to obtain definitive kinematic mass estimates for these galaxies. Sagittarius is denoted as an *open circle*. *Bottom panel*: $\log(M/L)_{tot}$ from Table 4 vs M_V; the *symbols* are the same as in the *top panel*. In each panel I have also plotted the function $\log M/L = 2.5 + 10^7/(L/L_\odot)$ as a *dashed line*.

component with $M/L_V = 2.5$. This is a lower limit to the halo mass because the dark matter may plausibly be more extended than the luminous material.

Local Group dwarfs have proven useful to restriction of some possible forms of DM. For example, massive neutrinos have been ruled out in dSph galaxies from phase-space arguments (Lin & Faber 1983, Lake 1989a, Gerhard & Spergel 1992). Massive black-hole models (Strobel & Lake 1994) are also incompatible with the generally smooth central surface brightness distributions of the cores of dSph systems or the large global M/L ratios inferred in these systems (Demers et al 1995).

7.3   *Alternatives to Dark Matter*

The current fashion is to assume that the kinematic observations described above constitute part of a DM problem. However, it may be wise to remember that this already implies a solution to what remains a long-standing crisis in understanding the internal kinematics of galaxies. In this section, I discuss two possible alternatives to DM as they apply to Local Group dwarfs.

TIDES   Kuhn & Miller (1989) and Kuhn (1993) proposed that one way to mimic the kinematic effects of DM was through a resonance process between the orbital period of a dwarf and its natural radial oscillation period. Pryor (1996) and Olszewski (1998) reviewed recent studies that suggested that this mechanism is unlikely to have a significant effect on real dSph galaxies and for actual observational samples of stars used in kinematic studies. I add only two points here. First, tidal effects are indeed visible in many Local Group dwarfs (Section 8), but this alone does not imply that the central velocity dispersions, and hence the inferred mass-to-light ratios, are significantly affected until the galaxies are nearly completely disrupted. Second, the M/L ratios of isolated early-type galaxies such as LGS 3 and Leo II are sufficiently high to require DM, yet they are sufficiently far from any large galaxies that they cannot be affected significantly by tides. Kinematic studies of other isolated dwarfs such as Antlia and Tucana would be particularly helpful in settling this issue.

MODIFIED GRAVITY   Milgrom (1983a,b) introduced Modified Newtonian Dynamics, or MOND, to understand the rotation curves of disk galaxies (and some other related phenomena) with a modified form of Newton's law of gravity without resorting to DM. Only at very low accelerations (defined by the parameter $a_0 \sim 2 \times 10^{-8}$ cm sec^{-2}) is Newton's law substantially altered from its standard form.

A single unambiguous example of a galaxy strictly obeying Newtonian dynamics in the low-acceleration regime would falsify MOND instantly. I do not address here how MOND currently fares with regard to understanding the dynamics of large galaxies apart from noting that no unambiguous failures have

yet been reported (Sanders 1996, McGaugh & de Block 1998). Nor do I discuss the far-reaching implications of MOND on cosmology and other areas of astrophysics (Bekenstein & Milgrom 1984, Felton 1984, Sivaram 1994, Qiu et al 1995, Sanders 1997). Instead, I focus here on the use of Local Group dwarfs to test MOND.

Lake & Skillman (1989) and Lake (1989b) suggested that the rotation curves of IC 1613 and NGC 3109 could not be explained by MOND unless $a_0 \leq 3 \times 10^{-9}$ cm sec^{-2}, a value that is incompatible with that needed to interpret rotation curves of giant systems. Milgrom (1991) noted that (*a*) MOND successfully fit the shapes of the rotations curves of these and other galaxies discussed by Lake (1989b) and (*b*) the mixed success that MOND had in reproducing the amplitudes of the rotation curves could be understood given the errors in the galaxy distances, inclinations, and asymmetric-drift corrections. For NGC 3109 (Jobin & Carignan 1990), Milgrom was in fact justified in claiming the earlier rotation curve was in error, though in the case of IC 1613, it remains unclear if Milgrom's objection to Lake & Skillman's (1989) conclusion is valid. More recently, Sanders (1996) found that the rotation curves of both NGC 55 and NGC 3109 are fit well by MOND.

Gerhard & Spergel (1992b) argued that the internal kinematics of Local Group dSph galaxies demanded DM even if MOND was used to estimate their masses. Lo et al (1993) found that the MOND masses for many nearby dIrr galaxies were smaller than their integrated HI masses—an obvious failure if correct. Milgrom (1995) responded that if the observational errors and most recent results were considered, neither effect claimed by Gerhard & Spergel (1992b) was observed. In the second case, Lo et al (1993) used an incorrect expression to determine the MOND masses, leading to estimates that were too small by a factor of 20 (Milgrom 1994). When the proper relation is used ($M_{\mathrm{MOND}} = 81\sigma_0^4/4a_0 G$, where σ_0 is the observed central velocity dispersion for an isotropic system), the MOND masses are consistent with the inferred luminous (gaseous + stellar) masses without invoking a dark component.

The burden of proof remains squarely on MOND, but the kinematic data for Local Group dwarfs does not yet refute this alternative to DM.

8.   INTERACTIONS IN THE LOCAL GROUP

The Local Group is a dangerous place for dwarf galaxies. NGC 205 and Sagittarius have wandered too close to their dominant parents and exhibit clear kinematic and structural signatures of tidal distortions (Hodge 1973, Bender et al 1991, Pryor 1996, Ibata et al 1997). Irwin & Hatzidimitriou (1995) noted that many nearby dSph systems show a strong correlation of tidal radius or ellipticity with the strength of the external tidal field. Bellazzini et al (1996) have

shown convincingly that the central surface brightness, Σ_0, of dSph galaxies obey a bivariate relation in Σ_0, L_{tot}, and R_{GC}, where R_{GC} is the Galactocentric distance of the galaxy. They show that Sagittarius in particular appears to be unbound, even in its core (Mateo et al 1995c, but see Ibata et al 1992).

A number of models have investigated what dwarfs look like before, during, and after strong tidal encounters (Allen & Richstone 1988, Moore & Davis 1994, Johnston et al 1995, Oh et al 1995, Piatek & Pryor 1995, Velázquez & White 1995, Kroupa 1997). At early times in a strong interaction or in the weak-interaction limit, stars are lost from the dwarf into leading and trailing orbits. These stars quickly fill a larger volume than that of the original galaxy, and if they were included in kinematic samples, they would reveal streaming motions that could be interpreted as rotation. Extratidal stars might be seen at this stage, even though the majority of the galaxy's stars remain bound and the central velocity dispersion is unaffected (e.g. Gould et al 1992, Kuhn et al 1996; in both cases many of the stars discussed are actually within recent estimates of the tidal radii of the respective galaxies). At later stages of strong interactions, the dwarfs become strongly elongated but not necessarily parallel to the orbital path of their center of mass. Alcock (1997a) claimed to see such a tilt in Sagittarius, but Ibata et al (1997) did not. At very late stages of a nearly complete tidal disruption event, the dwarf becomes a long strand that is stretched along its orbit, with a small clump ($\leq 10\%$ of the original mass) as the only remnant of the original galaxy. At no time except the very end of the tidal episode does the central velocity dispersion significantly exceed its virial value, even for models with no initial dark component.

These disrupted dwarfs should produce relatively long-lived streams in the halos of galaxies such as M31 and the Milky Way (1–2 Gyr; P Harding, private communication). Lynden-Bell & Lynden-Bell (1995) concluded that one possible stream can be traced out with the Magellanic Stream (Wakker & van Woerden 1997), Ursa Minor, Draco, and possibly Carina and Sculptor. A recent determination of the proper motion of Sculptor (Schweitzer et al 1995) suggests that this galaxy is not part of this putative (or any other proposed) stream. There have been many intriguing claims of halo substructure in recent years (e.g. Arnold & Gilmore 1992, Majewski 1992, Côté et al 1993, Kinman et al 1996) that could possibly be remnants of disrupted dwarfs.

More recently, Alcock et al (1997b) and Zaritsky & Lin (1997) claimed to detect a possible signature of a foreground galaxy or galaxy tidal remnant towards the LMC. Gallart (1998) suggested instead that this new "galaxy" is in fact due to the signature of known but subtle stellar evolutionary phases that are becoming apparent in the large-scale photometric surveys carried out in the LMC. This is not the first time that a putative new galaxy has been detected directly in front of a known Local Group dwarf: Connolly (1985) identified a

Table 8 Summary of the contents of Local Group dwarf galaxies

Galaxy[a]	N_{RR}[b]	N_{Ceph}[c]	N_{Mira}[d]	N_{AC}[e]	Ref.[f]	N_{OBa}[g]	N_{WR}[h]	N_{HII}[i]	N_{Dust}[j]	Ref.[k]	N_{AGB}[l]	N_{PN}[m]	N_{GC}[n]	Ref.[o]
WLM[o]	—	15	—	—	64	—	—	21	—	37	10	2	1	2, 18, 32, 98
NGC 55	—	—	—	—		—	—	13	—	95	14+	1	5	55, 94, 96
IC 10	—	5–9	—	—	61, 97	—	16	144	—	34, 51, 76	—	5	3	98
NGC 147	32	—	—	—	60, 99	—	—	0	—	100	Yes	5	3	23, 28, 32, 101
And III											Yes?			5
NGC 185	151	—	—	—	59	—	—	1	2	42, 100, 102	Yes	5	9	16, 23, 32, 49
NGC 205[p,q]	30	—	12	~9	58	—	—	—	12	92	7+	28	12	16, 32, 47, 56, 92, 93
M32	—	—	—	—				0	0	103–105	Yes	30	0	16, 26, 32, 72, 73, 144
And I	4+	—	—	—	91	—	—	—	—		Yes	—	0	5, 6
Sculptor[p]	226+	—	1	11?	43, 52, 66, 82, 140	—	—	—	—		8	—	0	8, 9, 106–108, 143
LGS 3	—	—	—	—		—	—	0	—	37, 109	Yes	—	—	46
IC 1613	15	77+	—	—	13, 92, 110, 111	20	1	77	11	7, 31, 35, 54, 112	15	1	0	18, 32, 40, 71, 113
And II														
Phoenix	—	60?	—	—	69	—	—	—	—		—	—	—	114
Fornax[r,s]	400+	1	30	1	52, 70, 75, 136	—	—	—	—		82	1	5	10, 32, 106, 115, 116, 143
EGB 0427+63								25	—	37	—	—	—	
Carina[p]	69	—	—	9	43, 50, 52, 74, 83	—	—	—	—		9	—	—	8, 9, 143
Leo A	—	5?	—	—	38, 39	—	—	6–10	—	109, 117, 118	Yes	2–4	—	98, 117, 120
Sextans B	36	7	1	6	13, 53, 63	—	—	12	—	118, 121	Yes	0	—	98
NGC 3109	—	29	—	—	13, 14, 22, 65, 80	18	—	39	Yes	12, 14, 29	Yes	7	0–10	22, 57, 98, 122
Antlia								1	Yes?	78, 123, 124	Yes	—	—	78, 123, 124
Leo I[p]	Yes?	—	—	15	19, 50, 52, 85, 125	1+	—	—	—		19	—	—	8–10, 48, 143
Sextans A	—	10	—	—	13, 53, 62, 126	—	—	25	—	4, 33, 109, 127	Yes	1	—	98, 129
Sextans	36	—	1	6	50	—	—	—	—		0	—	—	143
Leo II[p]	152	—	—	4	21, 50, 52, 81	—	—	—	—		8	—	—	8–10, 20, 45, 130, 143
GR 8	—	1?	5?	—	67	—	0	32	—	36, 132	Yes	0	—	96, 133
Ursa Minor[p]	82	—	—	7	32, 52	—	—	—	—		1	—	—	9, 10
Draco[p]	280+	—	4	5+	52, 85, 134, 139	—	—	—	—		3–4	—	—	9, 10
Sagittarius	313+	—	4	—	1, 84, 135	—	—	—	—		4+	2	4	41, 84, 87–90
SagDIG	—	—	—	—		—	—	3	—	118	Yes	—	—	137

Galaxy													
NGC 6822[o,u]	—	13	—	13, 25, 44	16	157	4	—	7, 17, 30, 68, 131	40	8+	1	18, 24, 32, 138
DDO 210	—	0	—	69	—	—	—	—	—	Yes?	—	1	27
IC 5152	Yes	Yes?	—	69	—	—	—	—	—	—	—	—	—
Tucana	—	—	3?	15, 142	—	—	—	—	—	No?	—	—	15, 141, 142
UKS2323–326	—	—	—	38	—	—	—	—	11	—	—	—	—
Pegasus	—	7–10	—	38	—	1	—	1	3	Yes	1	—	3, 98

[a]Galaxy name.

[b–u]The census of known populations of variable stars: RR Lyr stars, Cepheids, Mira (long-period) variables, and Anomalous Cepheids.

[c–f]References for variable stars: 1, Alard 1996; 2, Ables & Ables 1977; 3, Aparicio 1994; 4, Aparicio & Rodriguez-Ulloa 1992; 5, Armandroff et al 1993; 6, Mould & Kristian 1990; 7, Armandroff & Massey 1991; 8, Azzopardi & Massey 1991; 9, Azzopardi et al 1985; 10, Aaronson et al 1983; 11, deleted in proof; 12, Bresolin et al 1993; 13, Capaccioli et al 1992; 14, Sandage & Carlson 1988; 15, Castellani et al 1996; 16, Ciardullo et al 1989; 17, Collier & Hodge 1994; 18, Cook et al 1986; 19, Demers et al 1994a; 20, Demers & Irwin 1993; 21, Swope 1967; 22, Demers et al 1985; 23, Ford et al 1977; 24, Gallart et al 1996a; 25, Gallart et al 1996c; 26, Grillmair et al 1996; 27, Greggio et al 1993; 28, Han et al 1997; 29, Hodge 1969; 30, Hodge 1977; 31, Hodge 1978; 32, Hodge 1988; 33, Hodge et al 1994; 34, Hodge & Lee 1990; 35, Hodge et al 1990; 36, Hodge et al 1989; 37, Hodge & Miller 1995; 38, Hoessel et al 1990; 39, Hoessel et al 1994; 40, Freedman 1988a; 41, Ibata et al 1994; 42, Hodge 1963b; 43, Kaluzny et al 1995; 44, Kayser 1967; 45, Lee 1995b; 46, Lee 1996; 48, Lee et al 1993a; 49, Lee et al 1993c; 50, Mateo et al 1995a; 51, Massey et al 1992; 52, Nemec et al 1988; 53, Piotto et al 1994; 54, Price et al 1990; 55, Pritchet et al 1987; 56, Richer & McCall 1992; 57, Richer et al 1984; 58, Saha et al 1992b; 59, Saha & Hoessel 1990; 60, Saha et al 1990; 61, Saha et al 1996; 62, Sandage & Carlson 1982; 63, Sandage & Carlson 1985a; 64, Sandage & Carlson 1985b; 65, Sandage & Carlson 1988; 66, Schweitzer et al 1995; 67, Tolstoy et al 1995; 68, Wilson 1992a; 69, Caldwell et al 1988; 70, Demers & Irwin 1987; 71, deleted in proof; 72, Freedman 1992; 73, Elston & Silva 1992; 74, Kuhn et al 1996; 75, Light et al 1986; 76, Massey et al 1992; 77, Saha et al 1992a; 78, Aparicio et al 1997c; 80, Musella et al 1997; 81, van Agt 1973; 82, van Agt 1978; 83, Saha et al 1986; 84, Whitelock et al 1996; 85, Hodge & Wright 1978; 86, deleted in proof; 87, Minniti & Zijlstra 1996; 88, Walsh et al 1997; 89, Da Costa & Armandroff 1995; 90, Zijlstra & Walsh 1996; 91, Da Costa et al 1996; 92, Hodge 1973; 93, Battistini et al 1987; 94, Da Costa & Graham 1982; 95, Ferguson et al 1996; 96, Liller & Alcaino 1983; 97, Wilson et al 1996; 98, Jacoby & Lesser 1981; 99, Saha & Hoessel 1987. 100, Young & Lo 1997a; 101, Hodge 1976; 102, Gallagher & Hunter 1981; 103, Ford & Jenner 1976; 104, Ford et al 1978; 105, van Dokkum & Franx 1995; 106, Richer & Westerlund 1983; 107, Hodge 1966; 108, Eskridge 1988b; 109, Hunter et al 1993; 110, Carlson & Sandage 1990; 111, Freedman 1988b; 112, Hodge 1980; 113, Lequeux et al 1987; 114, van de Rydt et al 1991; 115, Maran et al 1984; 116, Danzinger et al 1978; 117, Tolstoy 1996; 118, Strobel et al 1991; 119, Deleted in proof; 120, Tolstoy et al 1998; 121, Hodge 1974; 122, Davidge 1993; 123, Whiting et al 1997; 124, Sarajedini et al 1997; 125, Mateo et al 1998d; 126, Sakai et al 1996; 127, Hunter & Gallagher 1990; 128, Deleted in proof; 129, Dohm-Palmer et al 1997; 130, Mighell & Rich 1996; 131, Hodge et al 1988; 132, Drissen et al 1993; 133, Dohm-Palmer et al 1998; 134, Harris et al 1997. 135, Mateo et al 1995b; 136, Mateo et al 1998a; 137, Cook 1987; 138, Killen & Dufour 1982; 139, Baade & Swope 1961; 140, van Agt 1978; 141, Saviane et al 1996; 142, Lavery et al 1996; 143, Azzopardi 1994; 144, Davidge & Nieto 1992.

[g–j]The census of tracers of young populations: OB associations, Wolf-Rayet stars, HII regions, and discrete dust clouds.

[k]References for the young population tracers (see footnote f).

[l–m]The census of known intermediate-age and old-age population tracers: asymptotic giant branch (AGB) stars, planetary nebulae, and globular clusters.

[n]References for the intermediate-age and old-age tracers (see footnote f).

[o]The AGB census is for stars with $M_I \leq -4.4$.

[p]The AGB stars noted are principally C stars.

[q]The numbers of planetary nebulae are reported by Ciardullo et al (1989); see that paper for the original sources.

[r]Approximately 21 RR Lyr stars may be associated with Fornax cluster 1 (Smith et al 1996).

[s]The Cepheid is most likely a W Vir or Pop II Cepheid (Light et al 1986).

[t]Additional low-luminosity CH stars are also known on or near the AGB (Aaronson et al 1983).

[u]The numbers of Cepheids are reported by Capaccioli et al (1992); see that paper for the original sources.

number of "foreground" RR Lyr stars toward the LMC that he concluded are members based on their photometric properties but are nonmembers kinematically. Saha et al (1986) also identified some anomalously bright RR Lyr–like stars, apparently in front of the Carina dSph galaxy, that could be either part of an extended halo of the LMC or possibly associated with a foreground system. A more natural explanation may be that these are instead anomalous Cepheids in Carina itself (Mateo et al 1995a). In none of these cases is the true nature of all of these "foreground" stars conclusively established, and in the case of the LMC, it is not unreasonable to suppose that a tidal tail is present (Zaritsky & Lin 1997). Nevertheless, it seems wise to treat claims of the existence of galaxies or tidal features directly in front of known Local Group systems with particular caution.

Mateo (1996) and Unavane et al (1996) have discussed the possibility that a large fraction of the Galactic halo has been constructed from disrupted dSph systems. The latter considered Carina to be the template of such a system, while Mateo (1996) compared the properties of the ensemble of all Galactic dSph satellites with the halo. Neither approach is strictly correct. Carina arguably has the most unusual stellar population of any dSph system (Section 6.3; Figure 8); it is clearly not an appropriate choice as a template for the halo. On the other hand, present-day dSph systems are anomalous "survivors" that were able to form stars over a longer period than systems that were destroyed. They probably also follow orbits (relative to the Galaxy) that are quite distinct from the orbits of the galaxies that were consumed; thus, even an average of the stellar populations of all remaining dSph galaxies should not be expected to precisely match the current halo population. Given these differences in approach, the two studies nevertheless essentially agree: No more than 10% of the halo could have Carina-like progenitors (Preston et al 1994), but more than 50% of the halo could have formed from galaxies similar to the entire ensemble of Galactic dSph systems (though see van den Bergh 1994b).

9.   CONCLUSIONS

I hope that I have been able to convey the rich detail, the surprises, and the broad relevance of modern research on Local Group dwarfs. Nevertheless, this review only scratches the surface of this active field. Table 8 provides a census of various specific types of objects (variable stars; young, intermediate-age, and old ISM; and stellar population tracers) that can and have been used to study these systems in greater detail. Keep in mind that these dwarfs offer our best opportunities to study how stellar evolution proceeds in chemically young environments; they offer our best window into the nature of DM in what may be the smallest natural size scales of this material; and they may help us understand

if and how dwarfs help form larger galaxies via mergers. Many targets useful to attack these problems can be found in Table 8. We still have plenty of work to do with these nearby dwarfs to address these issues as well as the many others raised in this review.

But perhaps most exciting of all is that as we stand on the threshold of detailed studies of dwarf galaxies in other groups (e.g. Côté 1995, Côté et al 1997, Caldwell et al 1998), the Local Group dwarfs will serve as a benchmark against which other systems can be compared. We *know* that complex star-formation histories are common in the Local Group. We *know* that both dIrr and early-type dwarfs contain interstellar material, which manifests itself in many different ways. We *know* that Local Group dwarfs are kinematically peculiar, whether dominated by DM or not. Do dwarfs in other groups behave the same way? How do they differ? How many of these tendencies are truly universal, and how many due to the specific environmental circumstances of individual groups? These questions will lead to insights that we cannot gain from studies of only the galaxies in the Local Group. It will be an exciting adventure and one that is sure to uncover as many surprises as the dwarfs of the Local Group already have.

Literature Cited

Aaronson M. 1983. *Ap. J.* 266:L11–L15
Aaronson M. 1986. In *Star Forming Dwarf Galaxies and Related Objects*, ed. D Kunth, TX Thuan, JTT Van, pp. 125–44. Paris: Ed. Front.
Aaronson M, Olszewski EW, Hodge PW. 1983. *Ap. J.* 267:271–79
Ables HD. 1971. *US Naval Observatory*, Vol. 20, pt 4. Washington, DC: US Print. Off.
Ables HD, Ables PG. 1977. *Ap. J. Suppl.* 34: 245–58
Alard C. 1996. *Ap. J.* 458:L17–L20
Alcock C, Allsman RA, Alves DR, Axelrod TS, Becker AC, et al. 1997a. *Ap. J.* 474:217–22
Alcock C, Allsman RA, Alves DR, Axelrod TS, Becker AC, et al. 1997b. *Ap. J.* 490:L59–L63
Allen AJ, Richstone DO. 1988. *Ap. J.* 325:583–95
Allsopp NJ. 1978. *MNRAS* 184:397–404
Anders E, Grevesse N. 1989. *Geochim. Cosmochim. Acta* 53:197–214
Aparicio A. 1994. *Ap. J.* 437:L27–L30
Aparicio A, Dalcanton JJ, Gallart C, Martínez-Delgado D. 1997a. *Astron. J.* 114:1447–57
Aparicio A, Gallart C. 1995. *Astron. J.* 110: 2105–19
Aparicio A, Gallart C, Bertelli G. 1997b. *Astron. J.* 114:669–79
Aparicio A, Gallart C, Bertelli G. 1997c. *Astron. J.* 114:680–93
Aparicio A, García-Pelayo JM, Moles M. 1988. *Astron. Astrophys. Suppl.* 74:375–84
Aparicio A, Rodríguez-Ulloa JA. 1992. *Astron. Astrophys.* 260:77–81
Armandroff TE, Da Costa GS. 1986. *Astron. J.* 92:777–86
Armandroff TE, Da Costa GS, Caldwell N, Seitzer P. 1993. *Astron. J.* 106:986–98
Armandroff TE, Massey P. 1991. *Astron. J.* 102:927–50
Armandroff TE, Olszewski EW, Pryor C. 1995. *Astron. J.* 110:2131–65
Arnold R, Gilmore G. 1992. *MNRAS* 257:225–39
Ashman K. 1992. *PASP* 104:1109–38
Azzopardi M. 1994. See Layden et al 1994, pp. 129–40
Azzopardi M, Lequeux J, Westerlund BE. 1985. *Astron. Astrophys.* 144:388–94
Azzopardi M, Lequeux J, Westerlund BE. 1986. *Astron. Astrophys.* 161:232–36
Baade W, Swope H. 1961. *Astron. J.* 66:300–47
Babul A, Rees MJ. 1992. *MNRAS* 255:346–50

Battistini P, Bònoli F, Barccesi A, Federici L, Fusi Pecci F, et al. 1987. *Astron. Astrophys. Suppl.* 67:447–82
Beauchamp D, Hardy E, Suntzeff NB, Zinn R. 1995. *Astron. J.* 109:1628–44
Becker R, Henkel C, Wilson TL, Wouterloot JGA. 1993. *Astron. Astrophys.* 268:483–90
Bekenstein J, Milgrom M. 1984. *Ap. J.* 286:7–14
Bellazzini M, Fusi Pecci F, Ferraro FR. 1996. *MNRAS* 278:947–52
Bender R, Nieto JL. 1990. *Astron. Astrophys.* 239:97–112
Bender R, Paquet A, Nieto JL. 1991. *Astron. Astrophys.* 246:349–53
Bendinelli O, Parmeggiani G, Zavatti F, Djorgovski S. 1992. *Astron. J.* 103:110–16
Bertelli G, Bressan A, Chiosi C, Fagotto F, Nasi E. 1994. *Astron. Astrophys. Suppl.* 106:275–302
Bertelli G, Mateo M, Chiosi C, Bressan A. 1992. *Ap. J.* 388:400–14
Bica E, Alloin D, Schmidt AA. 1990. *Astron. Astrophys.* 228:23–36
Binggeli B. 1994. In *Panchromatic View of Galaxies*, ed. G Hensler, C Theis, J Gallagher, pp. 173–91. Paris: Ed. Front.
Bothun GD, Mould JR, Caldwell N, MacGillivray HT. 1986. *Astron. J.* 92:1007–19
Bothun GD, Thompson IB. 1988. *Astron. J.* 96:877–83
Bowen DV, Tolstoy E, Ferrara A, Blades JC, Brinks E. 1997. *Ap. J.* 478:530–35
Brandt WN, Ward MJ, Fabian AC, Hodge PW. 1997. *MNRAS* 291:709–16
Bresolin F, Capaccioli M, Piotto G. 1993. *Astron. J.* 105:1779–92
Brinks E, Taylor CL. 1994. See Meylan & Prugniel 1994, pp. 263–72
Buonanno R, Corsi CE, Fusi Pecci F, Hardy E, Zinn R. 1985. *Astron. Astrophys.* 152:65–84
Burstein D, Davies RL, Dressler A, Faber SM, Stone RPS, et al. 1987. *Ap. J. Suppl.* 64:601–42
Burstein D, Heiles C. 1982. *Astron. J.* 87:1165–89
Buta R, Williams KL. 1995. *Astron. J.* 109:543–57
Byrd G, Valtonen M, McCall M, Innanen K. 1994. *Astron. J.* 107:2055–59
Caldwell N, Armandroff TE, Da Costa GS, Seitzer P. 1998. *Astron. J.* 115:535–58

Caldwell N, Armandroff TE, Seitzer P, Da Costa GS. 1992. *Astron. J.* 103:840–50

Caldwell N, Schommer RA, Graham JA. 1988. *Bull. Am. Astron. Soc.* 20:1084

Capaccioli C, Piotto G, Bresolin F. 1992. *Astron. J.* 103:1151–58

Caputo F, Castellani V, Degl'Innocenti S. 1995. *Astron. Astrophys.* 304:365–68

Carignan C. 1985. *Ap. J.* 299:59–73

Carignan C, Beaulieu S, Côté S, Demers S, Mateo M. 1998. *Astron. J.* In press

Carignan C, Beaulieu S, Freeman KC. 1990. *Astron. J.* 99:178–90

Carignan C, Demers S, Côté S. 1991. *Ap. J.* 381:L13–L16

Carlson G, Sandage A. 1990. *Ap. J.* 352:587–94

Carney BW, Seitzer P. 1986. *Astron. J.* 92:23–42

Carter D, Jenkins CR. 1993. *MNRAS* 263:1049–74

Carter D, Sadler EM. 1990. *MNRAS* 245:P12–P16

Castellani M, Marconi G, Buonanno R. 1996. *Astron. Astrophys.* 310:715–21

Cesarsky DA, Lausten S, Lequeux J, Schuster HE, West RM. 1977. *Astron. Astrophys.* 61:L31–L33

Charbonnel C, Meynet G, Maeder A, Schaerer D. 1996. *Astron. Astrophys. Suppl.* 115:339–44

Chiosi C, Bertelli G, Bressan A. 1992. *Annu. Rev. Astron. Astrophys.* 30:235–85

Ciardullo R, Jacoby GH, Ford HC, Neill JD. 1989. *Ap. J.* 339:53–69

Collier J, Hodge P. 1994. *Ap. J. Suppl.* 92:119–23

Cook KH, Aaronson M, Norris J. 1986. *Ap. J.* 305:634–44

Connolly LP. 1985. *Ap. J.* 299:728–40

Cook KH. 1987. *Asymptotic giant branch populations in composite stellar systems*. PhD thesis. Univ. Ariz. Tempe

Corbelli E, Schneider SE, Salpeter EE. 1989. *Astron. J.* 97:390–404

Côté P, Welch DL, Fischer P, Irwin MJ. 1993. *Ap. J.* 406:L59–L62

Côté S. 1995. *Dwarf galaxies in nearby southern groups*. PhD thesis. Aust. N. Univ., Canberra

Côté S, Freeman KC, Carignan C, Quinn PJ. 1997. *Astron. J.* 114:1313–29

Da Costa GS. 1984. *Ap. J.* 285:483–94

Da Costa GS. 1992. In *The Stellar Populations of Galaxies*, ed. B Barbuy, A Renzini, pp. 191–200. Dordrecht: Kluwer

Da Costa GS. 1994a. See Meylan & Prugniel 1994, pp. 221–30

Da Costa GS. 1994b. See Layden et al 1994, pp. 101–14

Da Costa GS. 1998. In *Stellar Astrophysics for the Local Group*, ed. A Aparicio, A Herrero, F Sánchez, pp. 351–406. Cambridge: Cambridge Univ. Press

Da Costa GS, Armandroff TE. 1990. *Astron. J.* 100:162–81

Da Costa GS, Armandroff TE. 1995. *Astron. J.* 109:2533–52

Da Costa GS, Armandroff TE, Caldwell N, Seitzer P. 1996. *Astron. J.* 112:2576–95

Da Costa GS, Graham JA. 1982. *Ap. J.* 261:70–76

Da Costa GS, Hatzidimitriou D, Irwin MJ, McMahon RG. 1991. *MNRAS* 249:473–80

Danziger IJ, Webster BL, Dopita MA, Hawarden TG. 1978. *Ap. J.* 220:458–66

Davidge TJ. 1991. *Astron. J.* 101:884–91

Davidge TJ. 1993. *Astron. J.* 105:1392–99

Davidge TJ. 1994. *Astron. J.* 108:2123–27

Davidge TJ, Jones JH. 1992. *Astron. J.* 104:1365–73

Davidge TJ, Nieto JL. 1992. *Ap. J.* 391:L13–L16

Dekel A, Silk J. 1986. *Ap. J.* 303:39–55

Demers S, Battinelli P, Irwin MJ, Kunkel WE. 1995. *MNRAS* 274:491–98

Demers S, Beland S, Kunkel WE. 1983. *PASP* 95:354–57

Demers S, Irwin MJ. 1987. *MNRAS* 226:943–61

Demers S, Irwin MJ. 1993. *MNRAS* 261:657–73

Demers S, Irwin MJ, Gambu I. 1994a. *MNRAS* 266:7–15

Demers S, Irwin MJ, Kunkel WE. 1994b. *Astron. J.* 108:1648–57

Demers S, Kunkel WE, Irwin MJ. 1985. *Astron. J.* 90:1967–81

Demers S, Mateo M, Kunkel WE. 1998. *MNRAS*. In press

Dettmar RJ, Heithausen A. 1989. *Ap. J.* 344:L61–L64

de Vaucouleurs G, Ables H. 1965. *PASP* 77:272–82

de Vaucouleurs G, Ables HD. 1968. *Ap. J.* 151:105–16

de Vaucouleurs G, Ables HD. 1970. *Ap. J.* 159:425–33

de Vaucouleurs G, de Vaucouleurs A, Buta R. 1981. *Astron. J.* 86:1429–40

de Vaucouleurs G, de Vaucouleurs A, Corwin HG, Buta RJ, Paturel G, Fouqué P. 1991. *Third Reference Catalogue of Bright Galaxies*. New York: Springer-Verlag

de Vaucouleurs G, Freeman KC. 1972. *Vistas Astron.* 14:163–294

de Vaucouleurs G, Moss C. 1983. *Ap. J.* 271:123–32

De Young DS, Heckman TM. 1994. *Ap. J.* 431:598–603

Dohm-Palmer RC, Skillman ED, Saha A, Tolstoy E, Mateo M, et al. 1997. *Astron. J.* 114:2527–44

Dohm-Palmer RC, Skillman ED, Saha A, Tol-

stoy E, Mateo M, et al. 1998. *Astron. J.* In press

Dressler A, Richstone DO. 1988. *Ap. J.* 324: 701–13

Dufour RJ, Talent DL. 1980. *Ap. J.* 235:22–29

Dunn AM, Laflamme R. 1993. *MNRAS* 264: 865–74

Ellis RS. 1997. *Annu. Rev. Astron. Astrophys.* 35:389–443

Elston R, Silva DR. 1992. *Astron. J.* 104:1360–64

Epchtein N, de Batz B, Capoani L, Chevallier L, Copet E, et al. 1997. *ESO Mess.* 87:27–34

Eskridge PB. 1988a. *Astron. J.* 95:1706–16

Eskridge PB. 1988b. *Astron. J.* 96:1336–51

Eskridge PB. 1988c. *Astron. J.* 96:1352–61

Eskridge PB, White RE. 1987. *Bull. Am. Astron. Soc.* 190:02.01

Fabbiano G. 1989. *Annu. Rev. Astron. Astrophys.* 27:87–138

Faber SM, Lin DNC. 1983. *Ap. J.* 266:L17–L20

Fahlman GG, Mandushev G, Richer HB, Thompson IB, Sivaramakrishnan A. 1996. *Ap. J.* 459:L65–L68

Feitzinger JV, Galinski T. 1985. *Astron. Astrophys. Suppl.* 61:503–15

Felton JE. 1984. *Ap. J.* 286:3–6

Ferguson AMN, Wyse RFG, Gallagher JS. 1996. *Astron. J.* 112:2567–75

Ferguson HC, Binggeli B. 1994. *Astron. Astrophys. Rev.* 6:67–122

Ferguson HC, Sandage A. 1991. *Astron. J.* 101: 765–82

Ferraro FR, Fusi Pecci F, Tosi M, Buonanno R. 1989. *MNRAS* 241:433–52

Ferraro FR, Fusi Pecci F, Testa V, Greggio L, Corsi CE, et al. 1995. *MNRAS* 272:391–422

Fich M, Hodge P. 1991. *Ap. J.* 374:L17–L20

Fich M, Tremaine S. 1991. *Annu. Rev. Astron. Astrophys.* 29:409–45

Fisher JR, Tully RB. 1975. *Astron. Astrophys.* 44:151–71

Fisher JR, Tully RB. 1979. *Astron. J.* 84:62–70

Fitzgibbons GL. 1990. *Visual, red, and infrared photographic surface photometry of NGC55 and NGC253.* PhD thesis. Univ. Fla., Gainsville

Ford HC, Ciardullo R, Jacoby GH, Hui X. 1987. In *Planetary Nebulae*, ed. S Torres-Piembert, pp. 335–50. Dordrecht: Reidel

Ford HC, Jacoby G, Jenner DC. 1977. *Ap. J.* 213:18–26

Ford HC, Jacoby G, Jenner DC. 1978. *Ap. J.* 223:94–97

Ford HC, Jenner DC. 1976. *Ap. J.* 208:683–87

Fouqué R, Bottinelli L, Durand N, Gouguenheim L, Paturel G. 1990. *Astron. Astrophys. Suppl.* 86:473–502

Freedman WL. 1988a. *Astron. J.* 96:1248–306

Freedman WL. 1988b. *Ap. J.* 326:691–709

Freedman WL. 1992. *Astron. J.* 104:1349–59

Gallagher JS, Hunter DA. 1981. *Astron. J.* 86: 1312–22

Gallagher JS, Hunter DA, Gillett FC, Rice WL. 1991. *Ap. J.* 371:142–47

Gallagher JS, Hunter DA, Mould J. 1984. *Ap. J.* 281:663–665

Gallagher JS, Hunter DA, Tutukov AV. 1984. *Ap. J.* 284:544–56

Gallagher JS, Wyse RFG. 1994. *PASP* 106: 1225–38

Gallart C. 1998. *Ap. J.* 495:L43–L46

Gallart C, Freedman WL, Mateo M, Chiosi C, Thompson I, et al. 1998. *Astron. J.* In press

Gallart C, Aparicio A, Bertelli G, Chiosi C. 1996a. *Astron. J.* 112:1950–68

Gallart C, Aparicio A, Bertelli G, Chiosi C. 1996b. *Astron. J.* 112:2596–606

Gallart C, Aparicio A, Vílchez JM. 1996c. *Astron. J.* 112:1928–49

Garnett DR. 1989. *Ap. J.* 345:282–97

Garnett DR. 1990. *Ap. J.* 363:142–53

Garnett DR, Kennicutt RC, Chu YH, Skillman ED. 1991. *Ap. J.* 373:458–64

Gerhard OE. 1994. See Meylan & Prugniel 1991, pp. 335–50

Gerhard OE, Spergel DN. 1992a. *Ap. J.* 389:L9–L11

Gerhard OE, Spergel DN. 1992b. *Ap. J.* 397:38–43

Gizis JE, Mould JR, Djorgovski S. 1993. *PASP* 105:871–74

Godwin PJ, Lynden-Bell D. 1987. *MNRAS* 229:P7-P13

González J. 1993. *Line strength gradients and kinematic profiles in elliptical galaxies.* PhD thesis. Univ. Calif., Santa Cruz

Gottesman ST, Weliachew L. 1977. *Astron. Astrophys.* 61:523–30

Gould A, Guhathakurta P, Richstone D, Flynn C. 1992. *Ap. J.* 388:345–53

Grebel EK. 1997. *Rev. Mod. Astron.* 10:29–60

Gregg M, Minniti D. 1997. *PASP* 109:1062–67

Greggio L, Marconi G, Tosi M, Focardi P. 1993. *Astron. J.* 105:894–932

Grillmair CJ, Lauer TR, Worthey G, Faber SM, Freedman WL, et al. 1996. *Astron. J.* 112:1975–87

Grillmair CJ, Mould JR, Holtzman JA, Worthey G, Ballester GE, et al. 1998. *Astron. J.* 115: 144–51

Gurzadyan VG, Kocharyan AA, Petrosian AR. 1993. *Astron. Space Sci.* 201:243–48

Han M, Hoessel JG, Gallagher JS, Holtzman J, Stetson PB, et al. 1997. *Astron. J.* 113:1001–10

Hargreaves JC, Gilmore G, Annan JD. 1996a. *MNRAS* 279:108–20

Hargreaves JC, Gilmore G, Irwin MJ, Carter D. 1994a. *MNRAS* 269:957–74

Hargreaves JC, Gilmore G, Irwin MJ, Carter D. 1994b. *MNRAS* 271:693–705

Hargreaves JC, Gilmore G, Irwin MJ, Carter D. 1996b. *MNRAS* 282:305–12

Harris HC, Silbermann NA, Smith HA. 1997. In *A Half Century of Stellar Pulsation Interpretations: A Tribute to AN Cox*, ed. PA Bradley, JA Guzik, *Conf. Ser. 135*, pp. 164–68. San Francisco: Astron. Soc. Pac.

Hatzidimitriou D. 1991. *MNRAS* 251:545–54

Heckman TM, Dahlem M, Lehnert MD, Fabbiano G, Gilmore D, Waller WH. 1995. *Ap. J.* 448:98–118

Heisler CA, Hill TL, McCall ML, Hunstead RW. 1997. *MNRAS* 285:374–86

Held EV, de Zeeuw T, Mould J, Picard A. 1992. *Astron. J.* 103:851–56

Held EV, Mould JR, de Zeeuw PT. 1990. *Astron. J.* 100:415–19

Henning PA. 1997. *Publ. Astron. Soc. Aust.* 14:21–24

Hewitt JN, Haynes MP, Giovanelli R. 1983. *Astron. J.* 88:272–95

Ho LC, Fillippenko AV, Sargent WLW. 1995. *Ap. J. Suppl.* 98:477–593

Ho LC, Fillipenko A, Sargent W. 1997. *Ap. J. Suppl.* 112:315–90

Hodge P. 1994. See Layden et al 1994, pp. 57–64

Hodge P, Kennicutt RC, Strobel N. 1994. *PASP* 106:765–69

Hodge P, Lee MG, Gurwell M. 1990. *PASP* 102:1245–62

Hodge P, Lee MG, Kennicutt RC. 1988. *PASP* 100:917–34

Hodge P, Lee MG, Kennicutt RC. 1989. *PASP* 101:640–48

Hodge P, Miller BW. 1995. *Ap. J.* 451:176–87

Hodge PW. 1963a. *Astron. J.* 68:470–74

Hodge PW. 1963b. *Astron. J.* 68:691–96

Hodge PW. 1964. *Astron. J.* 69:438–42

Hodge PW. 1966. *Astron. J.* 71:204–5

Hodge PW. 1969. *Ap. J. Suppl.* 18:73–84

Hodge PW. 1971. *Annu. Rev. Astron. Astrophys.* 9:35–66

Hodge PW. 1973. *Ap. J.* 182:671–95

Hodge PW. 1974. *PASP* 86:289–93

Hodge PW. 1976. *Astron. J.* 81:25–29

Hodge PW. 1977. *Ap. J. Suppl.* 33:69–82

Hodge PW. 1978. *Ap. J. Suppl.* 37:145–67

Hodge PW. 1980. *Ap. J.* 241:125–31

Hodge PW. 1981. *Atlas of the Andromeda Galaxy*. Seattle: Univ. Wash. Press

Hodge PW. 1982. *Astron. J.* 87:1668–70

Hodge PW. 1989. *Annu. Rev. Astron. Astrophys.* 27:139–59

Hodge PW, Lee MG. 1990. *PASP* 102:26–40

Hodge PW, Smith DW. 1974. *Ap. J.* 188:19–25

Hodge PW, Smith T, Eskridge P, MacGillivray H, Beard S. 1991a. *Ap. J.* 379:621–30

Hodge PW, Smith TR, Eskridge PB, MacGillivray HT, Beard SM. 1991b. *Ap. J.* 369:372–81

Hodge PW, Wright FW. 1978. *Astron. J.* 83:228–33

Hoessel JG, Abbott MJ, Saha A, Mossman AE, Danielson GE. 1990. *Astron. J.* 100:1151–58

Hoessel JG, Saha A, Danielson GE. 1988. *PASP* 100:680–82

Hoessel JG, Saha A, Krist J, Danielson GE. 1994. *Astron. J.* 108:645–52

Hoffman GL, Salpeter EE, Farhat B, Roos T, Williams H, Helou G. 1996. *Ap. J. Suppl.* 105:269–98

Holmberg E. 1958. Medd Lunds Astron Obs II, No.136

Holtzman JA, Mould JR, Gallagher JS, Watson AM, Grillmair CJ, et al. 1997. *Astron. J.* 113:656–68

Hoopes CG, Walterbos RAM, Greenawalt BE. 1996. *Astron. J.* 112:1429–37

Hopp U, Schulte-Ladbeck RE. 1995. *Astron. Astrophys. Suppl.* 111:527–63

Huchtmeier WK, Richter OG. 1986. *Astron. Astrophys. Suppl.* 63:323–43

Huchtmeier WK, Richter OG. 1988. *Astron. Astrophys.* 203:237–49

Humason ML, Mayall NU, Sandage AR. 1956. *Astron. J.* 61:97–162

Hummel E, Dettmar RJ, Wielebinski R. 1986. *Astron. Astrophys.* 166:97–106

Hunter DA, Gallagher JS. 1985. *Ap. J. Suppl.* 58:533–60

Hunter DA, Gallagher JS. 1990. *Ap. J.* 362:480–90

Hunter DA, Hawley WN, Gallagher JS. 1993. *Astron. J.* 106:1797–811

Hunter DA, Plummer J. 1996. *Ap. J.* 462:732–39

Hurley-Keller D, Mateo M, Nemec J. 1998. *Astron. J.* In press

Huterer D, Sasselov DD, Schechter PL. 1995. *Astron. J.* 110:2705–14

Ibata RA, Gilmore G, Irwin MJ. 1994. *Nature* 370:194–96

Ibata RA, Wyse RFG, Gilmore G, Irwin MJ, Suntzeff NB. 1997. *Astron. J.* 113:634–55

Irwin M. 1994. See Meylan & Prugniel 1994, pp. 27–36

Irwin M, Hatzidimitriou D. 1995. *MNRAS* 277:1354–78

Irwin MJ, Bunclark PS, Bridgeland MT, McMahon RG. 1990. *MNRAS* 244:P16-P19

Israel FP. 1997. *Astron. Astrophys.* 317:65–72

Israel FP, Tacconi LJ, Baas F. 1995. *Astron. Astrophys.* 295:599–604

Jacoby GH, Lesser MP. 1981. *Astron. J.* 86:185–92

James P. 1991. *MNRAS* 250:544–54

Jobin M, Carignan C. 1990. *Astron. J.* 100:648–62

Johnson DW, Gottesman ST. 1983. *Ap. J.* 275:549–58

Johnston KV, Spergel DN, Hernquist L. 1995. *Ap. J.* 451:598–606

Jones BF, Klemola AR, Lin DNC. 1994. *Astron. J.* 107:1333–37

Jones DH, Mould JR, Watson AM, Grillmair C, Gallagher JS, et al. 1996. *Ap. J.* 466:742–49

Kaluzny J, Kubiak M, Szymanski M, Udalski A, Krzeminski W, Mateo M. 1995. *Astron. Astrophys. Suppl.* 112:407–28

Karachentsev I. 1996. *Astron. Astrophys.* 305:33–41

Karachentsev ID, Makarov DA. 1996. *Astron. J.* 111:794–803

Karachentsev ID, Makarov DA. 1998. *Astron. Astrophys.* 331:891–93

Karachentsev ID, Tikhonov NA. 1993. *Astron. Astrophys. Suppl.* 100:227–35

Karachentsev ID, Tikhonov NA, Sazonova LN. 1994. *Astrophys. Lett.* 20:84–88

Karachentseva VE, Karachentsev ID. 1998. *Astron. Astrophys. Suppl.* 127:409–19

Karachentseva VE, Karachentsev ID, Börngen F. 1985. *Astron. Astrophys. Suppl.* 60:213–27

Karachentseva VE, Prugniel P, Vennik J, Richter GM, Thuan TX, Martin JM. 1996. *Astron. Astrophys. Suppl.* 117:343–68

Kayser SE. 1967. *Astron. J.* 72:134–48

Kennicutt RC. 1983. *Ap. J.* 272:54–67

Kennicutt RC. 1994. See Layden et al 1994, pp. 28–40

Kent SM. 1987. *Astron. J.* 94:306–14

Killen RM, Dufour RJ. 1982. *PASP* 94:444–52

Kinman TD, Pier JR, Suntzeff NB, Harmer DL, Valdes F, et al. 1996. *Astron. J.* 111:1164–68

Kirkpatrick JD, Beichman CA, Skrutskie MF. 1997. *Ap. J.* 476:311–18

Klein U, Gräve R. 1986. *Astron. Astrophys.* 161:155–16

Knapp GR, Guhathakurta P, Kim DW, Jura M. 1989. *Ap. J. Suppl.* 70:329–87

Knapp GR, Kerr FJ, Bowers PF. 1978. *Astron. J.* 83:360–62

Knapp GR, Turner EL, Cunniffe PE. 1985. *Astron. J.* 90:454–68

Kochanek CS. 1996. *Ap. J.* 457:228–43

Kodaira K, Okamura S, Ichikawa S. 1990. *Photometric Atlas of Northern Bright Galaxies*. Tokyo: Univ. Tokyo Press

König CHB, Nemec JM, Mould JR, Fahlman GG. 1993. *Astron. J.* 106:1819–25

Koribalski B, Johnston S, Otrupcek R. 1994. *MNRAS* 270:L43–L45

Kormendy J, Richstone D. 1995. *Annu. Rev. Astron. Astrophys.* 33:581–624

Kroupa P. 1997. *New Astron.* 2:139–64

Kuhn JR. 1993. *Ap. J.* 409:L13–L16

Kuhn JR, Miller RH. 1989. *Ap. J.* 341:L41–L45

Kuhn JR, Smith HA, Hawley SL. 1996. *Ap. J.* 469:L93–L96

Lake G. 1989a. *Astron. J.* 98:1253–59

Lake G. 1989b. *Ap. J.* 345:L17–L19

Lake G, Skillman ED. 1989. *Astron. J.* 98:1274–84

Lausten S, Richter W, van der Lans J, West RM, Wilson RN. 1977. *Astron. Astrophys.* 54:639–40

Lavery RJ, Mighell KJ. 1992. *Astron. J.* 103:81–83

Lavery RJ, Seitzer P, Walker AR, Suntzeff NB, Da Costa GS. 1996. *Bull. Am. Astron. Soc.* 188:09.03

Layden A, Smith RC, Storm J, eds. 1994. *The Local Group*. Garching: Eur. South. Obs.

Lee MG. 1993. *Ap. J.* 408:409–15

Lee MG. 1995a. *Astron. J.* 110:1129–40

Lee MG. 1995b. *Astron. J.* 110:1155–63

Lee MG. 1996. *Astron. J.* 112:1438–49

Lee MG, Freedman W, Mateo M, Thompson I, Roth M, Ruiz MT. 1993a. *Astron. J.* 106:1420–35

Lee MG, Freedman WL, Madore BF. 1993b. *Astron. J.* 106:964–85

Lee MG, Freedman WL, Madore BF. 1993c. *Ap. J.* 417:553–59

Lehnert MD, Bell RA, Hesser JE, Oke JB. 1992. *Ap. J.* 395:466–74

Lequeux J, Meyssonnier N, Azzopardi M. 1987. *Astron. Astrophys. Suppl.* 67:169–79

Lequeux J, Rayo JF, Serrano A, Piembert M, Torres-Piembert S. 1979. *Astron. Astrophys.* 80:155–66

Light RM, Armandroff TE, Zinn R. 1986. *Astron. J.* 92:43–47

Liller W, Alcaino G. 1983. *Ap. J.* 264:53–57

Lin DNC, Faber SM. 1983. *Ap. J.* 266:L21–L25

Lin DNC, Jones BF, Klemola AR. 1995. *Ap. J.* 439:652–71

Lo KY, Sargent WLW, Young K. 1993. *Astron. J.* 106:507–29

Longmore AJ, Hawarden TG, Goss WM, Mebold U, Webster BL. 1982. *MNRAS* 200:325–46

Longmore AJ, Hawarden TG, Webster BL, Goss WM, Mebold U. 1978. *MNRAS* 183:P97-P100

Longo G, de Vaucouleurs A. 1983. *University of Texas Monograph Series*, No. 3

Longo G, de Vaucouleurs A. 1985. *University of Texas Monograph Series*, No. 3A

Lu NY, Hoffman GL, Groff T, Roos T, Lamphier C. 1993. *Ap. J. Suppl.* 88:383–413

Lugger PM, Cohn HN, Cederbloom SE, Lauer TR, McClure RD. 1992. *Astron. J.* 104:83–91

Luppino GA, Tonry JL. 1993. *Ap. J.* 410:81–86

Lynden-Bell D. 1982. *Observatory* 102:202–8

Lynden-Bell D, Lynden-Bell RM. 1995. *MNRAS* 275:429–42

Lyo AR, Lee MG. 1997. *J. Korean Astron. Soc.* 30:27–70

Madore BF, Freedman WL. 1991. *PASP* 103: 933–57

Madden SC, Poglitsch A, Geis N, Stacey GJ, Townes CH. 1997. *Ap. J.* 483:200–9

Maeder A, Meynet G. 1988. *Astron. Astrophys. Suppl.* 76:411–25

Majewski SR. 1992. *Ap. J. Suppl.* 78:87–152

Maran SP, Gull TR, Stecher TP, Aller LH, Keyes CD. 1984. *Ap. J.* 280:615–17

Marconi G, Buonanno R, Castellani M, Iannicola G, Molaro P, et al. 1998. *Astron. Astrophys.* 330:453–63

Marconi G, Focardi P, Greggio L, Tosi M. 1990. *Ap. J.* 360:L39–L41

Marconi G, Tosi M, Greggio L, Focardi P. 1995. *Astron. J.* 109:173–99

Markert T, Donahue M. 1985. *Ap. J.* 297:564–71

Martínez-Delgado D, Aparicio A. 1997. *Ap. J.* 480:L107–10

Marzke RO, Da Costa LN. 1997. *Astron. J.* 113:185–96

Massey P. 1998. In *Stellar Astrophysics of the Local Group*, ed. A Aparicio, A Herrero, F Sánchez, pp. 95–147. Cambridge: Cambridge Univ. Press

Massey P, Armandroff TE. 1995. *Astron. J.* 109:2470–79

Massey P, Armandroff TE, Conti PS. 1992. *Astron. J.* 103:1159–65

Mateo M. 1994. See Meylan & Prugniel 1994, pp. 309–22

Mateo M. 1996. In *Formation of the Galactic Halo... Inside and Out*, ed. H Morrison, A Sarajedini, *ASP Conf. Ser. 92*, pp. 434–43. San Francisco: Astron. Soc. Pac.

Mateo M. 1996. In *The Nature of Elliptical Galaxies*, ed. M Arnaboldi, GS Da Costa, P Saha, *ASP Conf. Ser. 116*, pp. 259–69. San Francisco: Astron. Soc. Pac.

Mateo M. 1998. In *Stellar Astrophysics for the Local Group*, ed. A Aparicio, A Herrero, F Sánchez, pp. 407–57. Cambridge, UK Cambridge Univ. Press

Mateo M, Demers S, Kunkel WE. 1998a. *Astron. J.* In press

Mateo M, Fischer P, Krzemiński W. 1995a. *Astron. J.* 110:2166–82

Mateo M, Hurley-Keller DA, Nemec J. 1998b. *Astron. J.* In press

Mateo M, Kubiak M, Szymański M, Kaluzny J, Krzemiński W, Udalski A. 1995b. *Astron. J.* 110:1141–54

Mateo M, Mirabal N, Udalski A, Szymański M, Kaluzny J, et al. 1996. *Ap. J.* 458:L13–L16

Mateo M, Nemec J, Irwin M, McMahon R. 1991a. *Astron. J.* 101:892–910

Mateo M, Olszewski E, Welch DL, Fischer P, Kunkel W. 1991b. *Astron. J.* 102:914–26

Mateo M, Olszewski EW, Hodge P. 1998c. *Astron. J.* In press

Mateo M, Olszewski EW, Pryor C, Welch DL, Fischer P. 1993. *Astron. J.* 105:510–26

Mateo M, Olszewski EW, Vogt SS, Keane M. 1998d. *Astron. J.* In press

Mateo M, Udalski A, Szymański M, Kaluzny J, Kubiak M, Krzemiński W. 1995c. *Astron. J.* 109:588–93

Mathewson DS, Ford VL. 1984. In *Structure and Evolution of the Magellanic Clouds*, ed. S van den Bergh, K de Boer, pp. 125–36. Dordrecht: Reidel

McGaugh S, de Blok E. 1998. *Ap. J.* In press

McNamara DH. 1995. *Astron. J.* 109:1751–56

Melisse JPM, Israel FP. 1994a. *Astron. Astrophys.* 285:51–68

Melisse JPM, Israel FP. 1994b. *Astron. Astrophys. Suppl.* 103:391–412

Mermilliod JC. 1981. *Astron. Astrophys.* 97: 235–44

Merrifield MR, Kent SM. 1990. *Astron. J.* 99:1548–57

Meylan G, Prugniel P, eds. 1994. *Dwarf Galaxies*. Garching: Eur. South. Obs.

Meynet G, Maeder A, Schaller G, Schaerer D, Charbonnel C. 1994. *Astron. Astrophys. Suppl.* 103:97–105

Meynet G, Mermilliod JC, Maeder A. 1993. *Astron. Astrophys. Suppl.* 76:411–25

Michard R, Nieto JL. 1991. *Astron. Astrophys.* 243:L17–L20

Mighell KJ. 1990. *Astron. Astrophys. Suppl.* 82:1–39

Mighell KJ. 1997. *Astron. J.* 114:1458–70

Mighell KJ, Rich RM. 1996. *Astron. J.* 111:777–87

Milgrom M. 1983a. *Ap. J.* 270:365–70

Milgrom M. 1983b. *Ap. J.* 270:371–83

Milgrom M. 1991. *Ap. J.* 367:490–92

Milgrom M. 1994. *Ap. J.* 429:540–44

Milgrom M. 1995. *Ap. J.* 455:439–42

Miller BW. 1996. *Astron. J.* 112:991–1008

Minniti D, Zijlstra AA. 1996. *Ap. J.* 467:L13–L16

Moles M, Aparicio A, Masegosa J. 1990. *Astron. Astrophys.* 228:310–14

Moore B, Davis M. 1994. *MNRAS* 270:209–21

Morishima T, Saio H. 1995. *Ap. J.* 450:70–73

Morris M, Lo KY. 1978. *Ap. J.* 223:803–10

Morrison H, Sarajedini A, eds. 1996. *Formation of the Galactic Halo... Inside and Out, Conf. Ser. 92*. San Francisco: Astron. Soc. Pac.

Mould J. 1997. *PASP* 109:125–29

Mould J, Aaronson M. 1983. *Ap. J.* 273:530–38

Mould J, Kristian J. 1990. *Ap. J.* 354:438–45

Mould J, Kristian J, Da Costa GS. 1983. *Ap. J.* 270:471–84

Mould J, Kristian J, Da Costa GS. 1984. *Ap. J.* 278:575–81

Mould JR, Bothun GD, Hall PJ, Staveley-Smith L, Wright AE. 1990. *Ap. J.* 362:L55–L57

Musella I, Piotto G, Capaccioli M. 1997. *Astron. J.* 114:976–87

Nemec JM. 1985. *Astron. J.* 90:204–39

Nemec JM, Nemec AF, Lutz TE. 1994. *Astron. J.* 108:222–46

Nemec JM, Wehlau A, Mendes de Oliveira C. 1988. *Astron. J.* 96:528–59

Nolthenius R, Ford H. 1986. *Ap. J.* 305:600–8

O'Connell RW. 1992. In *The Stellar Populations of Galaxies*, ed. B Barbuy, A Renzini, pp. 233–43. Dordrecht: Kluwer

Oh KS, Lin DNC, Aarseth SJ. 1995. *Ap. J.* 442:142–58

Ohta K, Sasaki M, Saitō M. 1988. *Publ. Astron. Soc. Jpn.* 40:653–64

Ohta K, Tomita A, Saitō M, Sasaki M, Nakai N. 1993. *Publ. Astron. Soc. Jpn.* 45:L21–L26

Olszewski EW. 1998. In *Santa Cruz Workshop on Galaxy Halos*, ed. D Zaritsky, *Conf. Ser.*, pp. 70–78. San Francisco: Astron. Soc. Pac. In press

Olszewski EW, Aaronson M. 1985. *Astron. J.* 90:2221–38

Olszewski EW, Aaronson M, Hill JM. 1995. *Astron. J.* 110:2120–30

Olszewski EW, Pryor C, Armandroff TE. 1996a. *Astron. J.* 111:750–67

Olszewski EW, Suntzeff NB, Mateo M. 1996b. *Annu. Rev. Astron. Astrophys.* 34:511–50

Oosterloo T, Da Costa GS, Staveley-Smith L. 1996. *Astron. J.* 112:1969–74

Ortolani S, Gratton RG. 1988. *PASP* 100:1405–22

Pagel BEJ, Edmunds MG, Smith G. 1980. *MNRAS* 193:219–30

Paltoglou G, Freeman KC. 1987. In *Structure and Dynamics of Elliptical Galaxies*, ed. T de Zeeuw, pp. 447–48. Dordrecht: Reidel

Peebles PJE. 1989. *Ap. J.* 344:L53–L56

Peebles PJE. 1995. *Ap. J.* 449:52–60

Peletier RF. 1993. *Astron. Astrophys.* 271:51–64

Peterson CJ. 1993. In *Structure and Dynamics of Globular Clusters*, ed. SG Djorgovski, G Meylan, *Conf. Ser. 50*, pp. 337–45. San Francisco: Astron. Soc. Pac.

Peterson RC, Caldwell N. 1993. *Astron. J.* 105:1411–19

Phillips S, Parker QA, Schwartzenberg JM, Jones JB. 1998. *Ap. J.* 493:L59–L62

Piatek S, Pryor C. 1995. *Astron. J.* 109:1071–85

Pierce MJ, Tully RB. 1992. *Ap. J.* 387:47–55

Piotto G, Capaccioli M. 1992. *Mem. Soc. Astron. Ital.* 63:465–78

Piotto G, Capaccioli M, Pellegrini C. 1994. *Astron. Astrophys.* 287:371–86

Poulain P, Nieto JL. 1994. *Astron. Astrophys. Suppl.* 103:573–95

Preston GW, Beers TC, Shectman SA. 1994. *Astron. J.* 108:538–54

Price JS. 1985. *Ap. J.* 297:652–61

Price JS, Grasdalen GL. 1983. *Ap. J.* 275:559–70

Price JS, Mason SF, Gullixson CA. 1990. *Astron. J.* 100:420–24

Pritchet CJ, Richer HB, Schade D, Crabtree D, Yee HKC. 1987. *Ap. J.* 323:79–90

Prugniel P, Simien F. 1997. *Astron.* 321:111–22

Pryor C. 1994. See Meylan & Prugniel 1994, pp. 323–34

Pryor C. 1996. In *Formation of the Galactic Halo... Inside and Out*, ed. H Morrison, A Sarajedini, *Conf. Ser. 92*, pp. 424–33. San Francisco: Astron. Soc. Pac.

Pryor C, Kormendy J. 1990. *Astron. J.* 100:127–40

Puche D, Carignan C, Bosma A. 1990. *Astron. J.* 100:1468:1476

Puche D, Carignan C, Wainscoat RJ. 1991. *Astron. J.* 101:447–55

Puche D, Westpfahl D. 1994. See Meylan & Prugniel 1994, pp. 273–81

Qiu B, Wu XP, Zou ZL. 1995. *Astron. Astrophys.* 296:264–68

Queloz D, Dubath P, Pasquini L. 1995. *Astron. Astrophys.* 300:31–42

Reid N, Mould J. 1991. *Astron. J.* 101:1299–303

Richer HB, Crabtree DR, Pritchet CJ. 1984. *Ap. J.* 287:138–47

Richer HB, Westerlund BE. 1983. *Ap. J.* 264:114–25

Richer MG, McCall ML. 1992. *Astron. J.* 103:54–59

Richer MG, McCall ML. 1995. *Ap. J.* 445:642–59

Richstone DO, Tremaine S. 1986. *Astron. J.* 92:72–74

Richter GM, Schmidt KH, Thänert W, Stavrev K, Panov K. 1991. *AN* 312:309–14

Richter OG, Tammann GA, Huchtmeier WK. 1987. *Astron. Astrophys.* 171:33–40

Roberts MS, Hogg DE, Bregman JN, Forman WR, Jones C. 1991. *Ap. J. Suppl.* 75:751–99

Rowan-Robinson M, Phillips TG, White G. 1980. *Astron. Astrophys.* 82:381–84

Rozanski R, Rowan-Robinson M. 1994. *MNRAS* 271:530–52

Sage LJ, Wrobel JM. 1989. *Ap. J.* 344:204–9

Saha A, Freedman WL, Hoessel JG, Mossman AE. 1992a. *Astron. J.* 104:1072–85

Saha A, Hoessel JG. 1987. *Astron. J.* 94:1556–63

Saha A, Hoessel JG. 1990. *Astron. J.* 99:97–148

Saha A, Hoessel JG. 1991. *Astron. J.* 101:465–68

Saha A, Hoessel JG, Krist J. 1992b. *Astron. J.* 103:84–103

Saha A, Hoessel JG, Krist J, Danielson GE. 1996. *Astron. J.* 111:197–207

Saha A, Hoessel JG, Mossman AE. 1990. *Astron. J.* 100:108–26

Saha A, Monet DG, Seitzer P. 1986. *Astron. J.* 92:302–27

Saitō M, Sasaki M, Ohta K, Yamada T. 1992. *PASJ* 44:593–600

Sakai S, Madore BF, Freedman WL. 1996. *Ap. J.* 461:713–23

Sandage A. 1961. *The Hubble Atlas of Galaxies*. Washington, DC: Carnegie Inst. Wash.

Sandage A. 1986a. *Ap. J.* 307:1–19

Sandage A. 1986b. *Astron. J.* 91:496–506

Sandage A, Bedke J. 1994. *The Carnegie Atlas of Galaxies*. Washington, DC: Carnegie Inst. Wash.

Sandage A, Binggeli B. 1984. *Astron. J.* 89:919–31

Sandage A, Binggeli B, Tammann GA. 1985a. *Astron. J.* 90:395–404

Sandage A, Binggeli B, Tammann GA. 1985b. *Astron. J.* 90:1759–71

Sandage A, Carlson G. 1982. *Ap. J.* 258:439–56

Sandage A, Carlson G. 1985a. *Astron. J.* 90:1019–26

Sandage A, Carlson G. 1985b. *Astron. J.* 90:1464–73

Sandage A, Carlson G. 1988. *Astron. J.* 96:1599–613

Sandage A, Smith LL. 1966. *Ap. J.* 144:886–93

Sandage A, Wallerstein G. 1960. *Ap. J.* 131:598–609

Sanders RH. 1996. *Ap. J.* 473:117–29

Sanders RH. 1997. *Ap. J.* 480:492–502

Sarajedini A, Chaboyer B, Demarque P. 1997. *PASP* 109:1321–39

Sarajedini A, Claver CF, Ostheimer JC. 1997. *Astron. J.* 114:2505–13

Sarajedini A, Layden AC. 1995. *Astron. J.* 109:1086–94

Saviane I, Held EV, Piotto G. 1996. *Astron. Astrophys.* 315:40–51

Schaller G, Schaerer D, Meynet G, Maeder A. 1992. *Astron. Astrophys. Suppl.* 96:269–331

Schechter P. 1976. *Ap. J.* 203:297–306

Schild R. 1980. *Ap. J.* 242:63–65

Schmidt KH, Boller T. 1992. *AN* 313:189–231

Schweitzer AE, Cudworth KM, Majewski SR, Suntzeff NB. 1995. *Astron. J.* 110:2747–56

Sembach KR, Tonry JL. 1996. *Astron. J.* 112:797–805

Sérsic JL. 1968. *Atlas de Galaxias Australes*. Cordoba: Obs. Astron.

Sérsic JL, Cerruti MA. 1979. *Observatory* 99:150–51

Siegel MH, Majewski SR, Reid IN, Thompson I, Landolt AU, Kunkel WE. 1997. *Bull. Am. Astron. Soc.* 191:81.03

Shostak GS. 1974. *Astron. Astrophys.* 31:97–101

Shostak GS, Skillman ED. 1989. *Astron. Astrophys.* 214:33–42

Silva DR, Elston R. 1994. *Ap. J.* 428:511–43

Sivaram C. 1994. *Astrophys. Space Sci.* 215:185–89

Skillman ED. 1998. In *Stellar Astrophysics for the Local Group*, ed. A Aparicio, A Herrero, F Sánchez, pp. 457–525. Cambridge: Cambridge Univ. Press

Skillman ED, Bender R. 1995. *Rev. Mex. Astron. Astrophys. Conf. Ser.* 3:25–30

Skillman ED, Bomans DJ, Kobulnicky HA. 1997. *Ap. J.* 474:205–16

Skillman ED, Kennicutt RC, Hodge PW. 1989a. *Ap. J.* 347:875–82

Skillman ED, Terlevich R, Melnick J. 1989b. *MNRAS* 240:563–72

Skillman ED, Terlevich R, Teuben PJ, van Woerden H. 1988. *Astron. Astrophys.* 198:33–42

Smecker-Hane TA, Stetson PB, Hesser JE, Lehnert MD. 1994. *Astron. J.* 108:507–13

Smith EO, Neill JD, Mighell KJ, Rich RM. 1996. *Astron. J.* 111:1596–603

Sofue Y, Wakamatsu K. 1993. *PASJ* 45:529–38

Stasinska G, Comte G, Vigroux L. 1986. *Astron. Astrophys.* 154:352–56

Stetson PB. 1997. *Baltic Astron.* 6:3–10

Strobel NV, Hodge P, Kennicutt RC. 1991. *Ap. J.* 383:148–63

Strobel NV, Lake G. 1994. *Ap. J.* 424:L83–L86

Suntzeff NB, Aaronson M, Olszewski EW, Cook KH. 1986. *Astron. J.* 91:1091–95

Suntzeff NB, Mateo M, Terndrup DM, Olszewski EW, Geisler D, Weller W. 1993. *Ap. J.* 418:208–28

Swope H. 1967. *PASP* 79:439–40

Tacconi LJ, Young JS. 1987. *Ap. J.* 322:681–87

Talent DL. 1980. *A spectrophotometric study of HII regions in chemically young galaxies*. PhD thesis. Rice Univ., Houston, TX

Thronson HA, Hunter DA, Casey S, Harper DA. 1990. *Ap. J.* 355:94–101

Thuan TX, Martin GE. 1979. *Ap. J.* 232:L11–L16

Tikhonov N, Makarova L. 1996 *AN* 317:179–86

Tolstoy E. 1996. *Ap. J.* 462:684–704

Tolstoy E, Gallagher JS, Cole AA, Hoessel JG, Saha A, et al. 1998. *Ap. J.* In press

Tolstoy E, Saha A. 1996. *Ap. J.* 462:672–83

Tolstoy E, Saha A, Hoessel JG, Danielson GE. 1995. *Astron. J.* 109:579–87

Tomita A, Ohta K, Saitō M. 1993. *PASJ* 45:693–705

Tonry JL. 1984. *Ap. J.* 283:L27–L30

Tosi M, Greggio L, Marconi G, Focardi P. 1991. *Astron. J.* 102:951–74

Unavane M, Wyse RFG, Gilmore G. 1996. *MNRAS* 278:727–36

van Agt SLTJ. 1973. In *Variable Stars in Globular Clusters and Related Systems*, ed. JD Fernie, pp. 35–48. Dordrecht: Reidel

van Agt SLTJ. 1978. *Publ. David Dunlap Obs.* 3:205–35

van den Bergh S. 1994a. *Astron. J.* 107:1328–32

van den Bergh S. 1994b. *Astron. J.* 108:2145–53

van den Bergh S. 1994c. *Ap. J.* 428:617–19

van den Bergh S. 1995. *Ap. J.* 446:39–43

van de Rydt F, Demers S, Kunkel WE. 1991. *Astron. J.* 102:130–36

van Dokkum PG, Franx M. 1995. *Astron. J.* 110:2027–36

van Zee L, Maddalena RJ, Haynes MP, Hogg DE, Roberts MS. 1997. *Astron. J.* 113:1638–47

Velázquez H, White SDM. 1995. *MNRAS* 275:L23–L26

Verter F, Hodge P. 1995. *Ap. J.* 446:616–21

Vogt SS, Mateo M, Olszewski EW, Keane MJ. 1995. *Astron. J.* 109:151–63

Wakker BP, van Woerden H. 1997. *Annu. Rev. Astron. Astrophys.* 35:217–66

Walsh JR, Dudziak G, Minniti D, Zijlstra AA. 1997. *Ap. J.* 487:651–62

Webster BL, Smith MG. 1983. *MNRAS* 204:743–63

Welch GA, Mitchell GF, Yi S. 1996. *Ap. J.* 470:781–89

Westerlund BE. 1990. *Astron. Astrophys.* Rev 2:29-

Westerlund BE. 1997. *The Magellanic Clouds*. Cambridge, UK Cambridge Univ. Press

Whitelock PA, Irwin M, Catchpole RM. 1996. *New Astron.* 1:57–75

Whiting AB, Irwin MJ, Hau GKT. 1997. *Astron. J.* 114:996–1001

Wiklind T, Rydbeck G. 1986. *Astron. Astrophys.* 164:L22–L24

Wilson CD. 1992a. *Astron. J.* 104:1374–94

Wilson CD. 1992b. *Ap. J.* 391:144–51

Wilson CD. 1994a. See Layden et al 1994, pp. 15–27

Wilson CD. 1994b. *Ap. J.* 434:L11–L14

Wilson CD. 1995. *Ap. J.* 448:L97–L100

Wilson CD, Reid IN. 1991. *Ap. J.* 366:L11–L14

Wilson CD, Welch DL, Reid IN, Saha A, Hoessel J. 1996. *Astron. J.* 111:1106–9

Wyatt RJ, Dufour RJ. 1993. *Rev. Mex. Astron. Astrophys.* 27:213–18

Yahil A, Tammann GA, Sandage A. 1977. *Ap. J.* 217:903–15

Yang H, Skillman ED. 1993. *Astron. J.* 106:1448–59

Young JS, Zie S, Tacconi L, Knezek P, Viscuso P, et al. 1995. *Ap. J. Suppl.* 98:219–57

Young LM, Lo KY. 1996a. *Ap. J.* 462:203–14

Young LM, Lo KY. 1996b. *Ap. J.* 464:L59–L62

Young LM, Lo KY. 1997a. *Ap. J.* 476:127–43

Young LM, Lo KY. 1997b. *Ap. J.* 490:710–28

Zaritsky D, Lin DNC. 1997. *Astron. J.* 114:2545–55

Zaritsky D, Olszewski EW, Schommer RA, Peterson RC, Aaronson M. 1989. *Ap. J.* 345:759–69

Zijlstra AA, Walsh JR. 1996. *Astron. Astrophys.* 312:L21–L24

Zinn R. 1980. In *Globular Clusters*, ed. D Hanes, B Madore, pp. 191–212. Cambridge: Cambridge Univ. Press

Zinn R, West MJ. 1984. *Ap. J. Suppl.* 55:45–66